NTIS #

SSC-449

HYDRODYNAMIC PRESSURES AND IMPACT LOADS FOR HIGH-SPEED CATAMARAN / SES HULL FORMS

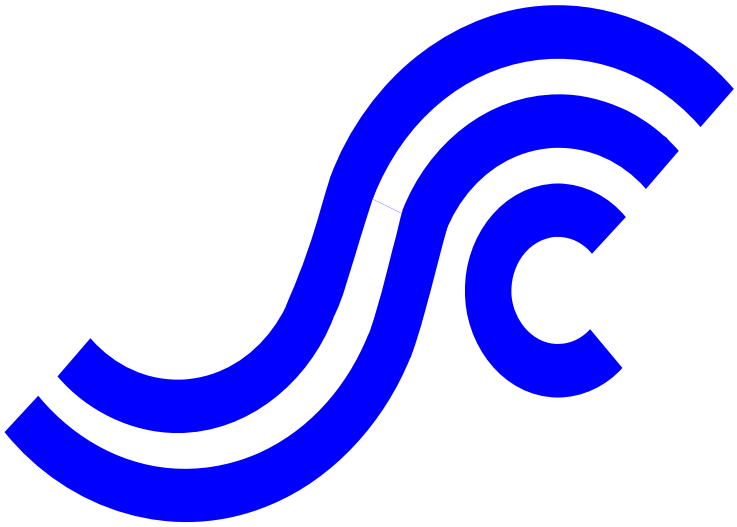

This document has been approved
For public release and sale; its
Distribution is unlimited

SHIP STRUCTURE COMMITTEE

2007

Ship Structure Committee

RADM Brian M. Salerno
U. S. Coast Guard Assistant Commandant,
Assistant Commandant for Marine Safety, Security and Stewardship
Chairman, Ship Structure Committee

{Name}
{Title}
Naval Sea Systems Command

Dr. Roger Basu
Senior Vice President
American Bureau of Shipping

Mr. Joseph Byrne
Director, Office of Ship Construction
Maritime Administration

Mr. William Nash
Director General, Marine Safety,
Safety & Security
Transport Canada

Mr. Kevin Baetsen
Director of Engineering
Military Sealift Command

Dr. Neil Pegg
Group Leader - Structural Mechanics
Defence Research & Development Canada - Atlantic

CONTRACTING OFFICER TECHNICAL REP.
Mr. Chao Lin / MARAD
Mr. Glenn Ashe / ABS
DRDC / USCG

EXECUTIVE DIRECTOR
Lieutenant Commander, Jason Smith
U. S. Coast Guard

SHIP STRUCTURE SUB-COMMITTEE

AMERICAN BUREAU OF SHIPPING

Mr. Glenn Ashe
Mr. Derek Novak
Mr. Phil Rynn
Mr. Balji Menon

DEFENCE RESEARCH & DEVELOPMENT CANADA ATLANTIC
Dr. David Stredulinsky
Mr. John Porter

MARITIME ADMINISTRATION
Mr. Chao Lin
Mr. Carl Setterstrom
Mr. Richard Sonnenschein

MILITARY SEALIFT COMMAND
Mr. Michael W. Touma
Mr. Paul Handler

ONR / NAVY/ NSWCCD
{Name}
{Name}
{Name}
{Name}

TRANSPORT CANADA
Paul Denis Vallee

US COAST GUARD

CDR Charles Rawson
Mr. James Person
Mr. Rubin Sheinberg

SOCIETY OF NAVAL ARCHITECTS AND MARINE ENGINEERS
Mr. Jaideep Sirkar
Mr. Al Rowen
Mr. Norman Hammer

Member Agencies:

American Bureau of Shipping
Defence Research Development Canada
Maritime Administration
Military Sealift Command
Naval Sea Systems Command
Society of Naval Architects & Marine Engineers
Transport Canada
United States Coast Guard

Ship
Structure
Committee

Address Correspondence to:

Executive Director
Ship Structure Committee
U.S. Coast Guard (CG-5212/SSC)
2100 2nd Street, SW
Washington, D.C. 20593-0001
Web site: http://www.shipstructure.org

SSC – 449
SR – 1441

OCTOBER 3, 2008

HYDRODYNAMIC PRESSURES AND IMPACT LOADS FOR HIGH SPEED CATAMARAN/SES

The objective of this research was to develop design guidelines for maximum pressure and impact loads on catamaran and catamaran/Surface Effect Ship (SES) hull forms intended for very high speeds; i.e. 50 to 104 knots. Previous guidelines, promulgated by the various Classification Societies produced significantly different values of hydrodynamic and impact pressure loads at service speeds above 50 knots. The guidelines proposed in this paper provide more accurate load values and reduce the corresponding variations in scantling requirements, particularly for hulls with sandwich-skin composite construction.

The report represents the results of two dependant projects. In the first project, zero gravity planing theory was used to calculate motions and load distributions on a generic Air-Enhanced Vessel (AEV) and also on a generic SES. At the conclusion of that effort it was realized that while the Froude numbers for the vessels of interest were quite high, it was probably not high enough to justify the assumption of zero gravity. The second report extended the code to non-zero gravity hydrodynamics, reevaluated some of the calculations, and validated the predictive capability of the extended CatSeaAir code.

The two projects are combined in this report with separate conclusions and references:

(A) Zero Gravity Hydrodynamics
(B) Non-Zero Gravity Hydrodynamics, Structural Loading, and Experimental Data Comparisons

BRIAN M. SALERNO
Rear Admiral, U.S. Coast Guard
Chairman, Ship Structure Committee

Technical Report Documentation Page

1. Report No. **SSC - 449**	2. Government Accession No.	3. Recipient's Catalog No.	
4. Title and Subtitle Hydrodynamic Pressures and Impact Loads for High Speed Catamaran / SES Hull Forms		5. Report Date **February 1, 2007** 6. Performing Organization Code	
7. Author(s) W. Vorus		8. Performing Organization Report No. SR-1441	
9. Performing Organization Name and Address Vorus & Associates Incorporated 2726 St. Charles Avenue New Orleans, LA 70130		10. Work Unit No. (TRAIS) 11. Contract or Grant No.	
12. Sponsoring Agency Name and Address Ship Structure Committee C/O Commandant (CG-3PSE/SSC) United States Coast Guard 2100 Second Street, SW Washington, DC 20593-0001		13. Type of Report Final Report 14. Sponsoring Agency Code CG- 5	
15. Supplementary Notes Sponsored by the Ship Structure Committee and its member agencies			

16. Abstract

The criteria most widely available to the design community for determining design pressures are embodied in Guidelines and Rules promulgated by various Classification Societies. When applied to fast catamaran or catamaran/SES hull design, with service speeds of 50 to 60 knots or higher, formulas published by ABS, DnV, and Lloyd's Register (for example) may produce significantly different values of design and impact pressure loads. This produces a corresponding variation in scantling requirements, particularly for hulls with sandwich-skin composite construction.

17. Key Words	18. Distribution Statement Distribution Available From: National Technical Information Service U.S. Department of Commerce Springfield, VA 22151 Ph. (703) 605-6000		
19. Security Classif. (of this report)	20. Security Classif. (of this page)	21. No. of Pages	22. Price

CONVERSION FACTORS
(Approximate conversions to metric measures)

To convert from	to	Function	Value
LENGTH			
inches	meters	divide	39.3701
inches	millimeters	multiply by	25.4000
feet	meters	divide by	3.2808
VOLUME			
cubic feet	cubic meters	divide by	35.3149
cubic inches	cubic meters	divide by	61,024
SECTION MODULUS			
$inches^2$ $feet^2$	$centimeters^2$ $meters^2$	multiply by	1.9665
$inches^2$ $feet^2$	$centimeters^3$	multiply by	196.6448
$inches^4$	$centimeters^3$	multiply by	16.3871
MOMENT OF INERTIA			
$inches^2$ $feet^2$	$centimeters^2$ meters	divide by	1.6684
$inches^2$ $feet^2$	$centimeters^4$	multiply by	5993.73
$inches^4$	$centimeters^4$	multiply by	41.623
FORCE OR MASS			
long tons	tonne	multiply by	1.0160
long tons	kilograms	multiply by	1016.047
pounds	tonnes	divide by	2204.62
pounds	kilograms	divide by	2.2046
pounds	Newtons	multiply by	4.4482
PRESSURE OR STRESS			
$pounds/inch^2$	$Newtons/meter^2$ (Pascals)	multiply by	6894.757
kilo $pounds/inch^2$	mega $Newtons/meter^2$ (mega Pascals)	multiply by	6.8947
BENDING OR TORQUE			
foot tons	meter tons	divide by	3.2291
foot pounds	kilogram meters	divide by	7.23285
foot pounds	Newton meters	multiply by	1.35582
ENERGY			
foot pounds	Joules	multiply by	1.355826
STRESS INTENSITY			
kilo $pound/inch^2$ $inch^{½}$($ksi\sqrt{in}$)	mega Newton $MNm^{3/2}$	multiply by	1.0998
J-INTEGRAL			
kilo pound/inch	$Joules/mm^2$	multiply by	0.1753
kilo pound/inch	kilo $Joules/m^2$	multiply by	175.3

Table of Contents *page*

Part A - 2005

Preface

The Ship Structures Committee project SR1441 was conducted over two years (2005 and 2006) and separate reports were written covering the work completed in both years. At the end of the second year the sponsor (SSC) requested that the two reports be combined to report the 2-year effort in one document.

Zero gravity planing theory was used in the first year to calculate motions and load distributions on a generic" Air-Enhanced" Vessel (AEV) and also on a generic SES. At the conclusion of that effort it was realized that while Froude number for the vessels of interest here is quite high (in excess of 1.), it is probably not high enough to justify the assumption of zero gravity in the hydrodynamics.

A new proposal was submitted to SSC for extending the code to non-zero gravity hydrodynamics, redoing some of the calculations, and attempting to validate the predictive capability of the extended CatSeaAir code. That second proposal was funded for 2006.

The overall report, which is this document, represents essentially the combined reports of the two years, with only one Table of Contents. The report segments combined are referred to as Parts A and B, respectively. Each report part contains the conclusions and references of that part. Analysis results and conclusions of Part A are considered to remain relevant and valid are not repeated in Part B, but linkage is provided in Part B in the interest of continuity. Part A remains as a valid part of the overall presentation and deserves first review.

Hydrodynamic Pressures and Impact Loads for High Speed Catamaran/SES Hull Forms

Ship Structures Committee Project SR 1441

Report Part A – 2005
Zero Gravity Hydrodynamics

I. Introduction

The criteria most widely available to the design community for determining hydrodynamic forces and hull surface pressure for use in vessel design are embodied in Guidelines and Rules promulgated by the various Classification Societies. When applied to fast multi-hull designs, with service speeds of 50 to 60 knots or higher, formulas published by ABS, DnV, and Lloyd's Register (for example) may produce significantly different values of design and impact pressure loads. This produces a corresponding variation in scantling requirements, particularly for hulls with sandwich-skin composite construction.

It has been recognized as a worthwhile service to the design community for the Ship Structure Committee (SSC) to sponsor a comprehensive evaluation of high-speed catamaran and catamaran/SES design pressure and impact load criteria. Ideally, this evaluation should be based on an analytical/numerical model, developed from first principles, and validated by comparison with full-scale test data for the hull forms of interest.

This work began in 2005.

II. Approach

At that time validation data for the subject analysis had not been uncovered. The approach taken was therefore to apply the codes developed to concept hydrodynamic design of one of each of the two basic types of interest: 1) the *active* air supported surface effect craft (SES), and 2) the *passive* air "enhanced" vessel (AEV), e.g., Stolkraft.

IIa. SES

An SES is basically a catamaran with skirt seals across the demi-hull openings forward and aft. See Figure 1 below. Lift fans are installed to pressurize the internal space between the demi-hulls to provide the required lift with reduced wetted hull surface area, and therefore reduced drag.

While reducing the hydrodynamic drag and associated power requirement, the total required power includes the lift-fan power. Nevertheless, the lift fans, operating under automatic control for adjustment to variable air leakage rate, are found to result in efficient operations when supporting up to 75-80% of the craft weight. The SES may be the best system for high-speed craft from considerations of both minimum resistance and minimum seaway dynamic response.

Figure 1: SKJOLD Class Norwegian SES Fast Patrol Boat

IIb. AEV

The air lubricated, or air-enhanced, vessel attempts to accomplish some of the function of the SES, but with natural ram air rather than lift fans. The most common form of the AEV is basically that of a trimaran with the center hull truncated at some relatively short distance behind the bow. The Australian Stolkraft AEV can be viewed at www.artanderson.com/stolkraft. A unique feature of the Stolkraft hull is the blunt truncation of the center-hull, opening abruptly into an air plenum formed by the space bounded by the demi-hull walls and the wet-deck overhead. This is shown in some detail on the lines and construction drawings of the bottom shape shown on the web pages cited above.

The explanation of the function of the bottom configuration provided by Stolkraft International of Queensland Australia is as follows:

"The air flow, generated by forward motion of the vessel, is ducted through two symmetrical scoops formed by the tri-hulled forebody. A vacuum caused by an amidships step combined with complex flow phenomena behind the three hulls, creates a cushion of air in the aft body recess between the two outer hulls, significantly reducing frictional resistance and subduing hull generated wake/wash."

This explanation is vague in several respects. While the air-flow between the two outer hulls produces a catamaran-type behavior aft of the step, it is not possible that the air pressure between the demi-hulls could be higher than the total head of the oncoming air stream. The static pressure corresponding to the full dynamic head of the 50 knot vessel is fully an order of magnitude lower than the internal pressure developed by the typical SES lift fan system, and therefore not capable of significant lift enhancement. This apparent conflict is explored further in the analysis section.

III. Assumptions and Approximations of the Analysis

The focus of the modeling is the hydrodynamics, versus the aerodynamics, but the aerodynamic approximations are rational and considered to lead to reliable conclusions regarding calm water and seaway performance of the two craft design types analyzed.

IIIa. Aerodynamics

1. The pressure of the internal air space is assumed to be incompressible. This is justified in view of the relatively low pressure developed.
2. The air pressure is assumed to be uniform in the plenum[1] and cushion space. This is considered consistent with the relatively low time scales of the calm water and seaway motions processes.
3. In the case of the SES, the pressure is taken as that required to support a specified fraction of the total vessel weight; the weight supported is the air (gauge)

pressure times the effective area of the wet-deck above the cushion. Thus, the effective weight of the craft is reduced by the air (but not it's mass). This approach simulates the function of the air control system in the SES. As it is understood, the control system adjusts the air flow to make-up for leakage losses while maintaining constant mean cushion pressure.

4. For the AEV, the uniform cushion pressure is taken as the static pressure corresponding to the dynamic head of the stream, i.e., craft speed, which is assumed constant. This assumes that a total conversion of the dynamic head occurs at the entry across the internal step; refer to Figure 3. This assumes, to large degree, that the cushion cross-sectional area is so much larger than the cross-section of the inlet passages that the inlet velocity drops immediately to zero on entry (Figure 3a). to recover the full dynamic head as a cushion pressure.

This is an upper bound assumption, and will produce an overestimate of the lift due to air pressure acting on the plenum ceiling. In neglecting pressure loss across the step, it also produces an underestimate of drag. Here the ceiling of the plenum, or cushion, is the wet deck area aft of the entry step. (This is the case provided the waterline length from the transom to entry is greater than the length from the transom to the step. Otherwise the plenum pressure does not develop due to leakage. This condition for non-zero plenum pressure has been assured for the design calm water case. It is not always achieved (at all times) in the seaway operations.

IIIb. Hydrodynamics

The hydrodynamic model that couples with the aerodynamics defined in the preceding is much better developed. It is based largely on the Vorus (1996). This work built upon a long history of work by many in planning/impact research.

The basic assumptions, approximations, and general capabilities of the hydrodynamics are as follows:

1) The water is incompressible, which is a clearly valid assumption.
2) The speed is high enough that gravity effects can be taken as higher order to convection in the hydrodynamic pressure. The approximation of zero gravity in the first order limit has been standard assumption for application of this general approach to small craft where the Froude numbers are very high ($U/\sqrt{gL}$ >2). This is clearly a limitation for larger high speed ships (with lower Froude number) which are of clear interest here. It is addressed in Part B of this report, as defined in the *preface*.
3) The dynamic model is 3 degree-of-freedom (heave-pitch-surge).

---

1 – here, air plenum and air cushion are used interchangeably, although they are often distinguished in SES terninology, the plenum being the air entry region out of the fans and into the cushion.

4) The analysis is in the time domain, stepped forward in time from the initial condition.
5) The analysis is three-dimensional, but assumes that variations axially (in x) are small, such that the solution is from entry downstream over the wetted hull length at every time step (non-linear slender body theory).
6) Irregular seaway analysis is included as a Jonswap spectrum inverted into the time domain.
7) At every time step a boundary value problem is solved with both kinematic and dynamic (pressure) boundary conditions satisfied on all wetted contours; the solutions are semi-analytic, so that the only iterations of carefully developed non-linear algebraic equations are required.
8) The geometry is general, only requiring that the hull flatness, in some sense, be observed. Slender body theory is the theoretical basis of the methodology.
9) Viscous drag is approximated by the empirical ITTC friction line in the traditional way. Pressure drag, computed directly from first principles, is composed of induced, spray, and transom hydrodynamic drag components. Additionally for SES, air momentum and seal drag exists, but are not included in the Part A work.
10) Contour pressure and resultant loads, along with surface accelerations, velocities, and displacements, are produced as functions of both space and time.

IV. Computer Codes

The base computer codes employed by the project, which implement the general hydrodynamics outlined above, existed originally in the VAI EDITH system. EDITH (Engineering Development in Theoretical Hydrodynamics) is a proprietary computer system dedicated to the application of sound hydrodynamics to relevant engineering challenges in marine hydrodynamics. With regard to the SR1441 project the relevant EDITH codes are:

EDITH 1 – VsSea (for high speed planing monohulls)
EDITH 2 – CatSea (for high speed planning catamarans)

A third base code was considered for application in this project:

EDITH 2a – VnvSea

VnvSea is for analysis of an inverse-V catamaran with lines employing the concept of the Hickman Sea Sled. This program was not utilized in the interest of consistency of the comparisons, but would be available for future extension of the work.

The new code series assembled for the SES/AEV analysis is EDITH 1-2 , or CatSeaAir.

IVa. Code Adaptations - Linkages

The truncated trimaran-type hull (Fig 3) was produced by dynamically linking VsSea and CatSea using the FORTRAN DLL software. The two codes are linked, in tact, as super-subroutines through a main program written specifically to handle the interfacing. That new system of three coupled codes constitutes the AEV component of CatSeaAir.

Actually this three component assembly applies to the SES as well, where the center monohull is simply deleted.

IVb. Code Adaptations - Air Effects

The effect of the pressurized air, as discussed in IVa above, was added in the CatSea component in two places to produce the 2005 version of CatSeaAir:

a. The uniform air pressure of the magnitudes stated in IIIa was imposed on the active length of the wet deck between the demi-hulls.

b. The second air involvement is less direct and more complex: Spray jets, modeled as vortex sheets, are shed both inward and outward from the instantaneous water separation points of the hull segments. The strengths of these sheets are determined such that the pressure along the free sheets is the local ambient pressure. The catamaran plenum in both hull types is at a local ambient pressure above atmospheric, and this modifies the dynamic boundary condition controlling the rate of sheet growth away from the demi-hull on both sides. The rate of shedding is increased by the higher ambient pressure, which in turn changes the trajectory of the sheet so that the hydrodynamic pressure on the demi-hull bottoms is increased, thereby increasing vessel lift. This is demonstrated in the Analysis section.

V. Designs Developed

The designs analyzed were developed arbitrarily, as were the speed and sea conditions applied. The purpose was to demonstrate the application of the codes primarily, as discussed in the Introduction.

It is considered helpful to provide some key geometric definitions before proceeding with the delineations. With the aid of the sketches, Figure 2:

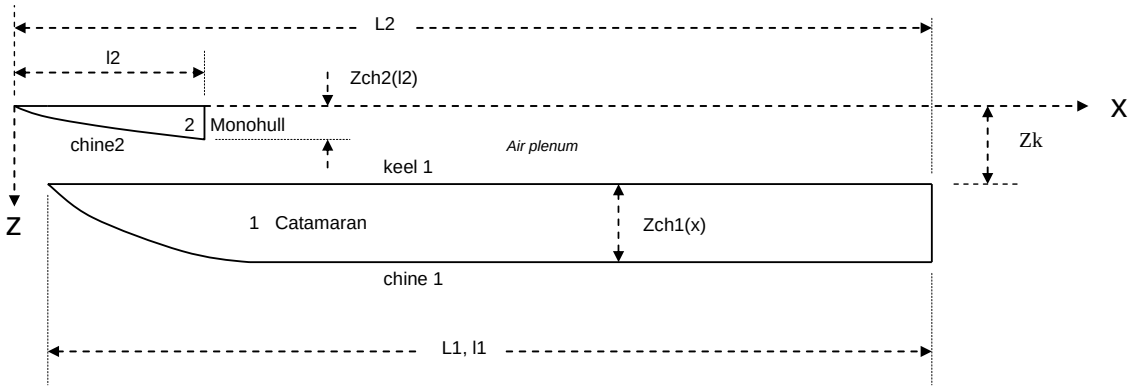

Figure 2a Half-Breadth Plan (AVL)

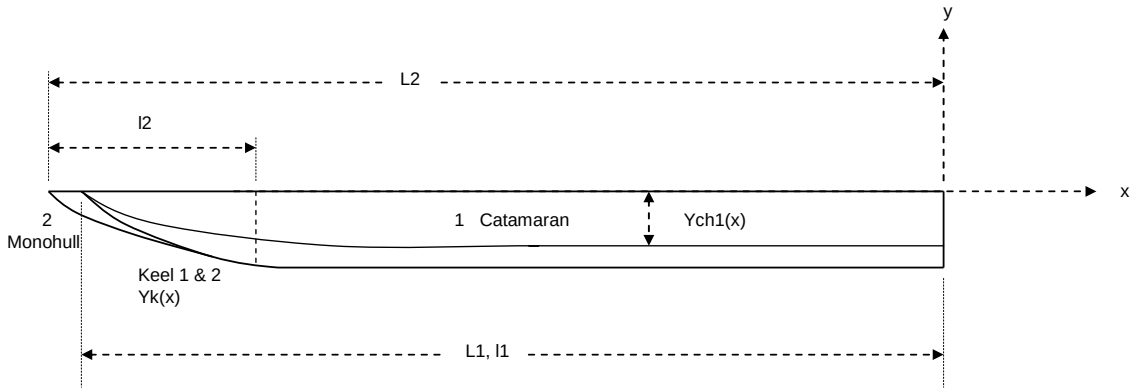

Figure 2b Profile

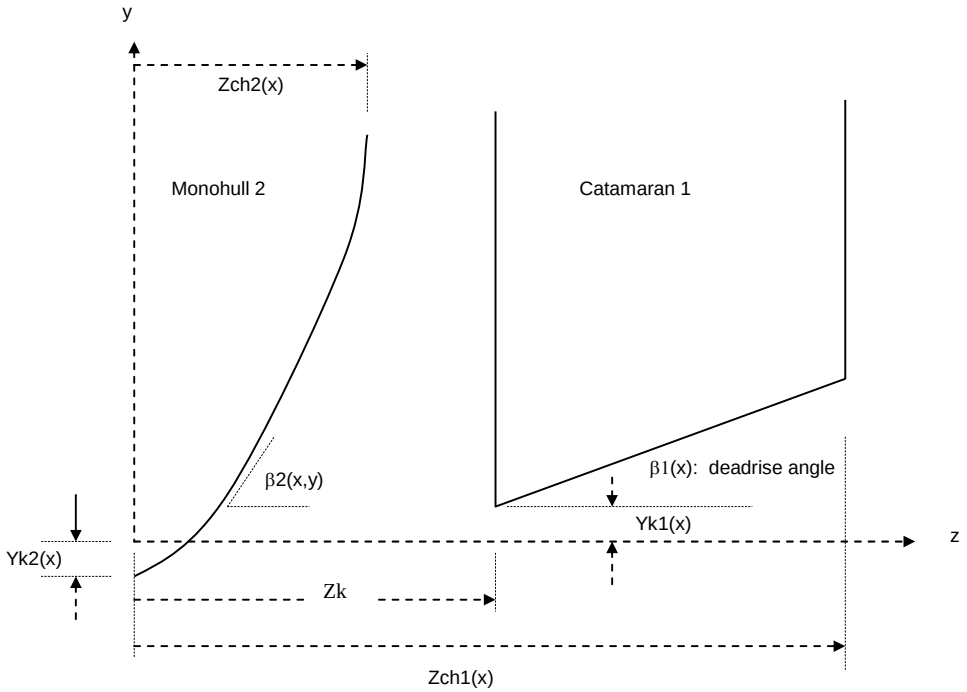

Figure 2c Body Plan at Section x

Figure 2 covers both designs analyzed. The SES design consists of the catamaran elements of Figure 2. The short monohull segment forward is added to the same catamaran data to model the AEV in this demonstration.

Va. Geometric Definitions

1) Catamaran keel offset, Zk (Figure 2c). Zk is taken as constant in x, and serves as the length by which all linear dimensions are made dimensionless. The monohull keel offset is zero by definition.
2) Overall hull lengths, l1 and l2, from segment transoms to stems. The corresponding *wetted* lengths (XMAX) are time dependent and of reduced value.

3) L1 and L2 are the lengths from the catamaran transom to the stems (forward extremity) of the respective segments; XENTRY1 and XENTRY2 are the corresponding time varying wetted values.
4) Most of the remaining geometry are arbitrary functions of the axial coordinate x or x and y and are fit (segmentally) with continuous polynomials.
5) Yk(x) is the keel upset from the baseline and Zch(x) is the chine offset from the centerline.
6) β(x) is the distribution of deadrise angle, Fig 2c. Transverse camber can be included in the analysis, in which case the deadrise angle is β(x,y).

Other definitions associated with the flow variables will be provided in the Analysis section.

The flowing table, Table 1, gives the principal dimensional characteristics selected. All dimensions are in meters (feet).

Table 1
Dimensions of Example Designs[1] (m)

	SES	AEV (monohull seg)
L	10.0 (32.8 ft)	10.29 (33.75)
l	10.0 (32.8)	3.43(11.25)
Yk(0)	.610(2.00)	.610 (2.00)
Yk(l)	0.	-.0686 (-.225)
Zk	.686 (2.25)	0.
Zch(0)	.686 (2.25)	0.
Zch(l)	1.37 (4.50 ft)	.610(2.00)
β(0,0)	90 deg	90
β(0,Ych(0))	90	90
β(l,0)[2,3]	12	14
β(l,Ych(l)[4])	12	50

1 - The distributions of the variables are plotted in the analysis section to follow.
2 – The deadrise angle of the SES catamaran sections is constant transversely but decreases in x
3 – The deadrise angle of the AEV short center section also decreases with x but is transversely cambered.
4 – The vertical upset to the chine is established by the intersection of the chine offset, Zch(x), and the contour rising from the keel.

Other input data related to vessel characteristics is listed in Table 2.

Table 2
Performance Characteristics of Example Designs

	SES	AEV (complete)
Vessel weight, W	(6.25 t, 15K lbs)	(6.25 t, 15K lbs)
Design speed, U (assumed constant)	50 knots	50 knots
Xcg/Zk (fwd of cat transom)	6.56[1]	6.56
GyRad/Zk (about cat transom)	7.60[2]	7.60
Ycg/Zk (above baseline)	1.20	1.20

1 - The center of gravity is placed rather far forward (45% of length from the transom) to achieve low trim over the speed range and avoid large trim changes with increasing speed in calm water; the center of lift due to the air pressure will be near mid-length at all speeds.
2 – The radius of gyration was taken as ¼ boat length about the CG, transferred to the transom.

As seen from Tables 1 and 2, the SES and the AEV designs are identical except for the added center monohull segment in the AEV configuration. The analysis to follow will therefore reflect the effect the hydrodynamic effects of the AEV monohull relative to the benefits of the maximum assumed cushion pressure naturally achieved (Section 2a).

VI. Analysis Procedure

The following are the procedural steps in the execution of the CatSeaAir system.

VIa. Calm Water Equilibrium

It is necessary to first establish calm-water equilibrium:

1. An estimate of the equilibrium trim and transom draft is entered in the input data file.
2. The time step is set at a large value relative to the small time scales required in the seaway calculations.
3. The calculation is commenced from zero time forward. In the first step the non-equilibrium trim and draft produces a flow, which produces pressures and integrated forces and moments.
4. Newton's law is then applied with the forces and moments to produce accelerations in the three degrees of freedom.
5. The accelerations are integrated as the time steps proceed to a continuously evolving updating of trim and draft displacements and surge velocity.
6. The new displacements produce new forces, which produce new accelerations by Newton's Law, updated displacements, and so forth …
7. This process produces reducing force and moment changes with time as the craft settles into an attitude such that the hydrodynamic load approaches the craft weight and the center of load converges to the axial position of the center of gravity. The ensuing accelerations converge toward zero with time as this equilibrium is approached.

8. When the accelerations have reached a state close enough to zero, the trim and draft are changing to even a smaller degree and calm-water equilibrium is considered as achieved.
9. The pressures and forces at equilibrium are available for powering and strength analysis as desired by the user.

VIb. Seaway Response

All of the same steps are executed in the seaway dynamics case:

1. The vessel is set with the determined calm water equilibrium trim and draft and time is restarted at zero.
2. The sea spectrum level is specified in the input, as a significant wave height and center band frequency for the Jonswap spectrum option; the significant wave height alone is input for the Pierson-Moskowitz option incorporated in 2006 in Part B. The spectrum is inverted in CatSeaAir by wave component superposition with randomized phase to calculate a wave height distribution in x at any time.
3. The sea wave distributions are ramped-up as a decaying exponential to the stationary level selected to avoid unrealistic starting gradients.
4. The sequential steps are then identical to 3. through 9. of the calm water case; a time dependent motion and load response to the seaway is thereby achieved.
5. Statistical quantities, such as RMS acceleration, are readily extracted as desired.

Sample Input/Output is contained in the Appendix following Part B of the report.

VII. Analysis

Calm water and seaway analysis of the two craft designed (Figure 4 and Tables 1 and 2) is now conducted by the above procedures.

VIIa. Calm Water Equilibrium

A. SES

As stated in Section IIIa., the SES is assumed to regulate the fan air flow so that constant pressure is maintained in the cushion. For the analysis the uniform cushion pressure has been set at four levels corresponding to support of the four fractions of the craft weight: 0, .25, .50, .75.

A1. Catamaran at zero air support

The analysis of the catamaran hull (Figure 4) at zero internal air pressure establishes a basis of evaluation of the air supported SES and AEV cases. Table 3 provides a summary of the equilibrium running geometry calculated for this base case.

Table 3

Base SES Case: Catamaran Running Geometry at Zero Cushion Pressure

Wetted Length/Total Length, Xmax/L	.715
Chine wetting point from transom/L	1. (chine unwetted)[1]
Trim angle, deg	.290
Transom draft, Ht/Zk	.148

1 - chine is unwetted when the jet-head has not progressed outward to the chine at the transom; chine-wetted otherwise.

The very low trim angle listed on Table 3 is due to location of the center of gravity forward to avoid large trim changes and air pressure variation, as discussed at Table 2. Low trim is a characteristic of the SES craft, as well as the AEV(see Figs 1 and 2). The transom draft, Ht, listed on Table 3 is the depth of the keel below the undisturbed water surface at the transom, which represents the second of the three degrees of freedom.

Figure 3 is the distribution of deadrise angle in XI at the equilibrium running condition of Table 3. The red portion of the curve is the unwetted region and the green is the wetted region aft of entry. XI is distance downstream from entry dimensionless on the keel offset Zk (refer to Section Va and Tables 1 and 2)

Decreasing deadrise angle increases local hydrodynamic hull surface pressure. The flat angle aft shown on Figure 5 limits the loading aft and helps to place the hydrodynamic load to match the forward-shifted position of the center of gravity; this is one of the equilibrium requirements. The other is that the total lift (hydrodynamic and hydrostatic) for the catamaran equal the craft weight, as discussed above.

A similar plot as Figure 3 for the keel upset distribution is Figure 4.

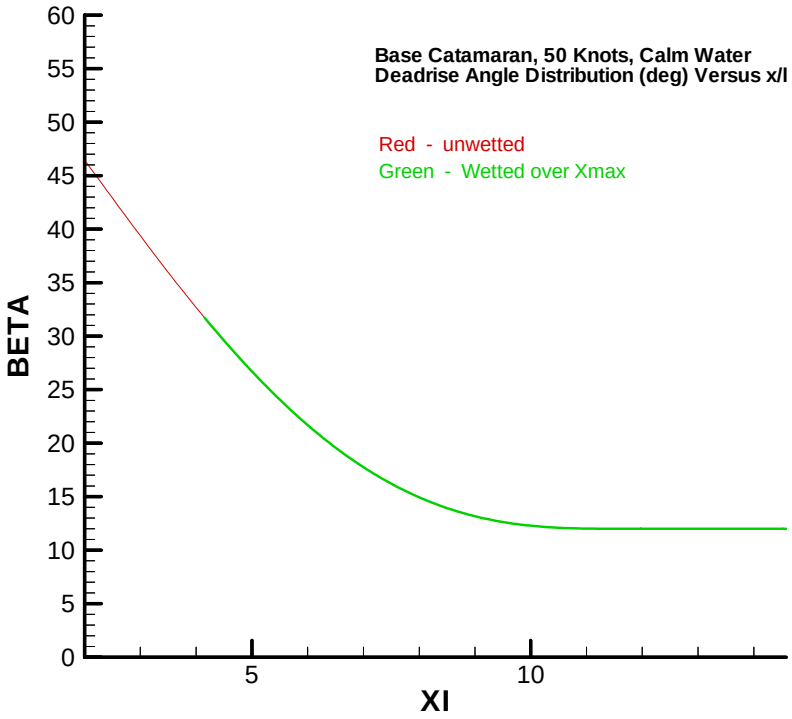

Figure 3 - Base Catamaran- Deadrise Angle Over Wetted Length

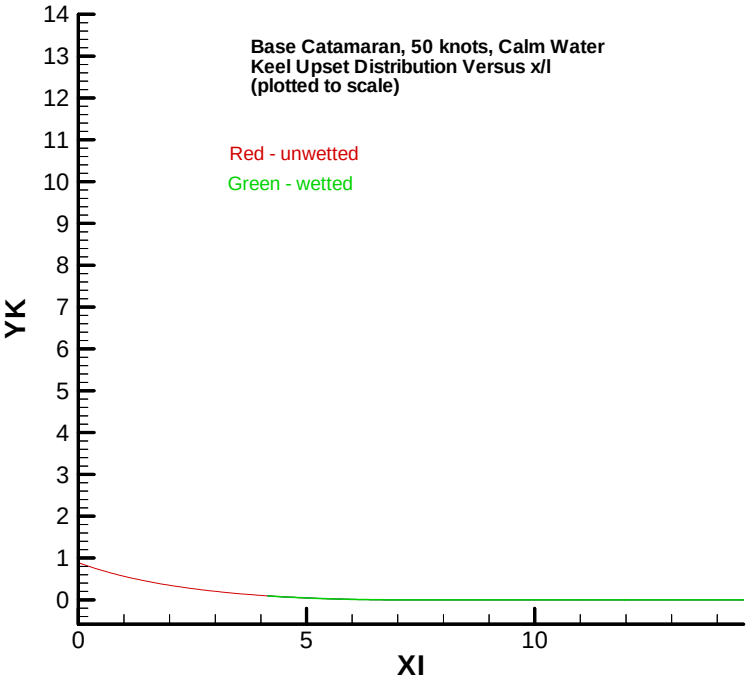

Figure 4 – Keel Upset Distribution Over Wetted Length

Figure 5 is a running half-breadth plan plotted from entry over X_{max}. The jet heads are the points where the spray jets separate from the main flow, Vorus (1996).

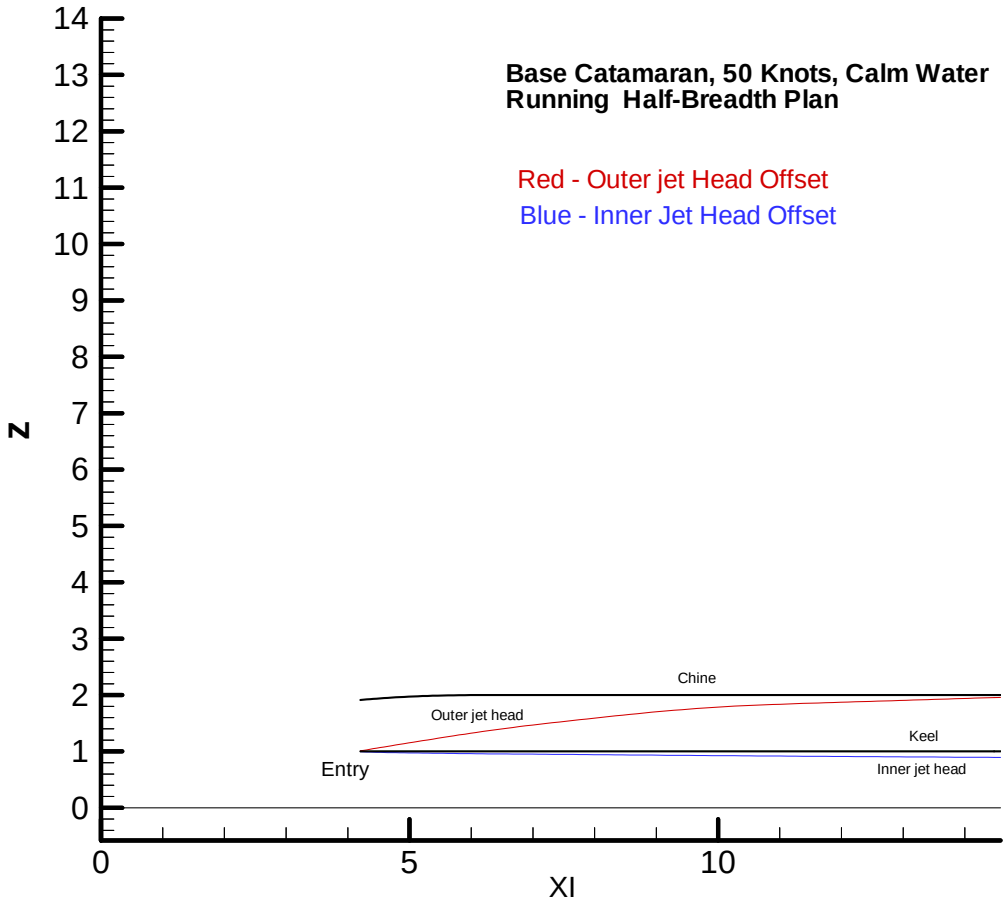

Figure 5 - Running Half-Breadth Plan Plotted (to scale) Over Wetted Length

The inner jet head shown on Figure 5 separates along the keel (Figure 3) and traverses inward as the leading edge of a free vortex sheet across the free surface between the demi-hulls. The trajectory of the inner jet-head is particularly important in the affects of internal air pressure on SES/AEV performance, as will be shown; refer to the discussion at IVbii). The outer jet-head on Figure 5 is in one way fundamentally different than the inner. It leads an attached vortex sheet, rather than a free sheet, up the deadrise, until it separates at the chine, or reaches the transom. In this case, due to the high speed, the outer jet-head has not quite reached the chine at the transom, as indicated on Figure 5. This is referred to as a chine-unwetted flow, versus the chine-wetted type where the jet head emerges from under the chine forward of the transom. CatSeaAir allows either mode to develop as the solution progresses downstream. The chine-unwetted flow is beneficial to achieving high lift-drag ratio, as lift drops to a lower level where chine-wetting occurs, and aft.

Figure 6 is a right-side plot of the wetted body plan at the Figure 5 running condition.

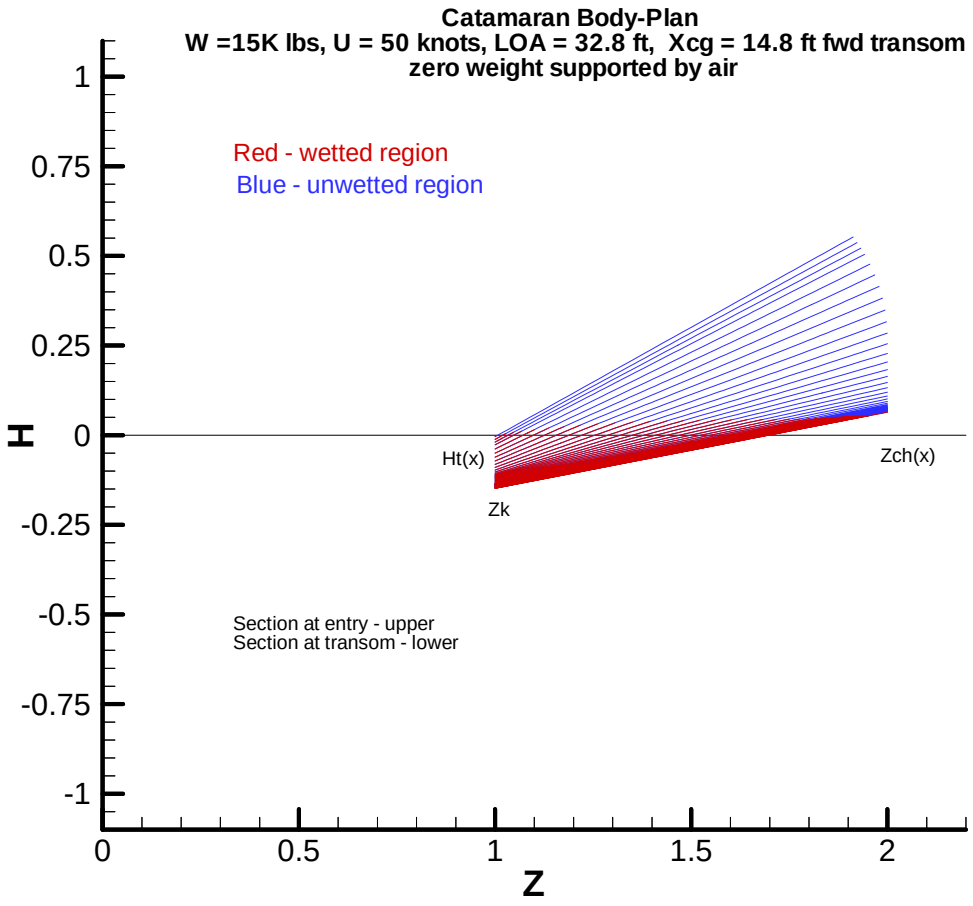

Figure 6 – Wetted Body Plan at Equilibrium

Figure 6 is an overlay of the cross-sections at 52 values of x from entry to the transom. Only those sections with some wetting are plotted. The wetting above the free surface at H = 0 is the jet-rise. Note that the transom section is at impending chine wetting, consistent with Figure 5. The chine is the outer extremity of the sections. The decreasing deadrise angle forward is clearly evident on Figure 6, and the close spacing of the section contours is evidence of the low trim angle of .29 degrees, Table 3.

Figure 7 plots the lift distribution over the vessel wetted length. Both the dynamic and the hydrostatic lift are included here in the single curve.

The normal force coefficient is defined, with consistent non-dimensionalization, as:

$$C_f(x) = \frac{f(x)}{\frac{1}{2}\rho U^2 Z_k}$$

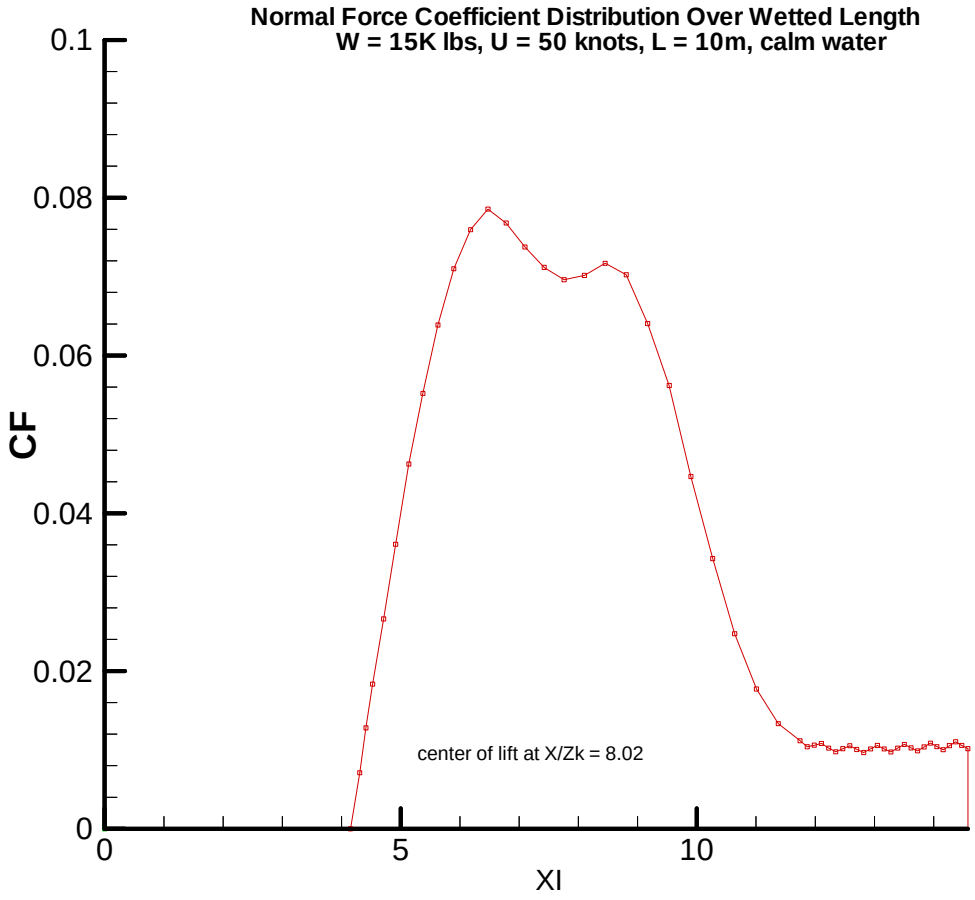

Figure 7 – Normal Force (Lift) Coefficient Distribution over Wetted Length

Figure 7 clearly shows the effects of the transition to constant deadrise angle on the lift distribution (Figure 3). This was in the interest in a forward shifted center of lift, which can be observed on Figure 7 to have been achieved. The oscillation exhibited in the constant deadrise region is due to the steep gradient in deadrise angle, β, just ahead. It is a numerical artifact, not physical, and is found to be inconsequential.

The lift/drag ratio predicted for the zero pressure case is a very respectable 9.04. This is somewhat remarkable in consideration that the very low trim angle is accompanied by a long waterline, which tends to produce large wetted surface area, and high viscous drag. But the pressure drag is low at the small trim angle. The main benefit of a low trim angle is usually found to be reduced pounding in sea waves. For conventional cases, a drag minimum is usually found to occur with a trim angle around 2 degrees. But with the high speed (Froude number), this is not a conventional case. The fact that this long waterline hull is predicted to run chine-unwetted is believed to be largely responsible for the high lift/drag ratio. However, it must be considered here that potentially significant components of both lift and drag are missing in this first analysis; these are components due to gravity waves. This is addressed specifically in Part B of this report and elaborated there.

It should be emphasized that lift/drag ratio is the measure of merit of calm water performance. For lift at equilibrium equal to the fixed craft weight, W:
Drag, D = W/(Cl/Cd) and EHP = DU. Therefore, maximization of Cl/Cd results in requirement of minimum power.

A2. SES with Air Support

The effects of plenum air pressure are discussed at IVb. Fig 8 plots variations of trim, draft, lift/drag, and plenum pressure for the fraction of weight supported by the air cushion. It must be kept in mind that the total lift = W = 15K lbs, such that the rising lift drag ratio represents a decrease in vessel drag, as argued in the above. The decrease in drag is due primarily to the decreasing draft at approximately constant trim, which results in a decrease in wetted surface and projected wetted surface.

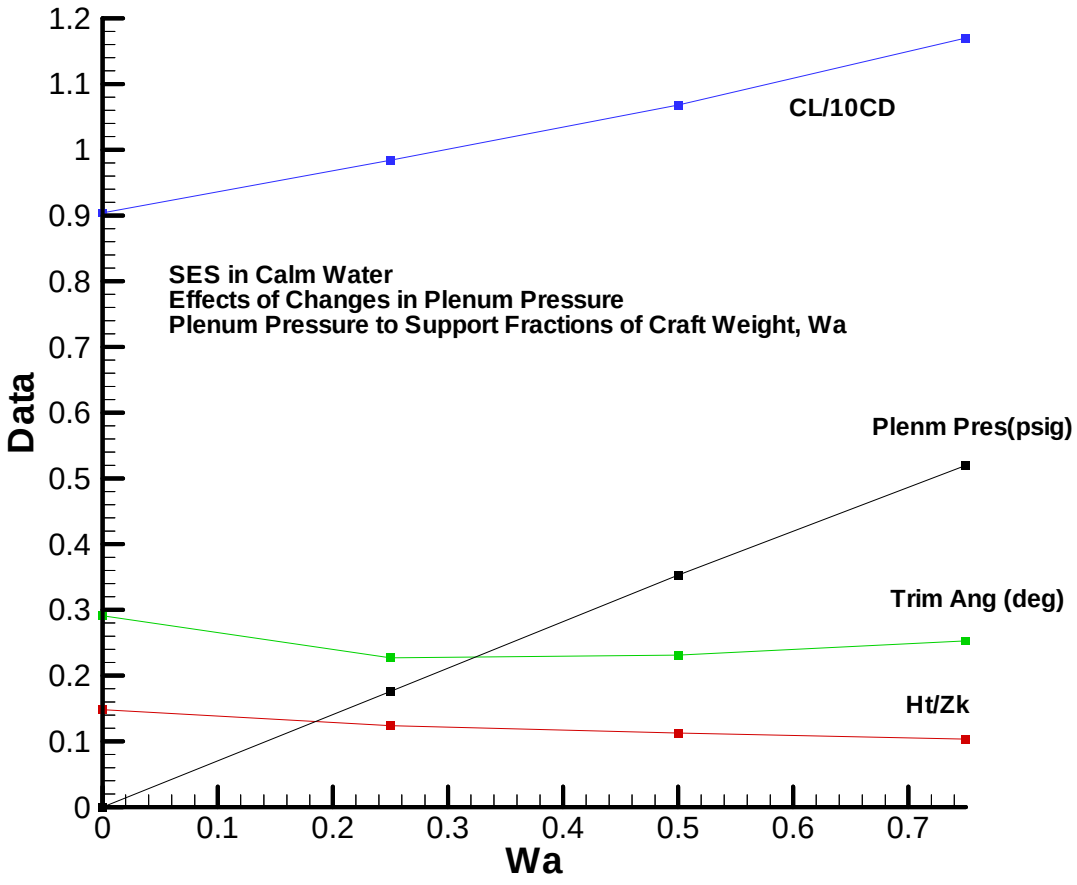

Figure 8 – SES Calm Water Performance versus Fraction of Weight Supported by Air

Note that the transom draft reduction is strongest at the lower weight fractions, flattening at higher Wa. This is the second effect of the air discussed at IVb. This is illucidated by

Fig 9. Fig 9 is the same half-breadth plan plot as Fig 5, but with all four of the jet-head trajectories plotted. The Figure 8 data is listed on the face of Figure 9.

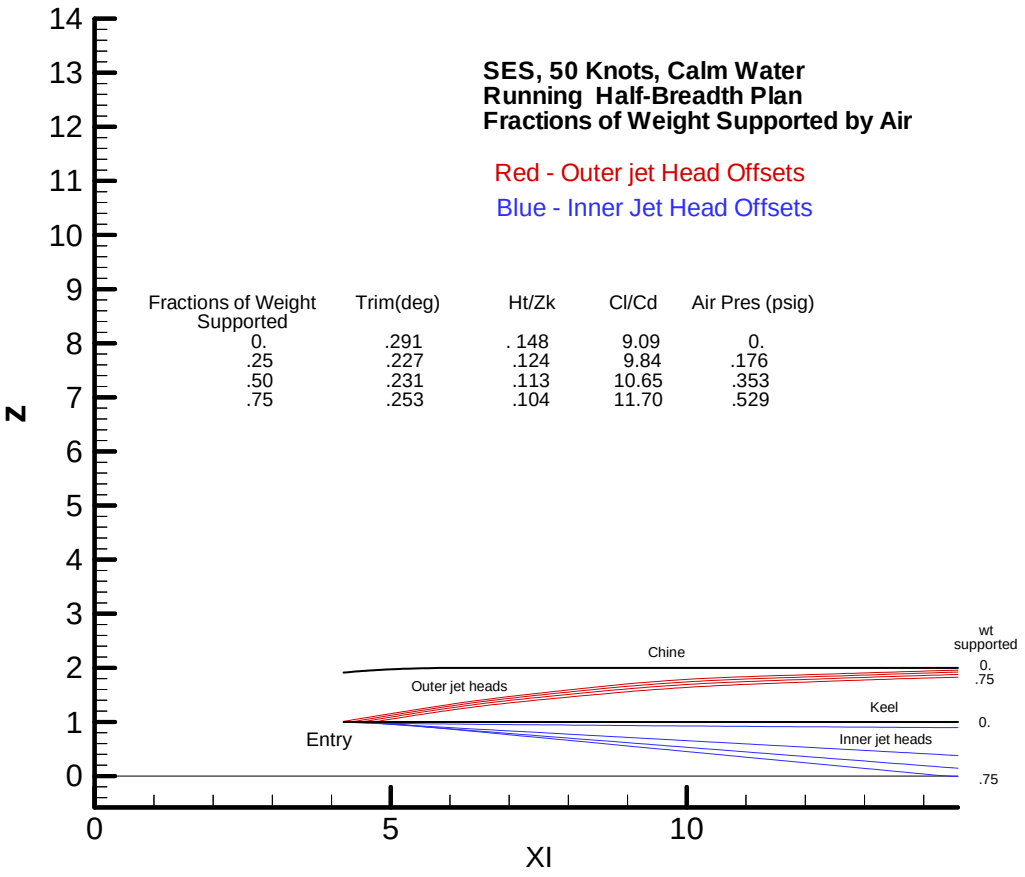

Figure 9 – Plan Plot of Jet-Head Trajectories Over Wetted Length with Variations in Fraction of Craft Weight Supported by Air

The origin of the jet-heads at the stem moves aft with increasing cushion pressure. This is because the waterline is shortening with the decreasing draft (Figure 8).

As noted in IVb, the closer the inner jet-heads to the demi-hull wall the higher the hydrodynamic downwash and the lower the hydrodynamic pressure on the demi-hull bottom. The spread away from the wall increases the hydrodynamic bottom pressure and decreases hydrostatic bottom pressure in reducing the draft to achieve the fixed lift equal to weight. This reduction in draft also reduces the drag, thus the higher lift/drag ratio.

This is believed to be new knowledge exposed by this first-principles analysis. But it is equivalent to the lift reductions and increases from hydrodynamic downwash familiar in lifting foil theory. Note from Fig 9 that the largest percentage effect is produced by the lower plenum pressure. That is, a 75% weight reduction by air pressure results in a 30% reduction in transom draft, while a 25% weight reduction by air results in a 17%

reduction in Ht/Zk. The largest jet-head spread rate is at the lower plenum pressure. This maximum rate of spreading at small plenum pressure is the reason why the AEV has measurably reduced wetted surface and increased lift/drag ratio with the small cushion pressure available from the stream dynamic head.

B. AEV

B1. AEV at Zero Air Support

Recall that the AEV catamaran hull component is the same as the SES. All else is the same as well except for the addition of the monohull center section to produce the truncated tri-hull, configured to funnel the stream air internally to achieve an elevated hull lifting pressure.

Figure 10 is the wetted half-body plan of the AEV, the equivalent of Figure 6 for the catamaran.

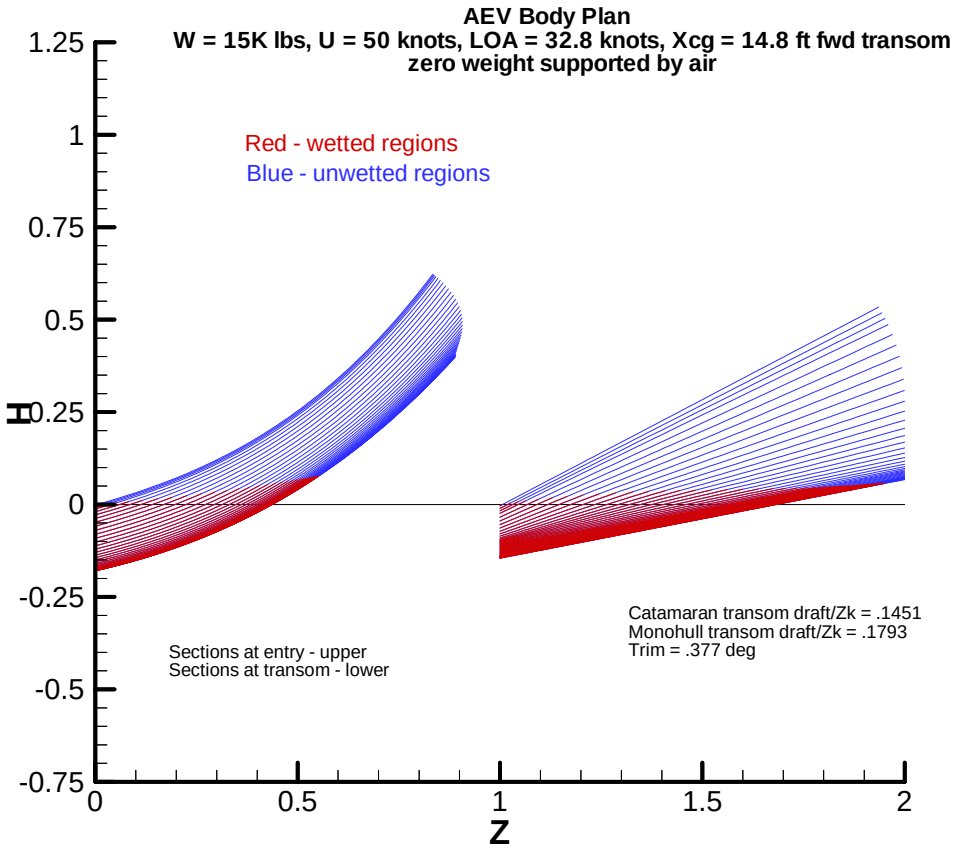

Figure 10 – Wetted Body Plan of AEV at Calm Water Equilibrium (with zero internal gauge pressure)

From Figure 10 the catamaran sub-hull of the AEV is again at impending chine-wetting, but the center-monohull is strongly chine-unwetted.

Figure 11 is the half-breath plan for the AEV at zero pressure, the equivalent of Figure 5 for the catamaran at zero air-supported weight.

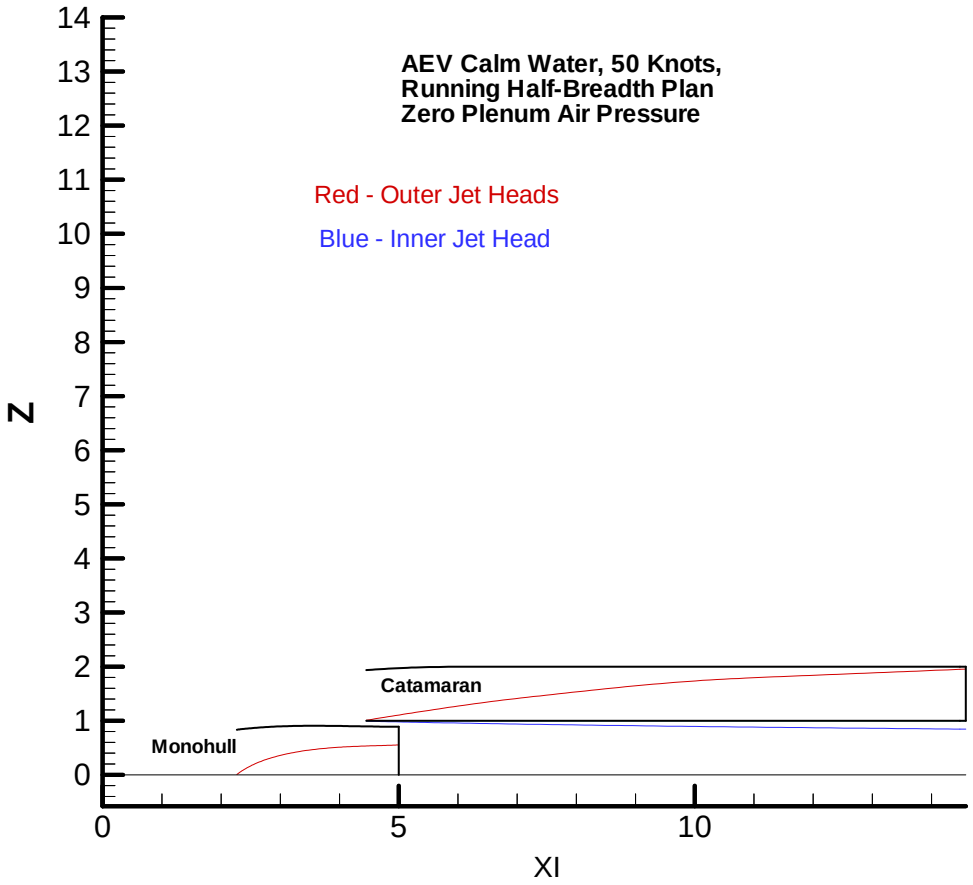

Figure 11 – AEV Running Half-Breadth Plan at Zero Air Support

Here, the transom closure line-segments have been added to the plot for clarity. Only the wetted regions are shown as previously. Keep in mind that the catamaran segment extends to x = 0 and the monohull stem is at slightly negative x (refer to Figure 2 and Table 1).

The small clearance between the two hull segments for the purpose of elevating the internal air pressure is evident on both Fig 11 and Fig 10. This clearance would be closed to suit by contouring the bow above the waterline (which is not shown and has been assumed to have no effect on the hydrodynamics).

B2. AEV with Air Support

Figure 12 is the wetted body plan with allowance for air support. The air cushion pressure has assumed a complete conversion of the stream dynamic head to a uniform static pressure aft of the AEV step, with no losses, as discussed at IIIa. This assumption produces an upper bound of the pressure available for added lift corresponding to 8.2% of craft weight supported.

The difference in wetted geometry without and with non-zero cushion pressure is hardly discernable on comparing Figures 10 and 12. The notations on these two Figures does indicate a slight decrease in both draft and trim in allowing for the pressurization.

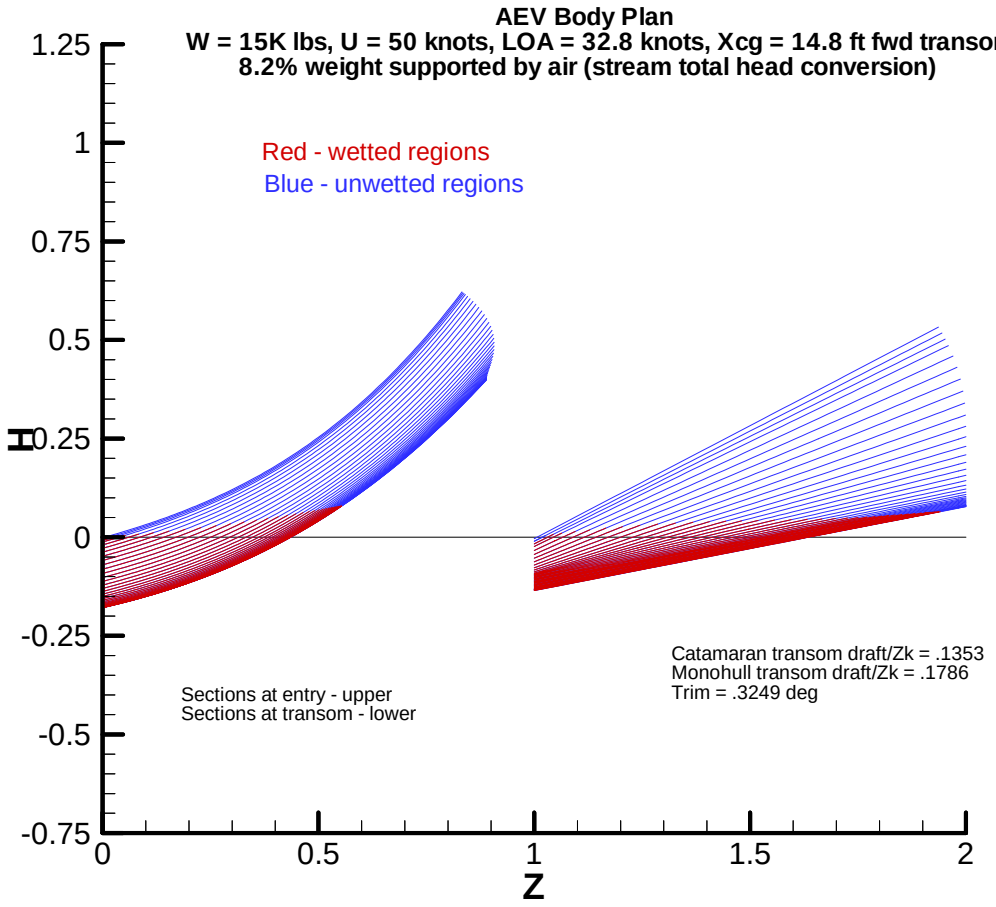

Figure 12 – Wetted Body Plan of AEV at Calm Water Equilibrium (with stream total-head cushion gauge pressure)

Figure 13 is the wetted half-breadth plan for the two cases, comparable to Figure 11. Note again the increased outward deflection of the inner jet head on Figure 13, implying a higher hydrodynamic pressure on the demi-hull bottoms, a reduced draft, and lower drag, as covered at Figure 9. The jet-head deflection on Figure 13 is, however, significantly less than the minimum pressure case of 25% weight support covered on Figure 9.

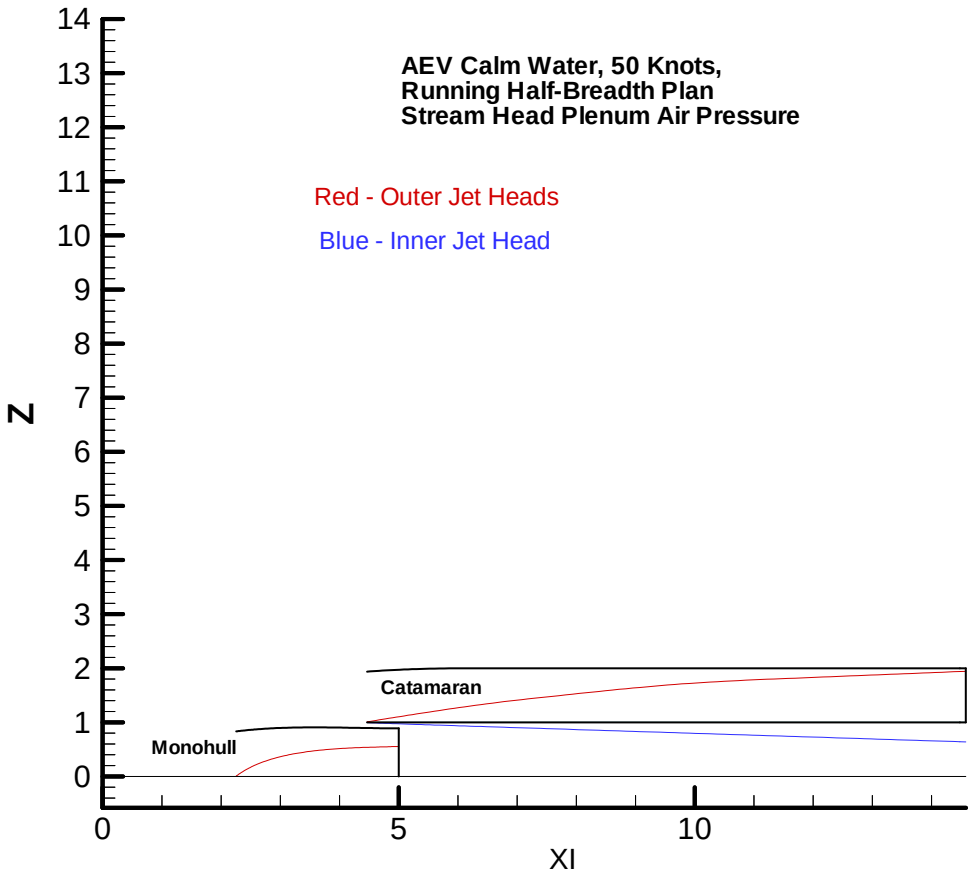

Figure 13 – AEV Running Half-Breadth Plan with Stream Air Support

The data is summarized on Table 4.

Table 4 – Effects of AEV Air Support

	Ht/Zk	Trim(deg)	Cl/Cd	p_g(psi)
Zero air support	.1451	.3771	6.76	0.
Air support by stream dynamic head[1]	.1353	.3249	6.84	.0578 (8.2%W)

1 – $p_g = \frac{1}{2}\rho_a U^2$; stream dynamic head assumed as the upper bound

The cushion pressure from the stream, as given by the formula in the Figure 2 footnote, is only .0578 psig. Comparing with Figure 11, this corresponds to only 8.2% of the craft weight. This implies the marginal drag reduction indicated. The lift/drag ratios of Table 4 give a drag reduction via the non-zero plenum pressure of 1.1%.

The lack of performance enhancement predicted for the natural ram air effects in the AEV case is not too surprising. 50 knots is generally considered the lower limit of speed for any effects of the air stream (lift or drag) on boat performance. A factor of 2 increase in boat speed, say, to 100 knots, would increase the static pressure by a factor of 4. At that level the internal lift would be significant (but so would the air drag acting on the craft external surfaces).

The enhanced calm-water performance claimed for AEV craft, such as Stolkraft (refer to II.), is not supported by this analysis. Admittedly, the assumptions of the air model used here is somewhat crude. But there is only so much energy extractable from the air stream corresponding to boat speed, and the maximum extraction has been assumed here.

It is possible that craft-generated gravity waves between the demi-hulls have some subtle interactions with the elevated air pressure, further along the lines of the jet-head deflections of Figs 9 and 13, that amplifies the drag reduction. This will be reconsidered in the extension of SR1441 in Part B to follow.

It seems more likely though that the air does indeed have negligible effect, and that the good performance qualities reported for AEV are purely hydrodynamic in origin, as associated with unusual hull lines. However, this is not supported by the comparative analyses with zero air pressure. That is, from Fig 8, the SES at zero air support, which is just the straight catamaran, is predicted to have a lift/drag ratio of 9.04. For the AEV, on the other hand, at zero pressure, Cl/Cd = 6.76 from Table 4 above. This is a significant drag difference, apparently due to the added drag of the center monohull. The monohull element is predicted to produce only 8% of the total lift, but 31% of the total drag. The center monohull, being a relatively short appendage, runs at lower Reynolds number with relatively high viscous drag.

The major benefits of the AEV-type hull may be more in its seaway dynamic characteristics that its calm water performance. The Stolkraft has hull geometry characteristics similar to the cathedral hull of Boston Whaler, which has developed such a good reputation for ride-ability.

Seaway dynamics is evaluated in the next sub-section for both the SES and the AEV using the zero-gravity hydrodynamic theory.

VIIb. Seaway Dynamics

While lift/drag ratio is the measure of merit for calm water performance, the measure of merit for seaway performance is impact acceleration. CatSeaAir computes all of the three degree of freedom force and displacement derivatives at every time step. The concentration in this Section of Part A is on accelerations and displacements, but force distributions, pressures etc. at specified points on the hull as functions of time are demonstrated in Part B and in the Appendix at the back of the complete report.

10,000 time steps were considered to generate a long enough record for meaningful statistical evaluations and this is the computation performed repeatedly here. The computation is in terms of the non-dimensional variables. The dimensionless time, τ, is defined as:

$$\tau = \frac{Ut}{Z_k}$$

with U = 50 knots = 84.45 fps, Z_k = 2.25 ft, τ =37.53t, with t in seconds. A non-dimensional time step of $\Delta\tau$ = .025 was selected for all cases based on experience. This gives τ_{max} = 250. The maximum real time of the computation is therefore:

$$t_{\max} = \frac{250}{37.5} = 6.66\,\text{sec}$$

In this time the vessel has traveled about 170m. After performing all of the computations at this time parameter it was recognized that τ_{max} = 250 was not large enough to achieve statistically stationary conditions in the response and that a longer record would be desirable. The number of time steps was increased from 10,000 to 20,000 and some of the calculations re-done to better demonstrate the evolution toward stationary conditions; recall that the start-up is from calm-water equilibrium, with the seaway ramped-up in time. The other calculations at the shorter time were considered adequate for comparing the differences in the various cases and to demonstrate the CatSeaAir programs (which is the main objective of this 2005 Part A report).

The computation proceeds identically as did the calm water cases, but with the calm sea surface replaced by the Jonswap sea wave spectrum, as explained in IIIb. All computations are for head seas. The dominant wave length, being that of a gravity wave at the spectrum center band frequency, is 40m, selected arbitrarily as allowed by the two parameter Jonswap spectrum.

A. SES

Seaway analysis for the four levels of active air support (0, .25, .50, .75 fractions of craft weight supported) is again performed, starting with the zero support catamaran case.

A1. Catamaran at zero air support

Figure 14 is the vertical acceleration plot for a ½ m significant wave height for the 6.66 sec maximum computation time.

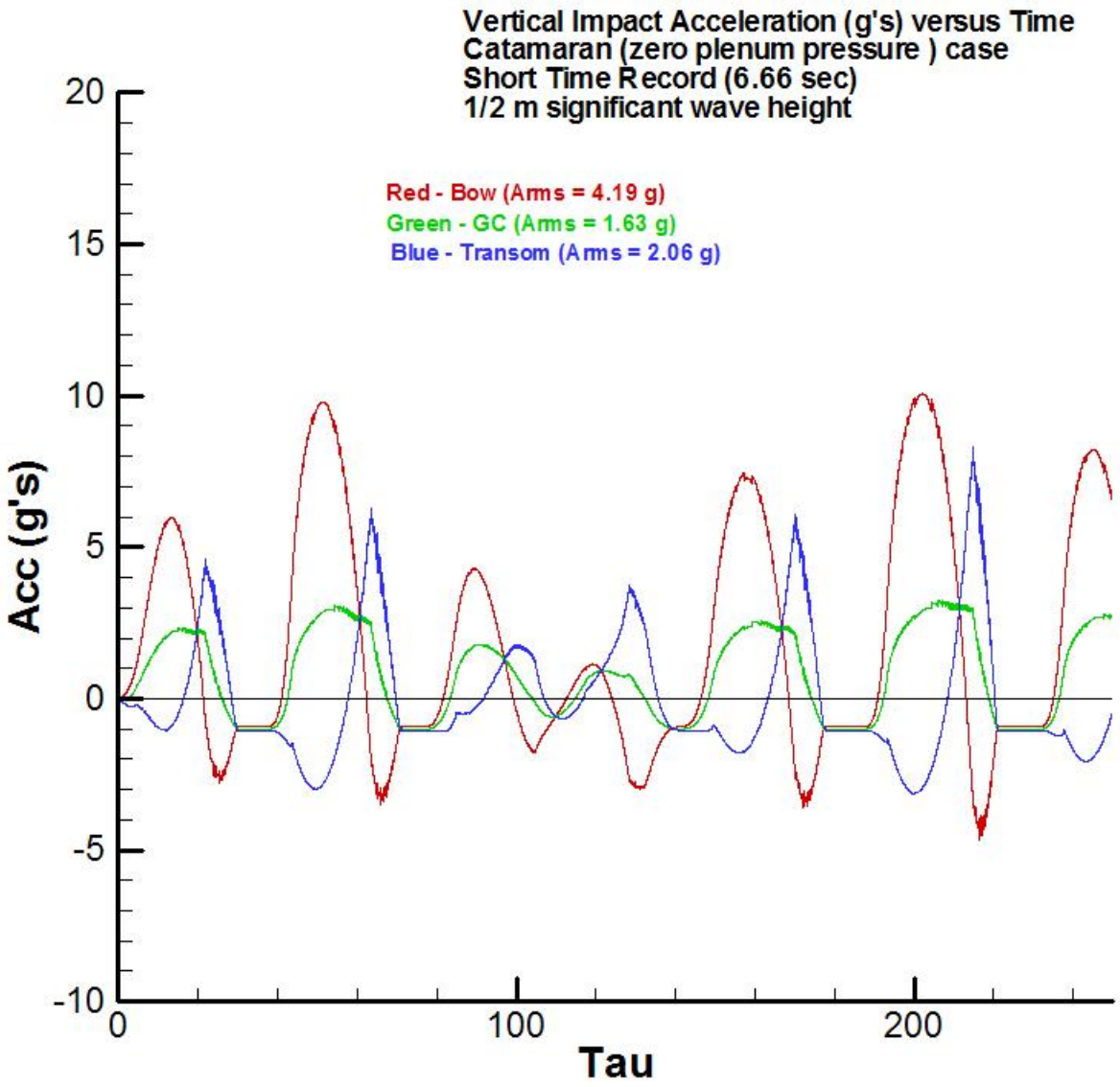

Figure 14 – Vertical Acceleration at Catamaran Bow, CG, and Transom for ½ m Significant Wave Height

At 50 knots in a 10m boat, a 1/2m significant seaway of this length is deceptively severe. Figure 14 predicts a 10g maximum at the bow, with an RMS bow acceleration of 4.19 g's, as indicated. The more peaked shape of the stern acceleration is consistent with the "launching" of the boat off the waves that immediately follows the sharp stern peaks. There it is seen that the accelerations are all essentially -1g, indicating free-fall following

launch off of the preceding wave. The bow is accelerating downward at slightly less than one g, and the transom at slightly more, indicating a slight bow-up rotation in the free-fall. The free-fall abruptly concludes with a sharp bow-up impact acceleration at the crash downward.

This sequence is also reflected in the waterline length characteristics of Fig 15.

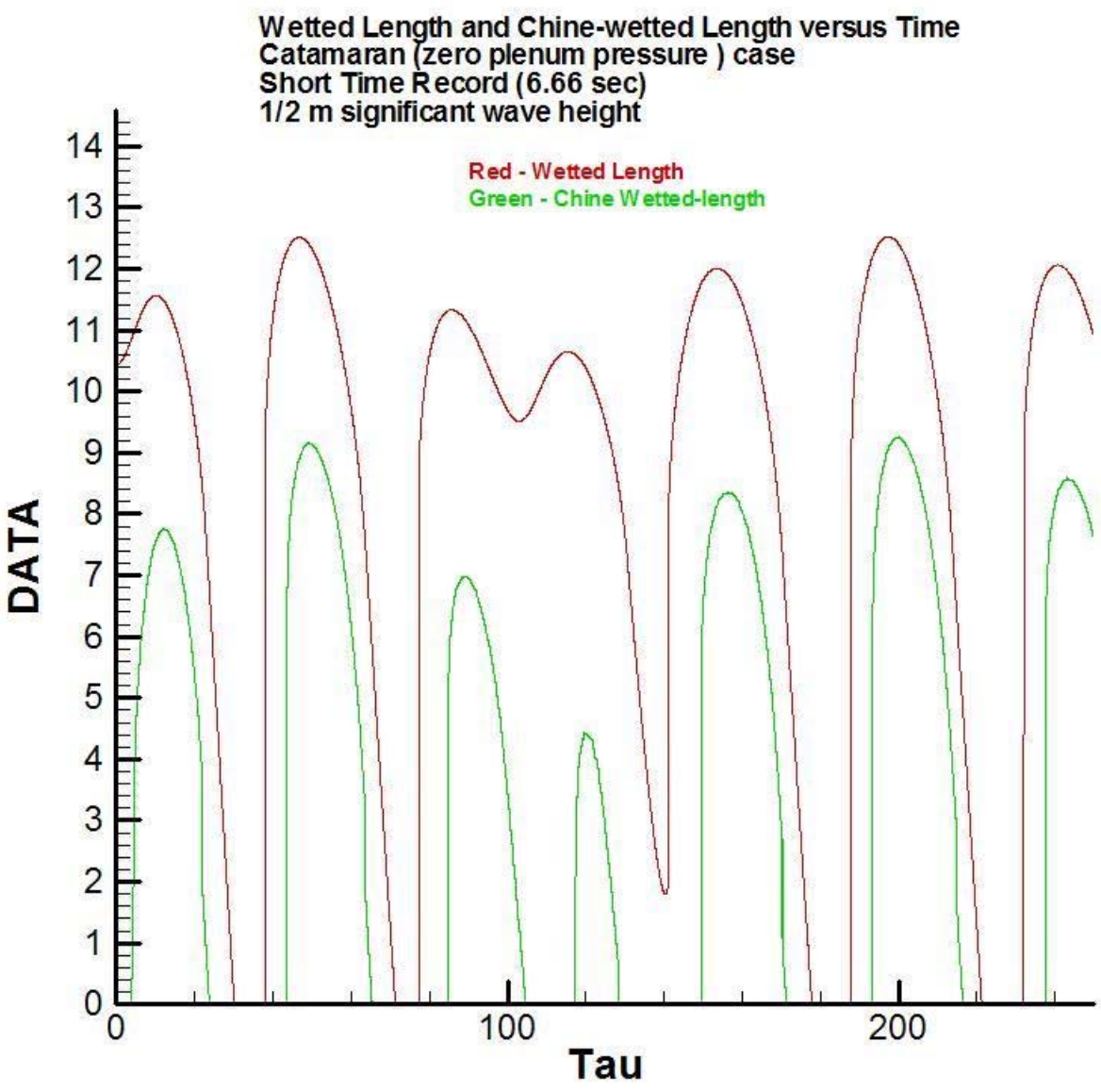

Figure 15 – Catamaran Wetted Length and Chine–wetted length for 1/2m Sig. Wave Height

The red curve of Figure 15 is the waterline length from the transom at any time and the green curve is the distance from the transom to the point of chine-wetting.

The computation starts from the calm-water equilibrium with the waterline length of Xmax/Zk = 10.41, and is fully chine-unwetted. From Figure 15, the first free-fall, where the wetted length is zero, commences at a τ of about 30 and ends with the commencement of the bow impact at around 40; this is consistent with Figure 14. On bow impact the wetted length expands almost instantaneously to the bow position. It is this very rapid time gradient of the waterline that is reflected in the intensity of the bow impact centered at approximately $\tau = 50$ on Figure 14. Note on Figure 15 the three other instances of free-fall in the record, which are consistent with the peaks of Figure 14.

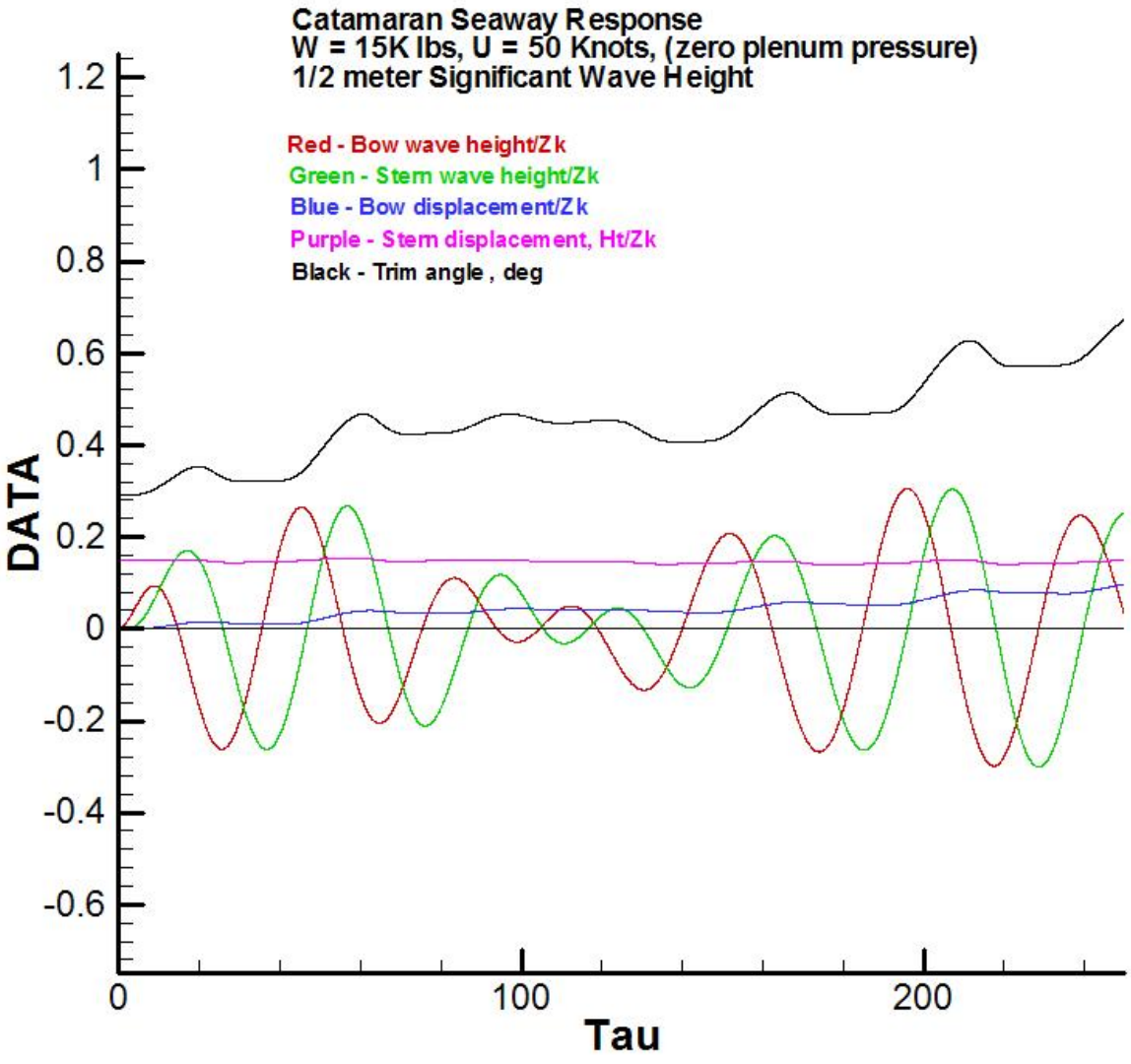

Figure 16 – Catamaran Displacement Responses; ½ m Sig Wave Height, Short Time Record

Figure 16 shows an array of time dependent displacements. As indicated on Figure 16, the red and green curves are the wave heights/Zk at the bow and stern versus time. The purple curve is the transom draft, Ht/Zk, which is decreasing slightly with time. The bow displacement (blue curve) is that due to the seaway alone and does not include the initial calm water value. The initially curious aspect of Figure 16 is the slowly rising trim angle; this is also seen in the increasing bow displacement (blue curve). This coupled with the decreasing Ht implies that the boat is rising in the seaway with time. This is reasonable in consideration of Figure 14, which indicates more acceleration up than down over time, producing a net rise.

Even more provocative, with less hull in the water, the mean-lift/mean-drag ratio is predicted to have risen from the calm water value of 9.04 to a value of 10.44 at $\tau = 250$. This does not necessarily imply a drag reduction in the seaway, as greater lift in the mean is required to elevate the boat to the higher mean position and keep it there; static equilibrium does not hold in the mean in this highly nonlinear dynamics. It does suggest more efficient operation of planing boats at high speeds in waves (if the personnel on-board can tolerate the pounding). There are many aspects of planing craft hydrodynamics that are opposite to that of displacement hulls. The suggestion here is energy extraction from the ambient wave system in elevating the craft to a reduced mean displacement relative to the still-water equilibrium position; refer to Figure 16. This would be the opposite of the well known, and well accepted, behavior of displacement craft, which experience a loss of energy to the ambient wave system, resulting in larger net waves and added resistance. Analysis independent of that here shows that the net waves in the wake of the planing craft are reduced, consistent with the extraction of wave energy from the seaway and the increased lift-drag ratio of the planing craft operating in the seaway.

This behavior has often been seen in the predictions of the EDITH codes. The curious aspect here that deserves further investigation is the Figure 16 indication that the response has not reached a statistically stationary condition. Response to a stationary random input is necessarily a stationary random output developed for a long enough time after start-up.

The computation was first re-run with the significant wave height increased from 1/2m to 1m. The acceleration record, parallel to Figure 14, is Figure 17.

The features of Figure 17 would be expected on the basis of Figure 14. There are more periods of “launch and crash” due to the larger waves. In addition, some of the upward stern acceleration peaks are larger than at the bow. This is what produces the launch, like a “diver off of a spring board.”

The concern over stationarity continues at Figure 18, which is the counterpart of Figure 16 for the 1 meter significant wave height.

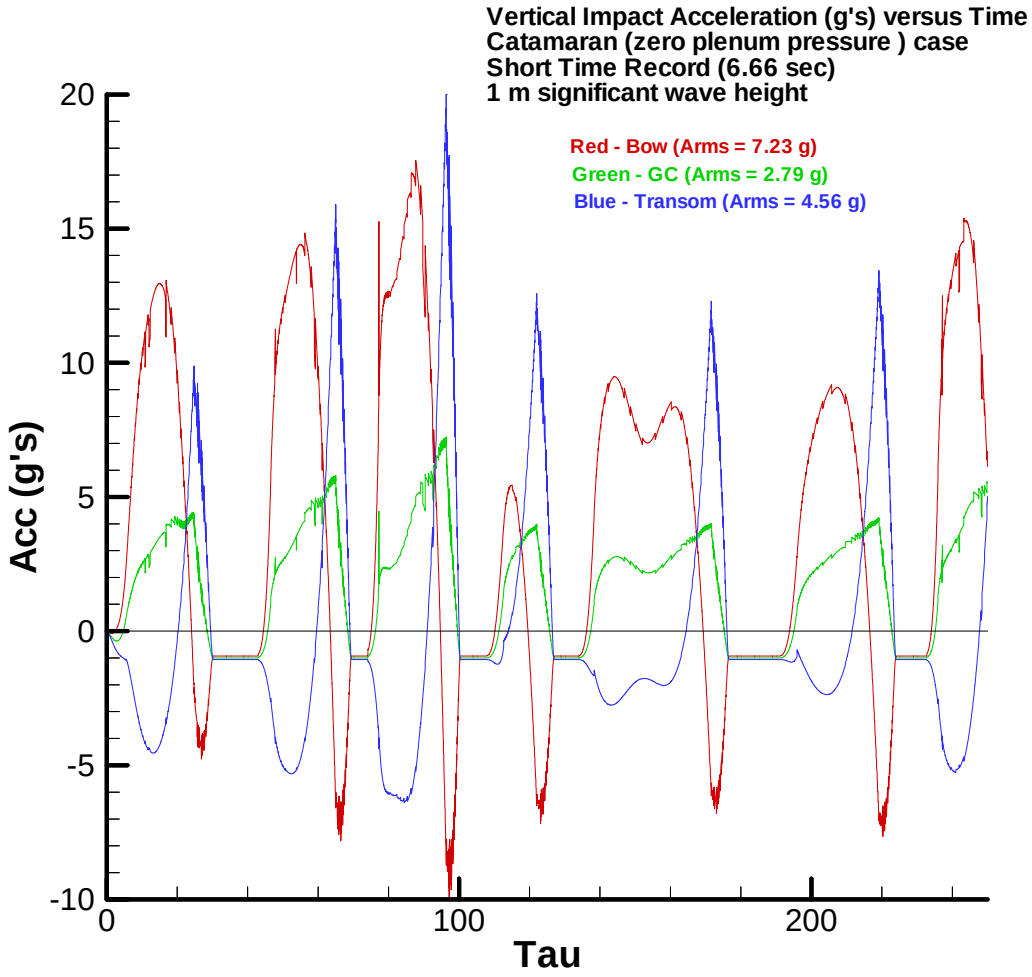

Figure 17 – Vertical Acceleration at Catamaran Bow, CG, and Transom for 1m Significant Wave Height, t_{max} = 6.66 sec

The trim rises even more strongly on Figure 18. At some point in time the trim and transom draft should evolve to stationary values which are no longer changing in the mean. If this does not occur, numerical inaccuracies accumulating in the time-domain nonlinear computation would have to be admitted.

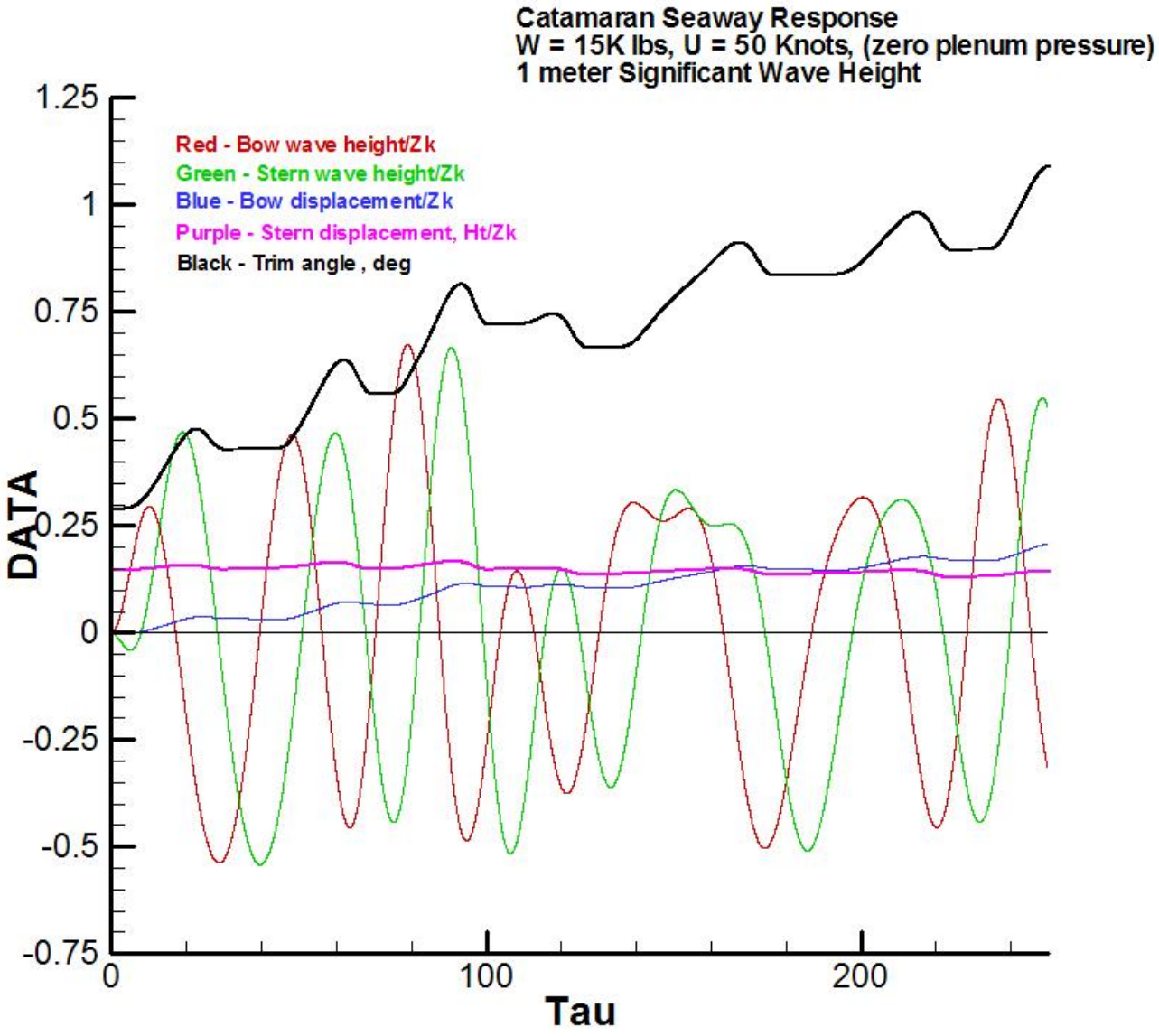

Figure 18 – Catamaran Displacement Responses; 1m Sig Wave Height, Short Time Record (6.66 sec)

This led to the computation time extension addressed at the beginning of VIIb above. The CatSeaAir code has a restart capability that was used here to extend the Figures 17 and 18 computations out to τ_{max} of 500, corresponding to 20K time steps. The results are shown on Figures 19 and 20.

The relative closeness of the RMS accelerations on Figuress 17 and 19 suggests that stationarity is approached at $\tau_{max} = 500$. The higher transom acceleration level is consistent

with the decreased transom draft to which the craft has risen and its greater tendency to launch off of the waves.

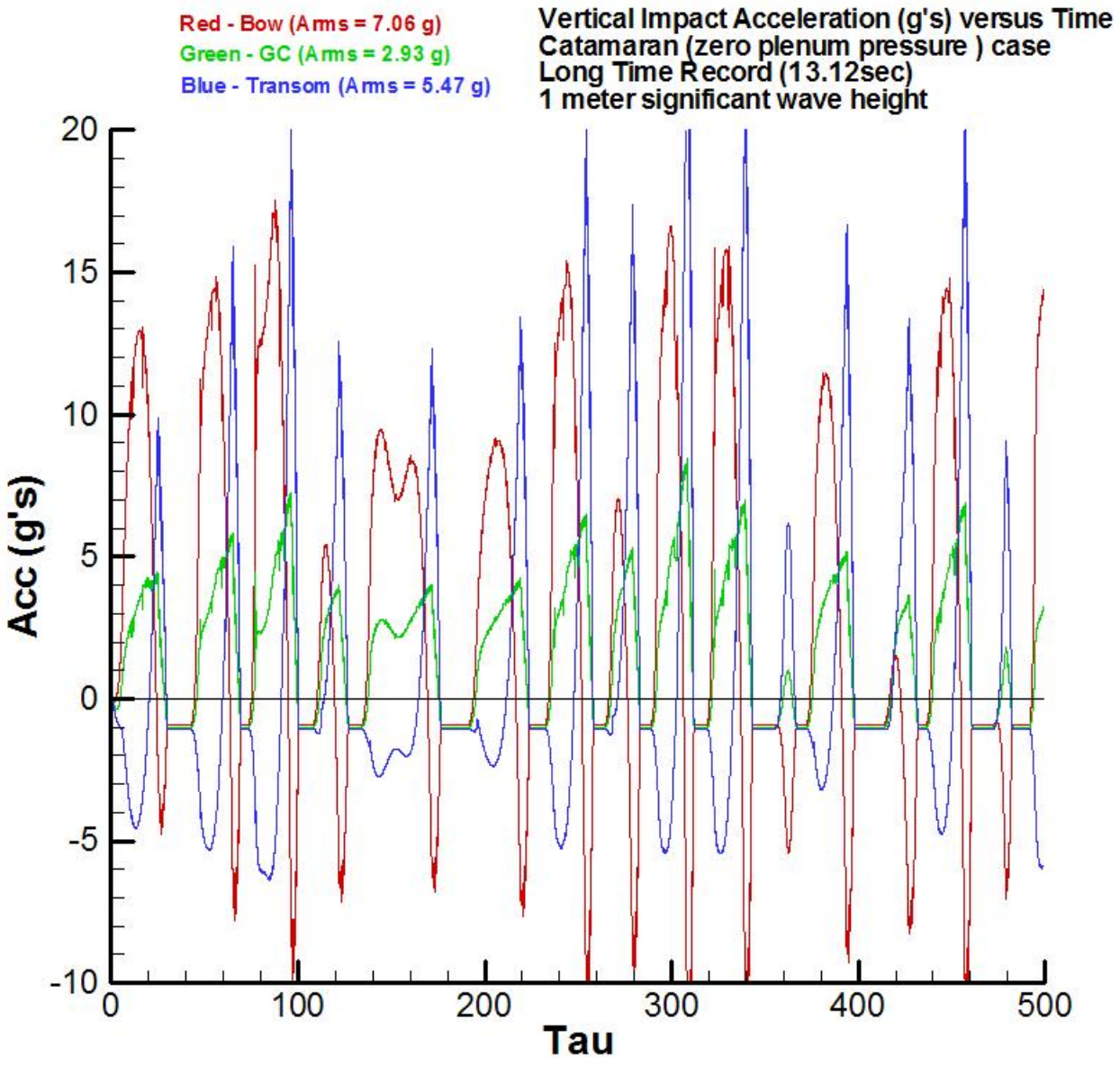

Figure 19 – Vertical Acceleration at Catamaran Bow, CG, and Transom for 1 m Significant Wave Height, t_{max} = 13.12 sec

Figure 20 is considered to be satisfactory evidence that the curves have "leveled-off" and that further time extension would not result in large time-scale changes, i.e., stationary conditions have been acceptably achieved. The high mean-lift/mean-drag ratio is also maintained at the 10.4 value out to the longer time.

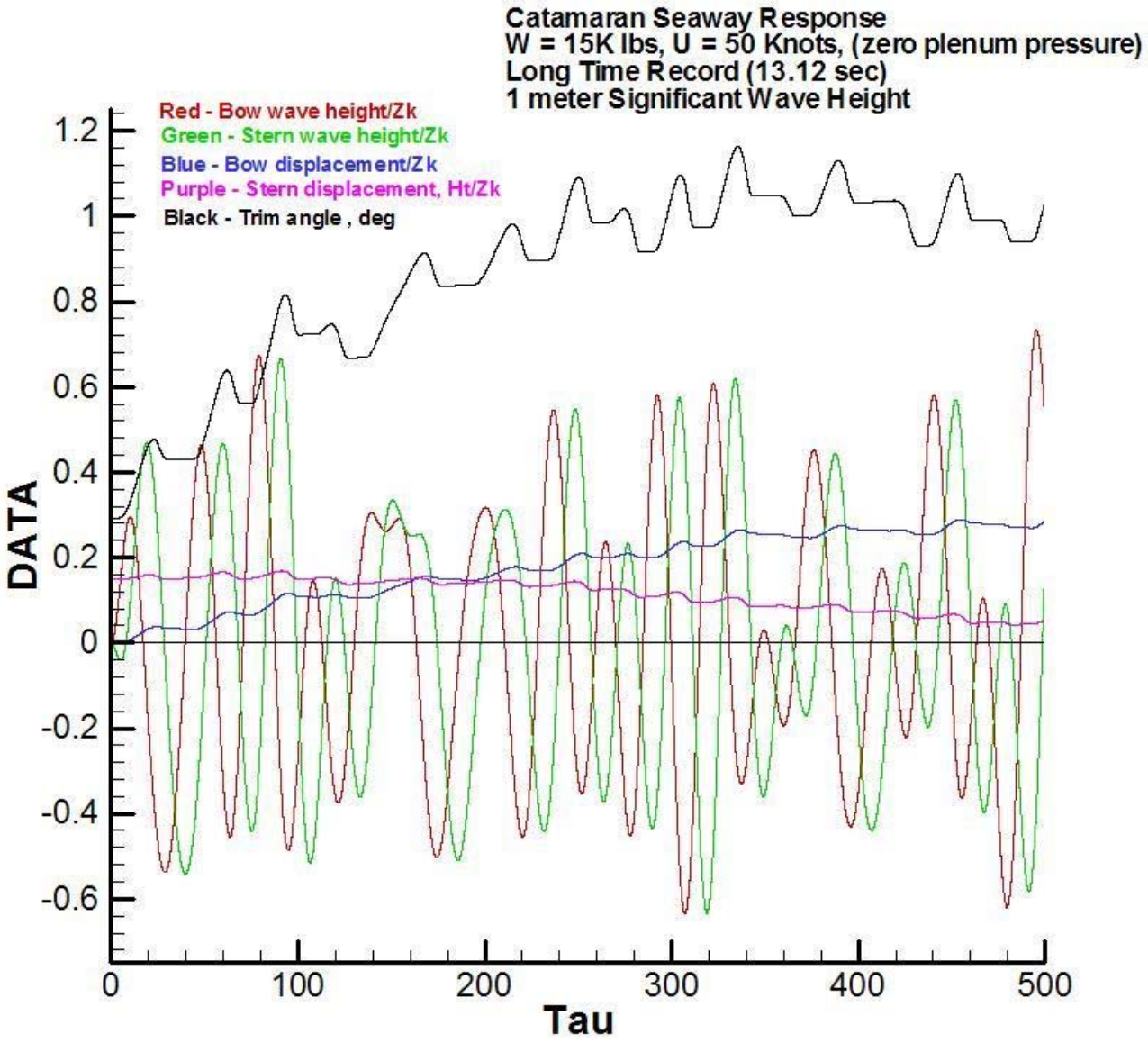

Figure 20 – Catamaran Displacement Responses; 1 meter Significant Wave Height, Long Time Record (13.12 sec)

A2. SES with Air Support

As stated at the beginning of this section, the remaining analysis of the SES and AEV was performed at the shorter time span, $\tau_{max} = 250$. The ½ meter significant sea was also used exclusively. This provides a valid basis for comparison even though statistically stationary conditions are not well achieved.

Figure 21 is a plot of the vertical accelerations at bow, CG, and transom superimposed for the four fractions of craft weight supported by air (see Figure 9). This includes and is the extension of Figure 14 for the zero pressure catamaran case.

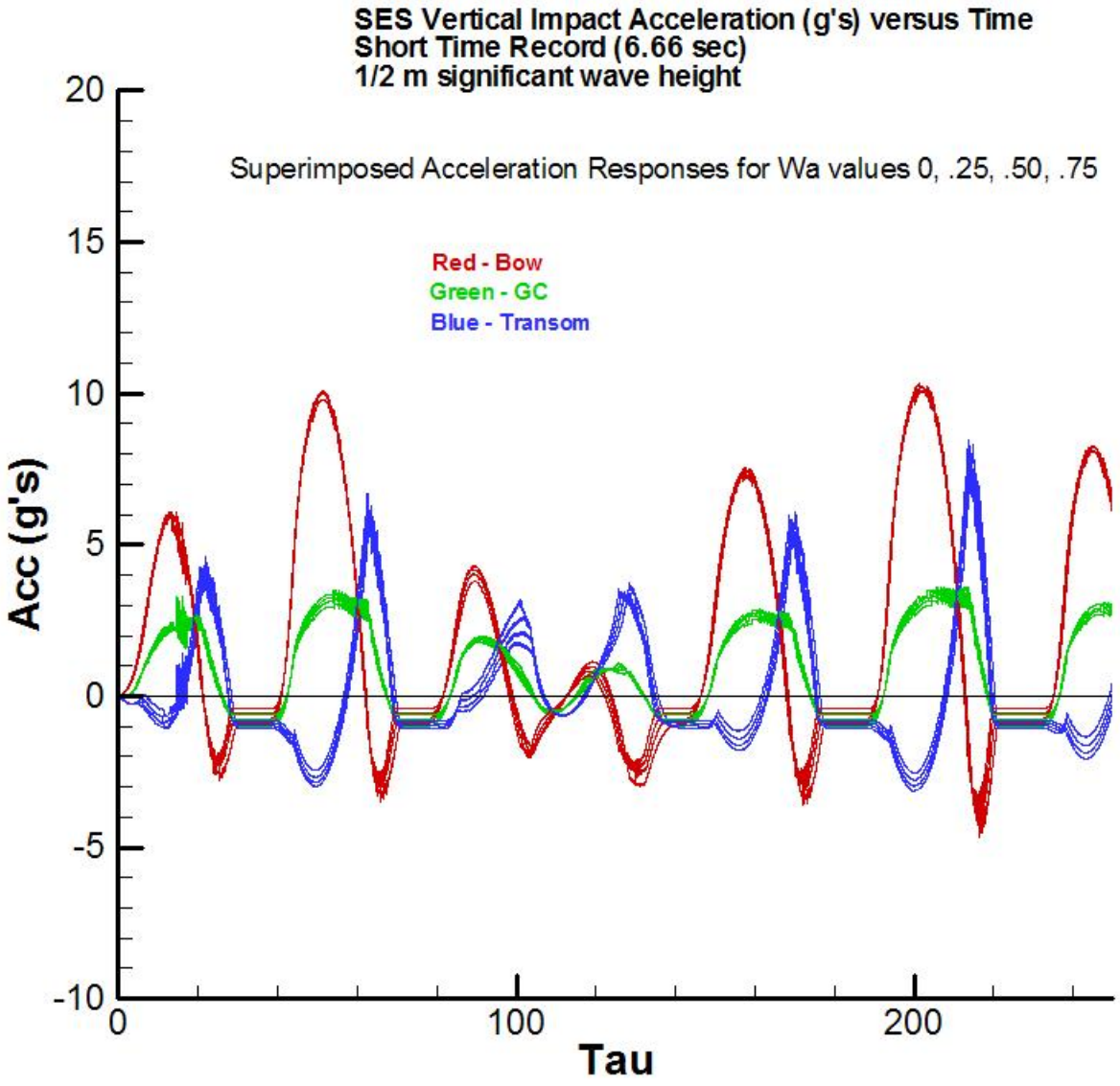

Figure 21 – Vertical Acceleration at SES Bow, CG, and Transom for 1/2m Significant Wave Height, t_{max} = 6.66 sec; Responses for Array of 4 Cushion Pressures Superimposed (0, .25, .50, .75)

Some differences in the four acceleration characteristics exist at the lower response levels of Figure 21, but diminish at the higher acceleration levels. The reason is that the pressure produced by the seaway motions is so much larger than the cushion pressures that they dominate the responses; the larger the response the more dominant are the seaway induced pressures in the superposition.

Figure 22 plots the superimposed displacement responses for the four pressure cases. This includes and extends the data of Figure 16 for the zero pressure catamaran case.

The differences in the calm water displacements are largely just the initial calm water values. Like the acceleration of Figure 21, the differences in cushion pressure have essentially no effect on the dynamic displacement components that evolve with time. This is for the same reason as was clear in the largely unchanging peak accelerations with cushion pressure at Figure 21; that is, the seaway dynamic pressures developed are an order of magnitude higher than any of the cushion pressures. The displacements are all just the integrations of the accelerations in time, with the constants at $\tau = 0$ added.

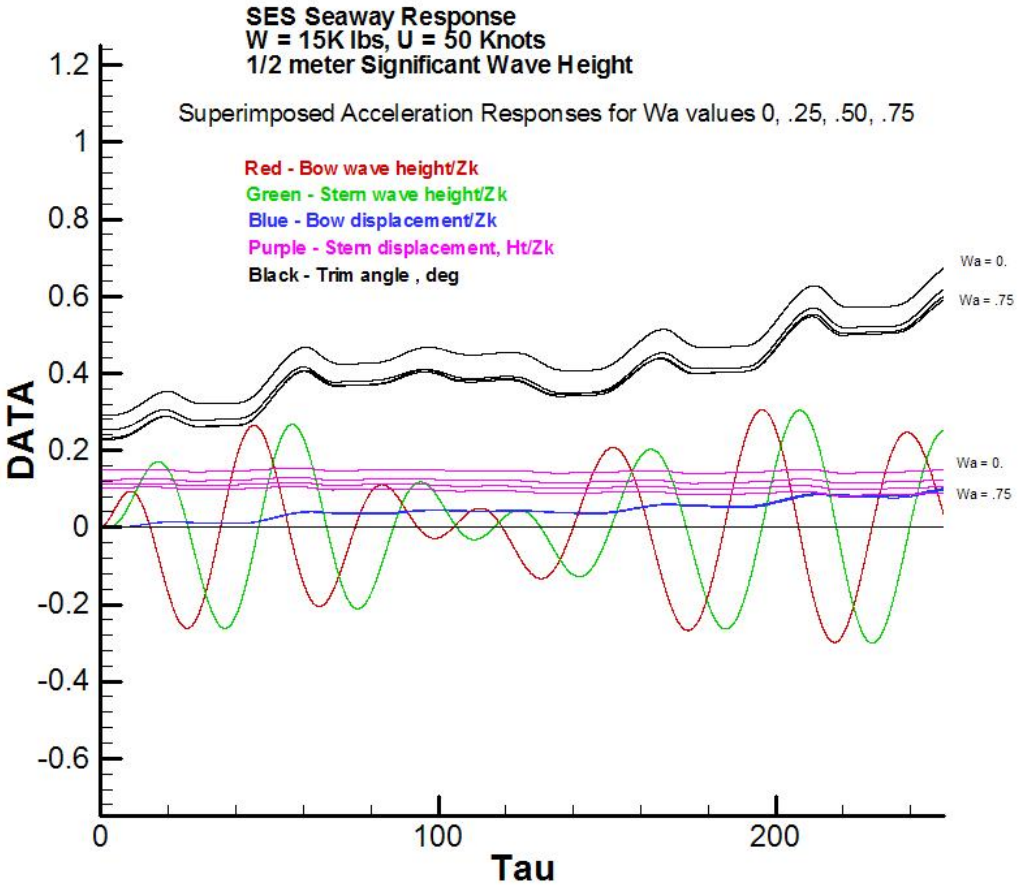

Figure 22 – SES Displacement Responses; ½ m Sig Wave Height, Short Time Record (6.66 sec); Responses for Array of 4 Cushion Pressures Superimposed (0, .25, .50, .75)

An obvious implication of this analysis, and for the reasons cited above, is that the active pressurization of the SES has little influence on the seaway response relative to an un-pressurized catamaran running at low trim angle. This is seen clearly in the bow displacement curve of Figure 22, which does not include the calm water equilibrium component.

B. AEV

The AEV vertical acceleration response predicted for the ½ m seaway is Figure 23. This is a superposition of the cases with and without non-zero cushion pressure effects. The AEV response is higher than the composite SES response of Figure 21, but only marginally so.

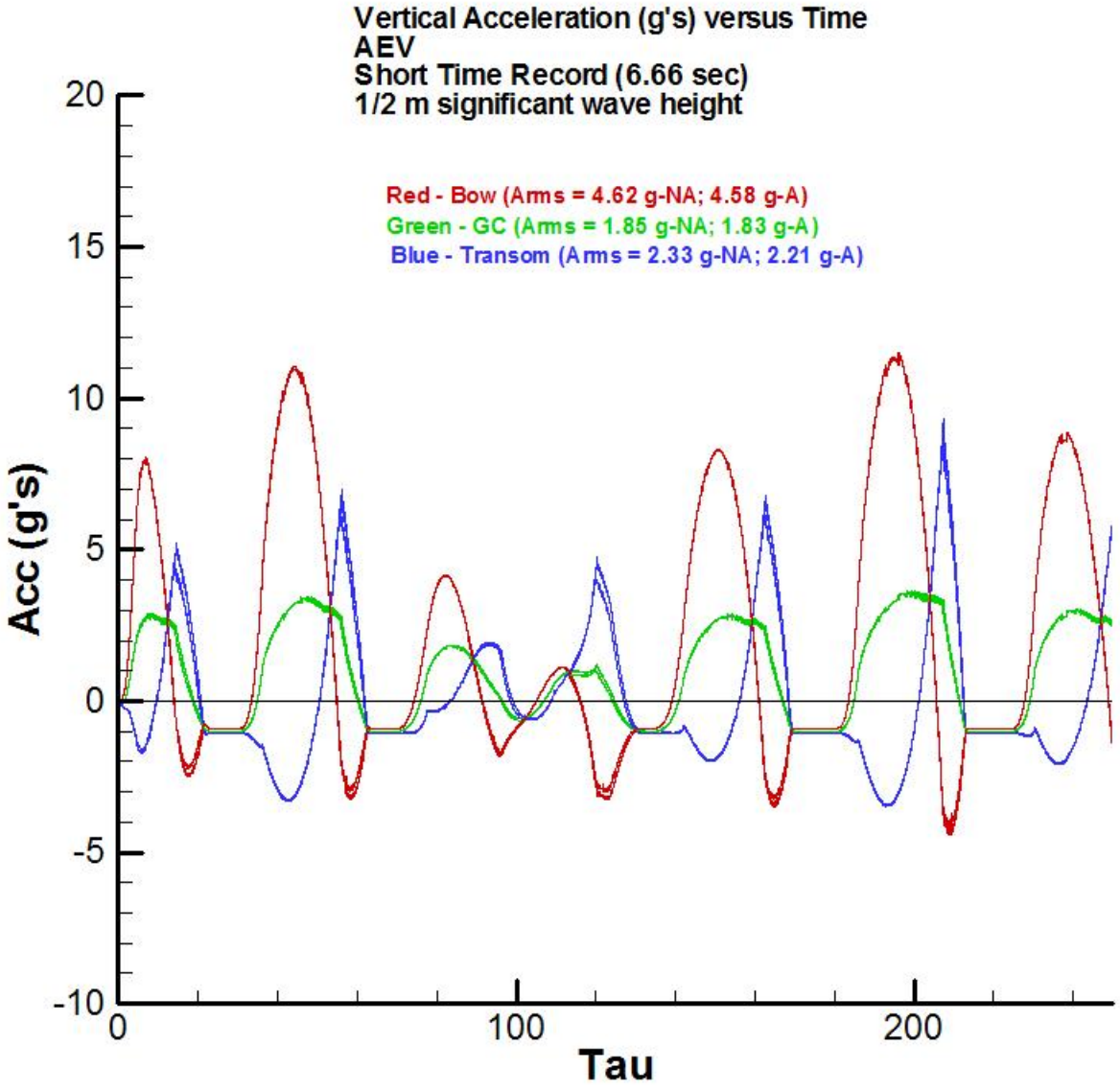

Figure 23 – Vertical Acceleration at AEV Bow, CG, and Transom for ½ m Significant Wave Height

The displacement response of the AEV, Figure 24, offers no surprises. For both the SES and the AEV, cushion pressure effects, while influential in the calm water performance, to varying degree, are predicted to be essentially irrelevant in seaway dynamic performance.

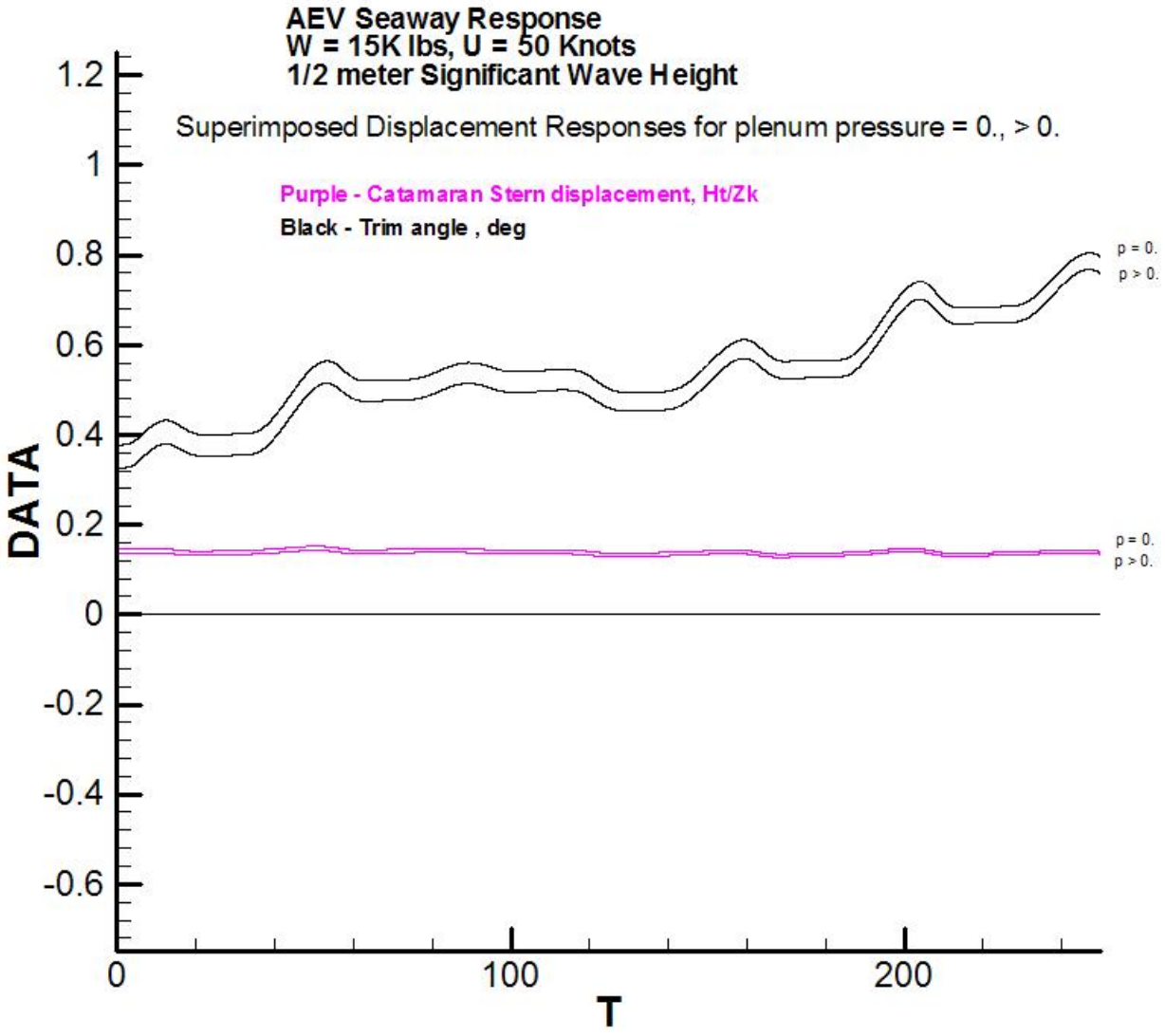

Figure 24 – AEV Displacement Responses; ½ m Sig Wave Height, Short Time Record (6.66 sec); Responses for Zero and Non-zero Cushion Pressures Superimposed (0, .25, .50, .75)

VIII. Summary and Conclusion-Report Part A

1. The CatSeaAir (EDITH 1-2) code has proved to be highly robust. In over 200,000 total time steps executed in the analysis presented there was not a single stop due to any kind of numerical or physical difficulty. The codes were generally run in 10,000 step blocks, with a planned restart to execute the 20,000 step case.

2. With lack of measured data in hand for comparison in this initial 1995 work, the approach was to design a 10m, 50 knot craft for analysis and comparison.

3. The main element in the configuration is an asymmetric catamaran hull. The SES analysis set the internal air pressure between the catamaran demi-hulls in steps on the basis of 0 to 75% of the craft weight supported by air. For the AEV analysis a short monohull segment was added between the catamaran demi-hulls forward; the pressure in the air plenum of the AEV formed between the demi-hulls aft was assumed to be the total dynamic head in the incoming air stream.

4. In the calm water analysis of the SES, and the AEV, it was discovered that an important contributing factor to the lift achieved is the effect of the elevated air pressure on the vortex shedding between the demi-hulls. Refer to Figure 9 and discussion.

5. Gravity wave effects, which may be important particularly in the calm water analysis are not included here, but this is the principal subject of Part B of this report, to follow.

6. Claimed advantages of natural air enhancement in the AEV craft could not be confirmed by the analysis conducted. Even complete conversion of the 50 knot stream dynamic head to static pressure, without losses, produces insignificant craft lift; refer to Table 4 and Figure 23. This outcome was expected.

7. Neither the SES nor the AEV show any appreciable effect of non-zero air pressure on the level of seaway dynamic response; see Figures 21 to 24. The reason deduced is that the uniform cushion pressures are so small relative to the seaway hydrodynamic impact pressures that they have little effect in the superposition to seaway dynamic forces.

8. The good seaway performance predicted for both of the craft is due mainly to a forward placed center of gravity (45% of length from the transom) in both cases. This was done to avoid high trim at low speeds and loss of cushion pressures. The center of pressure in the cushion is at approximately at boat mid-length.

   10g bow acceleration in a ½ m significant seaway (and 20g's is a 1m seaway) might sound to be not good seakeeping quality until it is considered that the boats are being run on a straight line into head seas at the fixed speed of 50 knots. This is not the usual operating scenario. Effort is made by the pilot to maneuver through the waves. In offshore racing, for example, a "throttleman" supports the "steerman" in avoiding the highest wave impacts.

IX. References - Report Part A

Vorus, W.S., "A Flat Cylinder Theory for Vessel Impact and Steady Planing Resistance," Journal of Ship Research, June 1996.

Hydrodynamic Pressures and Impact Loads for High Speed Catamaran/SES Hull Forms

Ship Structures Committee Project SR 1441

Report Part B – 2006

1) Non-Zero Gravity Hydrodynamics
2) Structural Loading
3) Experimental Data Comparisons

I Introduction

As stated in the preface, the SR1441 first year, 2005, exercised a zero gravity, or infinite Froude number, theory for catamaran, SES and AEV hydrodynamics. This is reported in Part A of this report. The craft to which the analysis was specifically applied was a bi-hull, 10 meters in overall length, with a 1.37m transom half-beam and a speed of 50 knots. Based on overall length, this corresponds to a Froude number, Fn, of 2.6. If, however, the vessel length was increased by a factor of 10, the Fn becomes .82. The Fn = 2.6 may be high enough to assume Fn = infinity in the hydrodynamic analysis. However, the high speed 50 knot ship at Fn = .82 will have much stronger gravity effects hydrodynamically. The computation in this Part B of the report is first continued with the 10m craft with non-infinite Fn, but is followed by a calculation for the same vessel with speed reduced from 50 to 30 knots.

Hull hydrodynamic pressures distributions, as would be required in structural analysis, are demonstrated for the 10m craft at 50 knots.

The report concludes with an analysis of the Bell-Halter 110 SES and comparison with its model test data. This is in an attempt to indicate an absolute measure of the validity of the assembled theory and analysis for the air supported craft type.

II Non-zero Gravity Theory

The base theory used here for gravity wave effects is the linearized planning monohull theory of Maruo (1967), adapted for catamaran, including SES. The AEV is not analyzed in Part B of the report. The Maruo formulation is based on ideal flow theory and represents a solution to the Laplace equation for a velocity potential, subject to the linearized free surface boundary condition, with gravity included, and a radiation condition of no waves upstream. It is a steady flow theory, and therein lies the major approximation of this application. The unsteady seaway dynamics assumes that the wave-making is quasi-steady. That is, with changing vessel attitudes in the seaway, this application assumes that at any instant the temporal effects in the wave-making, as regards loading changes, are small. The unsteady effects in the wave making are generated by the Maruo solution at any instant for the craft geometry varying generally with time.

Referring to Figure 26, x is downstream with the coordinate system located at the bow, and y is up. The planing surface is considered to occupy the region of the y = 0 plane corresponding to $-Z(x) \le z \le -Z_k$ *and* $Z_k \le z \le Z(x)$ with $0 \le x \le L$, L being the instantaneous waterline length. Z(x) is the waterline offset and Zk is the demi-hull keel offset, taken as constant in x. The kinematic boundary condition is satisfied on this plane surface, which requires that the craft bottom have a flat characterization. Planing craft are consistent with the assumption of flatness in satisfying boundary conditions on the y = 0 plane, and this has been a universal assumption for conventional analysis of planing craft at zero gravity, as built upon the original work of vonKarman(1929) and Wagner (1932). The current CatSeaAir code prior to the addition of the Mauro gravity routines used the non-linear slender-body formulation of Vorus (1996).

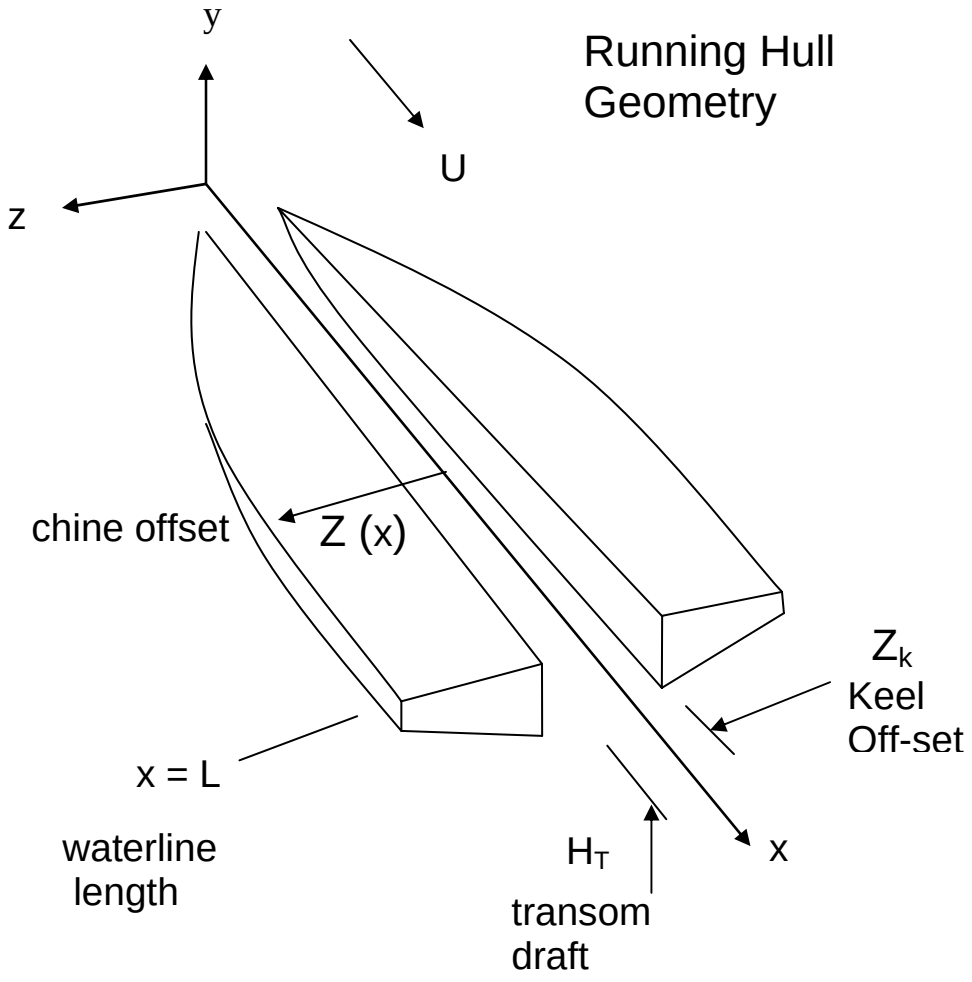

Figure 26: Catamaran/SES Geometry

The Maruo velocity potential, adapted for the Figure 28 catamaran geometry, is:

$$\Phi(x,y,z) = -\frac{1}{\pi}\int_{\zeta=-Z(x)}^{-Z_k} + \int_{Z_k}^{Z(x)}\int_{\xi=0}^{x}\gamma_z(\xi,\zeta)\int_{\lambda=0}^{\infty}\cos\left[\sqrt{\kappa\lambda}(x-\xi)\right]\cos\left[\lambda(z-\zeta)\right]e^{\lambda y}\,d\lambda\,d\xi\,d\zeta \tag{2}$$

Referring back to Figure 26, Φ is the velocity potential in the fluid region, $y \le 0$. γ_z is the unknown transverse (z-directed) vortex density component on the surface projection. (The companion axial vortex density component, γ_x, is the usual subject of the conventional zero gravity slender body formulation of planing, but the two components are related by the condition of zero divergence of the two dimensional surface vector.)

κ in (2) is the wave number:

$$\kappa = g/U^2 \tag{3}$$

κ entered the derivation of (2) in satisfying the linearized free surface boundary condition in allowing for gravity wave generation.

Note from (2) that only the sections at $\xi <$ x upstream convect into the current x – solution section; γ_z for $\xi <$ x will always be known from upstream computation steps. This x-marching characteristic of the elliptic solutions in the z-coordinate is common to the parabolic reduction in x associated with all slender body theories.

The linearized kinematic boundary condition on the planing surface is:

$$\frac{\partial \Phi}{\partial y} = U \frac{\partial y_0}{\partial x} \qquad \text{on y = 0, } -Z(x) \le z \le -Z_k \text{ and } Z_k \le z \le Z(x)\text{, } 0 \le x \le L \tag{4}$$

$y_0(x,z)$ is the definition of the planing surface $y - y_0(x,z) = 0$, which is presumed to be known.

Substitution of (2) into (4) produces an integral equation that is solved numerically for the vortex density $\gamma_Z(x,z)$. This solution is difficult in that it exhibits a higher order singularity that must be carefully treated, Tuck (1975). But it is made easier by the downstream marching in which each successive x-station is solved in terms of the already available solutions from the stations upstream.

The axial perturbation velocity on the surface is given in terms of $\gamma_Z(x,z)$ as:

$$u(x,z) = -\gamma_Z(x,z) \tag{5}$$

The coefficient of pressure on the surface is then:

$$C_p(x,z) = -2\left(\frac{u}{U}\right) \tag{6}$$

This pressure distribution, (6), is integrated over the surface to produce the force components needed in Newton's Law for stepping the vessel motion to the next time.

Note that $\kappa \to 0$ corresponds to vanishing gravity by (3). $\kappa = 0$ in (2) therefore gives the zero gravity solution $\gamma_{zi}(x,z)$. The vortex density due only to waves is therefore:

$$\gamma_{zw} = \gamma_z - \gamma_{zi} \tag{7}$$

(6) and (7) give the pressure due to wave-making as:

$$C_{pw}(x,z) = 2\left(\frac{\gamma_{zw}(x,z)}{U}\right) \tag{8}$$

A subroutine has been added to CatSeaAir to solve (2) and (4) and to compute (8) at each time step as the hull wetted geometry changes. $C_{pw}(x,z)$ is added to the g = 0 surface pressure currently calculated in CatSeaAir to obtain the total pressure field including the gravity wave effects.

Hydrostatic pressure relative to the undisturbed water surface is also included in the pressure sum in CatSeaAir, as well as is any air pressure associated with SES operations. The new version of CatSeaAir with the gravity routines included (as an option under user control) is designated as EDITH 1-2g.

EDITH 1-2g is simple to execute and interpret; sample I/O, with some explanation, is given in the Appendix. However, with the gravity option exercised, the code is time consuming. It executes about 200 time steps per hour. With 10,000 to 20,000 time steps desirable for achieving statistically stationary conditions in the random seaway analysis (see Part A), approximately 50 to 100 hours of running time is required. This is on a 3.2 Ghz workstation. Most of the calculation is serial in x and then serial in time, so it is not clear that parallel processing (or cluster computing) would help much. With the gravity option off, CatSeaAir runs about 20 time steps per minute.

The extended code is robust, however, and never crashes, and it has a restart capability. Effort will be made, by programming refinements, to reduce the time consumption requirement as time permits.

III Calculations with Gravity, Calm Water

IIIa. Zero Cushion Pressure

This section begins with the re-evaluation of the 50 knot catamaran of Part A of this report. Table 4 is the extension of Table 3 for steady speed of 50 knots in calm water, including the gravity effects in the hydrodynamics (last column of Table 4).

Table 4

Base SES Case: Catamaran Running Geometry at 50 knots with Zero Cushion Pressure

	g = 0	g ≠ 0
Froude number based on LOA, $\frac{V}{\sqrt{g \cdot LOA}}$	∞	2.6
Wetted Length/LOA, Xmax/LOA	.715	.718
Chine wetting point from stem/LOA	1.	1.
Trim angle, deg	.288[1]	.265
Transom draft, Ht/Zk	.148	.146
Lift/Drag Ratio	7.71[1]	7.72

1 – some g = 0 computed values changed slightly from Part A due to code refinements.

Perhaps the most surprising aspect of Table 4 is that the inclusion of wave making does not decrease the lift/drag ratio of the boat! It is essentially unchanged from the zero gravity prediction. An effect of gravity wave generation is to lift the stern of the planning boat and thereby decrease both the transom draft and the trim angle and increase the wetted length. The result is less wetted surface, which counters the resistance increase due to the waves. The running attitude of planning craft is very sensitive to the hydrodynamic loading developed and its resistance is very sensitive to the running attitude. This is a situation not encountered with displacement craft where the hull loading is dominated by buoyancy and

trim and draft are only weakly influenced by the distribution of gravity wave loading over the hull surface.

Table 4 can also be interpreted as a testament as to the validity of the usual assumption that gravity can be ignored in the hydrodynamics of high speed planning craft; the length Froude number of 2.6 in Table 4 is indeed high.

As a further evaluation, the speed of the catamaran was reduced from 50 to 30 knots, lowering the Froude number to 1.56. The results corresponding to Table 4 are listed in Table 5.

Table 5

Base SES Case: Catamaran Running Geometry at **30** knots with Zero Cushion Pressure

	g = 0	g ≠ 0
Froude number based on LOA, $\frac{V}{\sqrt{g \cdot LOA}}$	∞	1.56
Wetted Length/LOA, Xmax/LOA	.676	.713
Chine wetting point from stem/LOA	1.	1.
Trim angle, deg	1.60	1.09
Transom draft, Ht/Zk	.334	.290
Lift/Drag Ratio	10.1	10.5

Here, the gravity effects are stronger, as is necessary, but a higher lift/drag ratio is again developed at non-infinite Froude number. The reduction of drag by the rise of the stern of the boat is predicted to more than offset the increase in drag from the trailing wave system. The lift is a constant equal to the boat weight at all calm water conditions.

It is important to acknowledge again that planing craft behave differently than displacement craft with regard to the effects of running trim and draft on resistance. Most, if not all, of the codes that have been developed for catamaran resistance and seakeeping are for displacement catamarans. But most high-speed SES, and AEV, are developed with hard-chine planing demi-hulls that develop lift.

IIIb Non-Zero Cushion Pressure

This sub-section evaluate the effects of gravity wave-making with SES non-zero air cushion pressure. In view of the above tables little difference from the Part A predictions at 50 knots and zero gravity would be expected.

Table 6 is equivalent to Table 4 but with 75% of the craft weight supported by the air cushion.

Table 6

Base SES Case: Catamaran Running Geometry at 50 knots with **75%** of Craft Weight Supported by Cushion Pressure

	g = 0	g ≠ 0
Froude number based on LOA, $\frac{V}{\sqrt{g \cdot LOA}}$	∞	2.6
Wetted Length/LOA, Xmax/LOA	.612	.614
Chine wetting point from stem/LOA	1.	1.
Trim angle, deg	.332	.320
Transom draft, Ht/Zk	.0722	.0709
Lift/Drag Ratio	16.79	16.86

The Table 6 data at g = 0 is comparable to Figure 10 from the Part A report. Again, there are slight differences in the g = 0 prediction from Part A due to refinements in the CatSeaAir code at the time of incorporation of the non-zero gravity hydrodynamics. These refinements included adding seal and air momentum drag components in the SES analysis.

As expected, with the 10m craft at the high 50 knot Fn of 2.6, gravity effects in the hydrodynamics are predicted to contribute little. Lift/drag ratio is predicted to increase slightly by inclusion of gravity wave hydrodynamics. As offered in the preceding, with total lift constant in calm water, drag is reduced more by the lift of the boat aft via its stern wave than by the wave drag from wave radiation downstream. This is exhibited in Table 6.

Also note, same as in part A, the power required of the lift fans has not been added to the drag in the lift/drag calculation in this analysis. The other SES drag components, i.e., cushion drag, momentum drag, and seal drag have been accounted for in the CatSeaAir SES drag prediction for the cases with and without gravity.

In consideration of the slight differences between g = 0 and g > 0 in the above tables for the 10m boat operating at 50 knots, the g = 0 analysis of Part A is considered to cover the calm water analysis reasonably well, and it executes much faster.

IV Calculations with Gravity, Seaway Dynamics

Samples of the seaway dynamic analysis of the 10m craft at 50 knots are re-done with and without gravity to have a record of the comparison with identically the same EDITH 1-2g CatSeaAir code. 6,000 time steps, corresponding to $\tau = 150$, rather than 10,000 steps for $\tau = 250$, are computed here in view of the time intensity of the gravity computation; 6,000 steps are viewed as adequate for judging the relative influence of gravity in this high speed hydrodynamics. Figure 27 plots the bow vertical acceleration for zero air cushion support, both with and without gravity, in superposition. The same curves for 75% weight support in the SES is Figure 28. Figure 14 is the corresponding plot for zero gravity and zero air support from the earlier work in Part A. The corresponding curves for air support at g = 0 are Figure 21. The difference with and without inclusion of gravity in these two high Fn computations is hardly detectable. There are differences due to elevated cushion pressure.

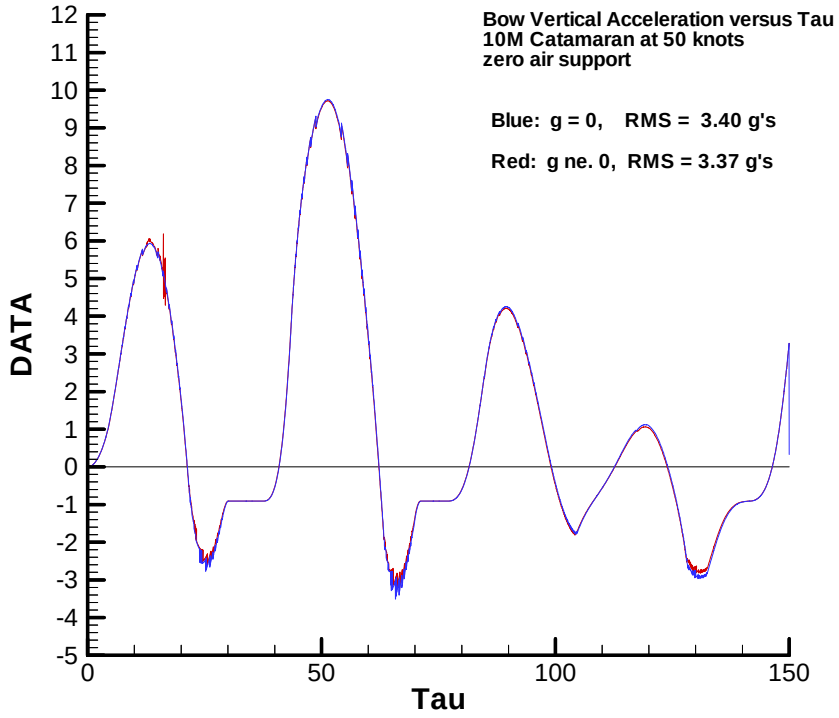

Figure 27: Bow Acceleration in g's for Zero Air Support, With and Without Gravity, Versus Time

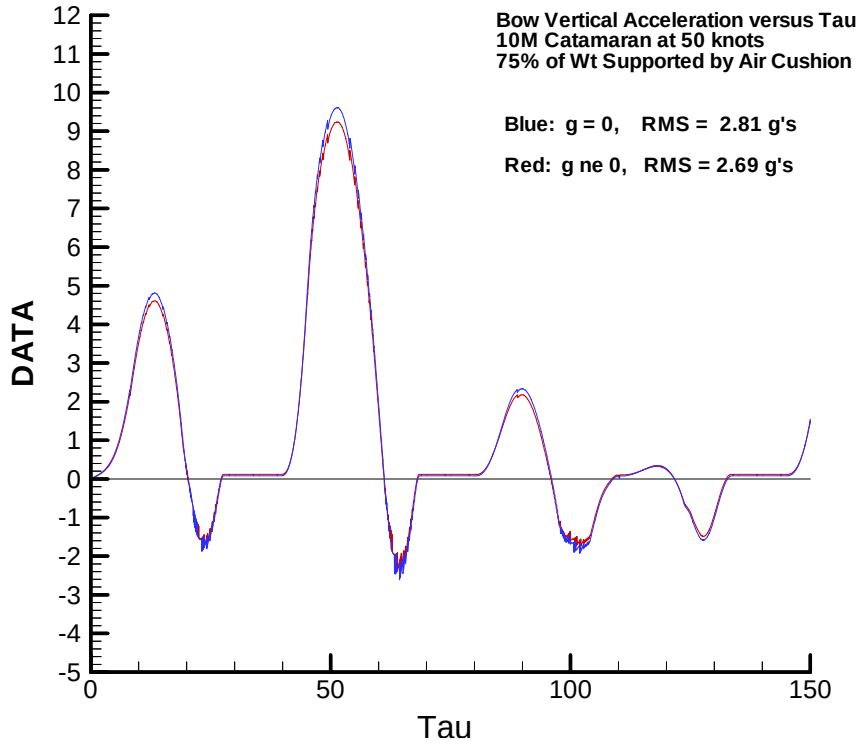

Figure 28: Bow Acceleration in g's for 75% Weight Air Support, With and Without Gravity, Versus Time

As discussed in Part A, the impact acceleration curves show little effect of air support except near free-fall, where the cushion pressure is significant relative to the vanishing hydrodynamic impact pressure. Here it is assumed that the SES lift fans are capable of maintaining fixed cushion pressure with increasing air leakage as free-fall is approached. The free-fall flats on these figures must obviously lie between the two levels shown due to large leakage. The large hydrodynamic impact pressure dominates the cushion pressure in the total demi-hull surface pressure in the vicinity of the positive and negative pressure peaks.

Figures 27 and 28 do indicate a 20% reduction in RMS acceleration due to air support, with gravity, as noted thereon.

A final demonstration for the dynamic analysis of the 10m craft consists of plotting dynamic pressure distributions over selected section contours corresponding to stations in x, at selected times. This is considered appropriate (even necessary) in view of the title of this SSC project; the loading for structural analysis is, of course, of primary interest.

Figure 29 is the distribution of force coefficient, $C_f(x,\tau)$, corresponding to the pressure sectionally integrated at $\tau = 50$ for the catamaran at zero air support, re Figure 27. Figure 30 plots the same data for 75% cushion support.

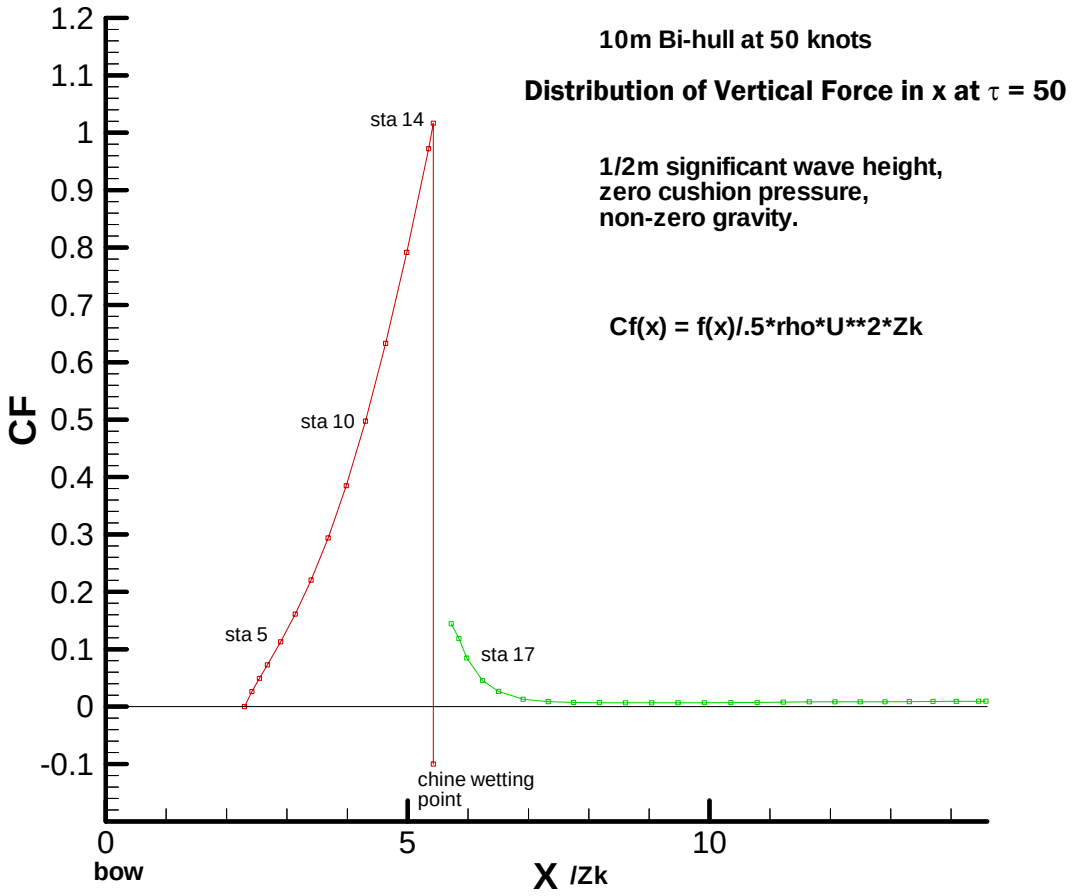

Figure 29: Vertical Force Distribution in x at time $\tau = 50$ for Zero Cushion Support, Non-zero Gravity (refer to Figure 27)

The near discontinuity on these two figures is the occurrence of chine-wetting. Just as in calm-water planning the hull pressure (and lift) drop by an order of magnitude when the jet-head reaches the chine, proceeding outward. This is for the case of cylindrical wetted geometry in x at chine-wetting and aft, which is the common case and the case here. Vessel-generated gravity waves then boost the pressure and lift aft in calm water. In the case of Figures 28 and 29, at $\tau = 50$ the instantaneous motions and ambient waves, along with the cylindrical geometry, are responsible for almost nullifying the pressure loading aft.

The impact acceleration is largest at the bow around this time, implying high sectional and contour pressure loading there; refer to Figures 27 and 28. Therefore, bow contour pressure distributions have been plotted at $\tau = 50$ at each of the four x-stations marked on Figures 29 and 30. The pressure plots are Figures 31 through 38; 31 through 34 are for zero cushion pressure and 35 through 38 for 75% cushion support. The plots are transversely in z from the demi-hull keel to the chine. The vertical component of the integral of this pressure across the section at each x are the values at the respective x on Figures 29 and Figure 30.

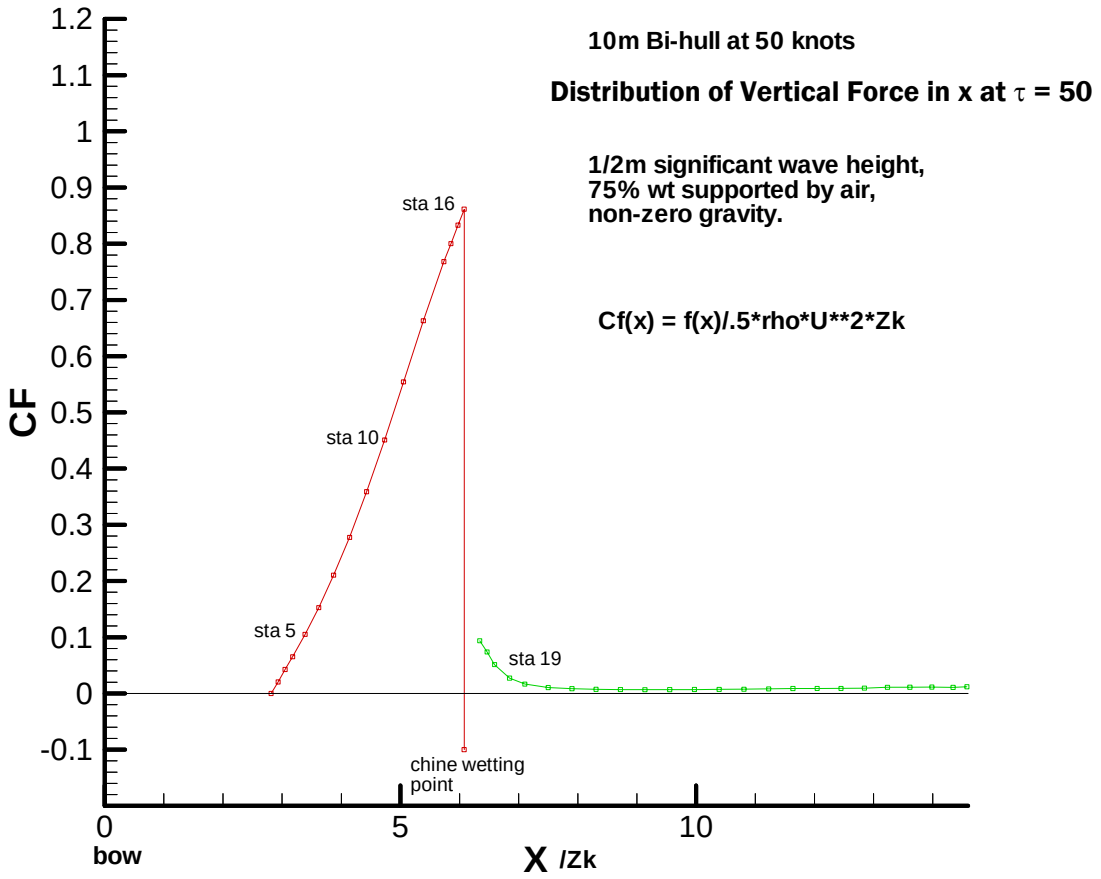

Figure 30: Vertical Force Distribution in x at time $\tau = 50$ for 75% Cushion Support, Non-zero Gravity (refer to Figure 28)

Turning to the pressure distribution plots at the x-stations:

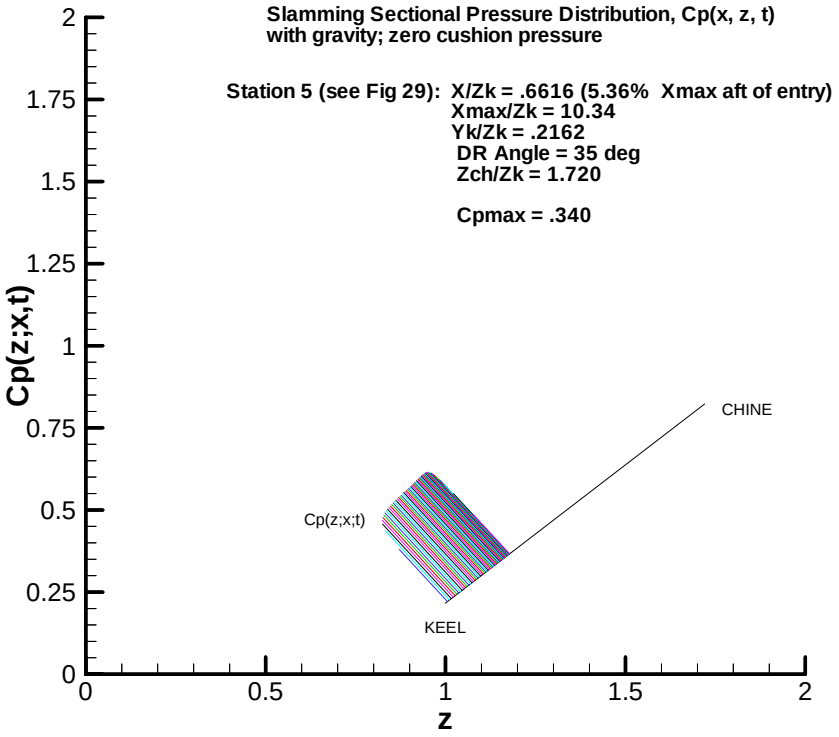

Figure 31: Half Demi-hull Section $C_p(x, z, t)$ at Station 5.36% of Wetted Length Aft of Entry (refer to Figure 29)

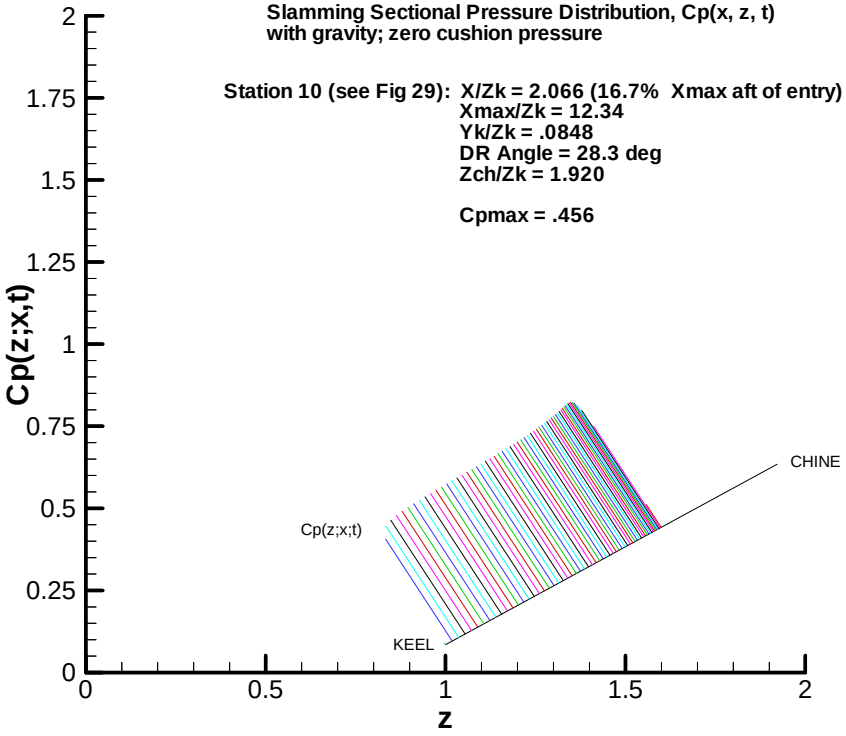

Figure 32: Half Demi-hull Section $C_p(x, z, t)$ at Station 16.7% of Wetted Length Aft of Entry (refer to Figure 29)

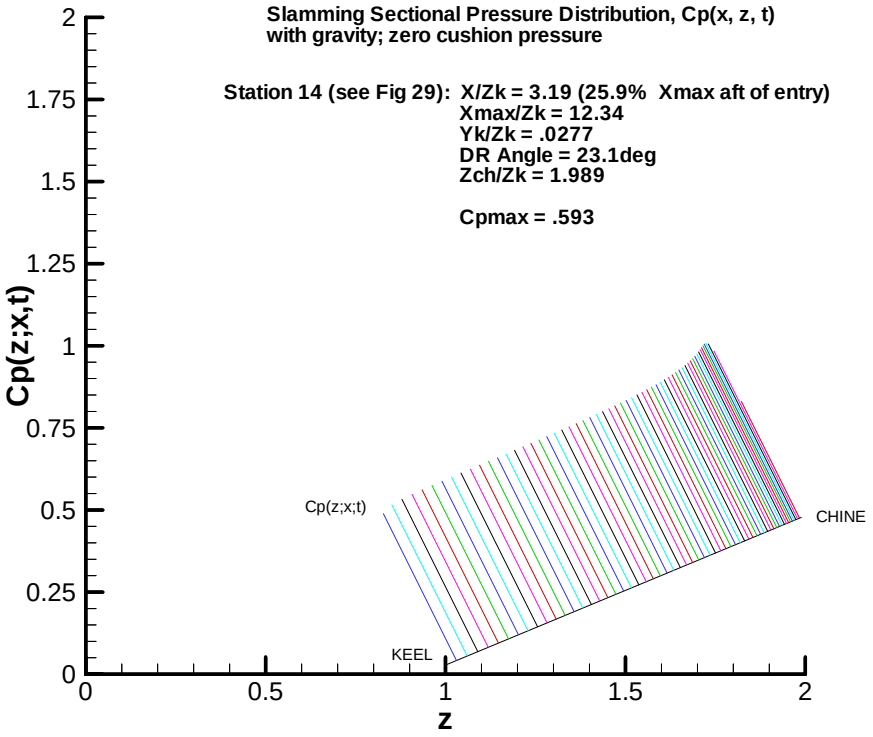

Figure 33: Half Demi-hull Section $C_p(x, z, t)$ at Station 29.5% of Wetted Length Aft of Entry (refer to Figure 29)

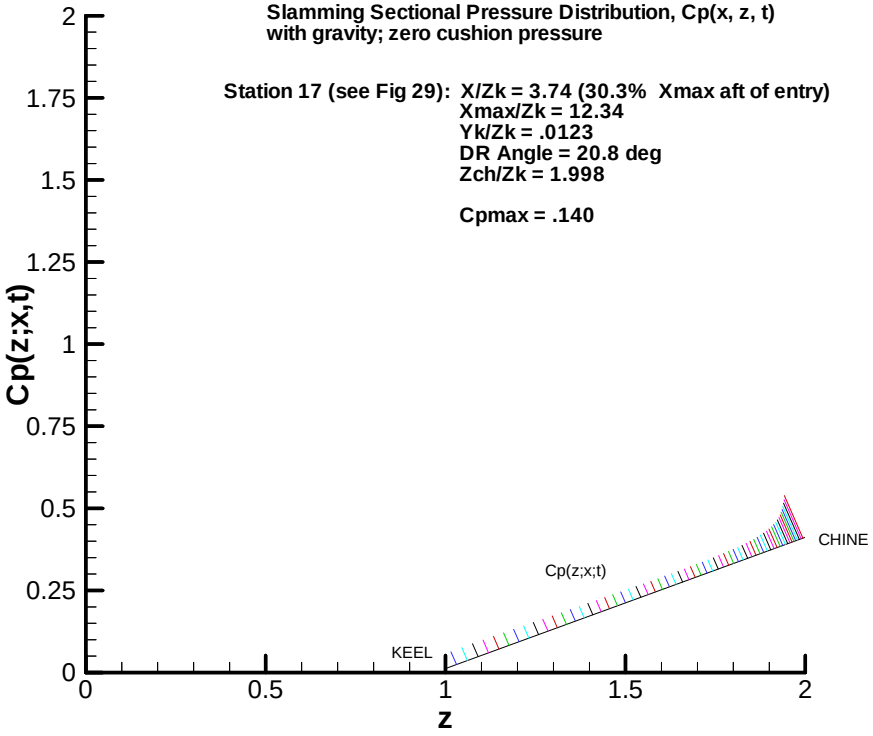

Figure 34: Half Demi-hull Section $C_p(x, z, t)$ at Station 30.3% of Wetted Length Aft of Entry (refer to Figure 29); Zero Cushion Pressure

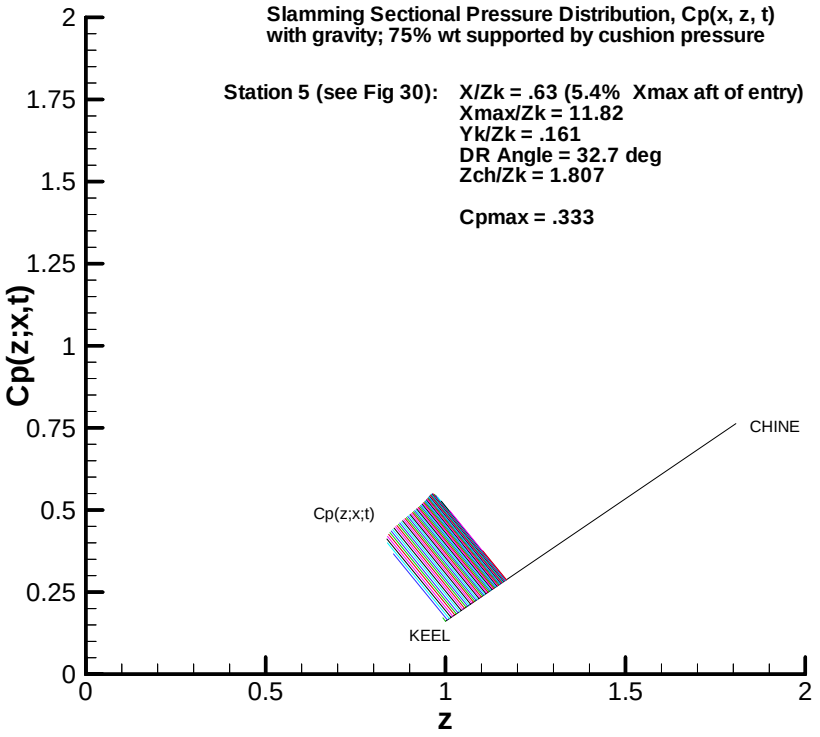

Figure 35: Half Demi-hull Section $C_p(x, z, t)$ at Station 5.4% of Wetted Length Aft of Entry (refer to Figure 30); 75% Wt by Cushion Pressure

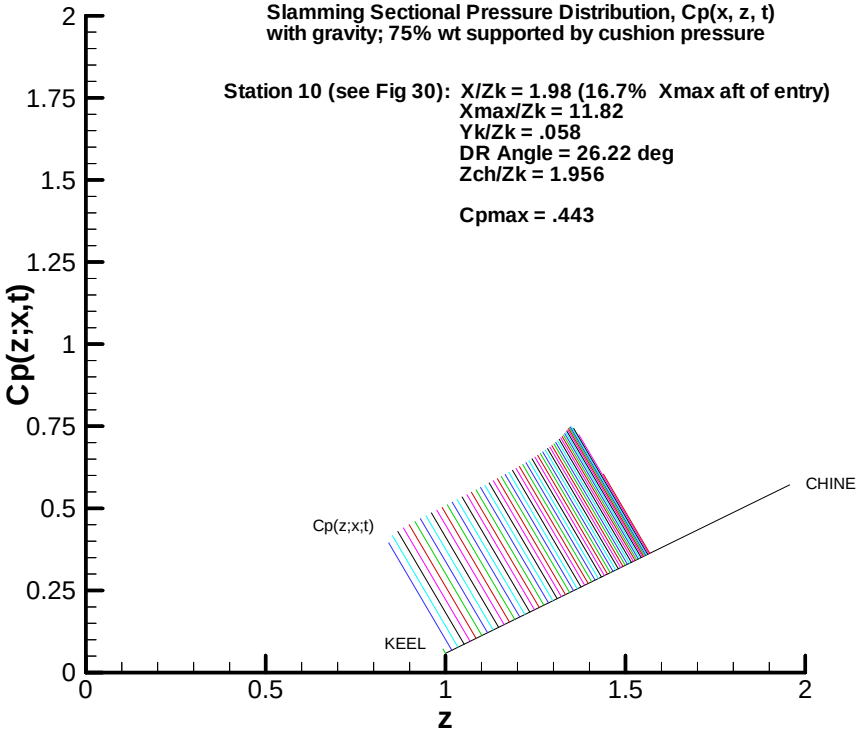

Figure 36: Half Demi-hull Section $C_p(x, z, t)$ at Station 16.7% of Wetted Length Aft of Entry (refer to Figure 30); 75% Wt by Cushion Pressure

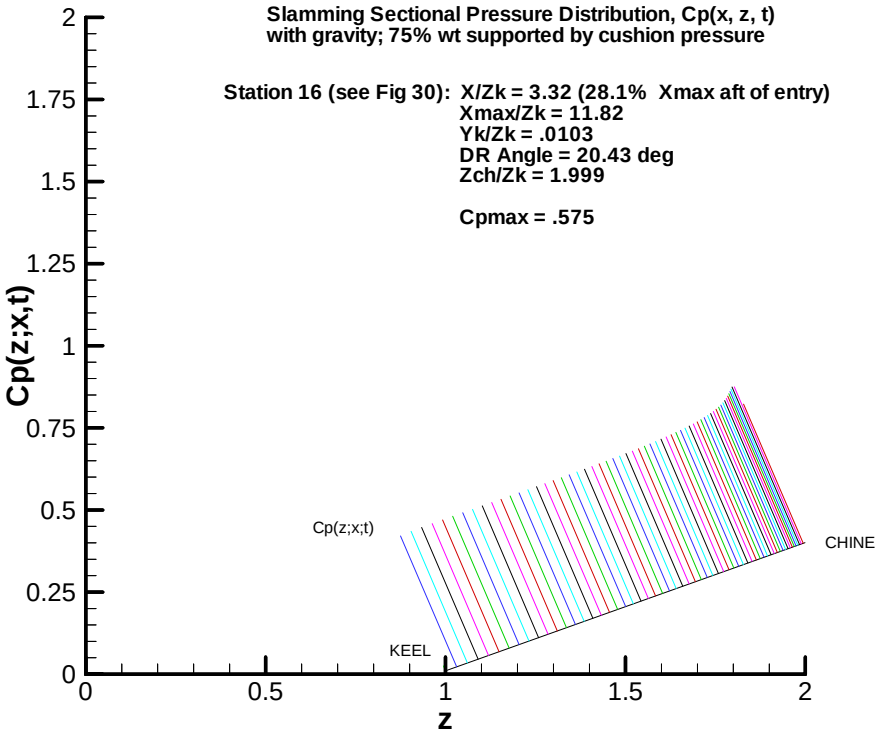

Figure 37: Half Demi-hull Section $C_p(x, z, t)$ at Station 28.1% of Wetted Length Aft of Entry (refer to Figure 30); 75% Wt by Cushion Pressure

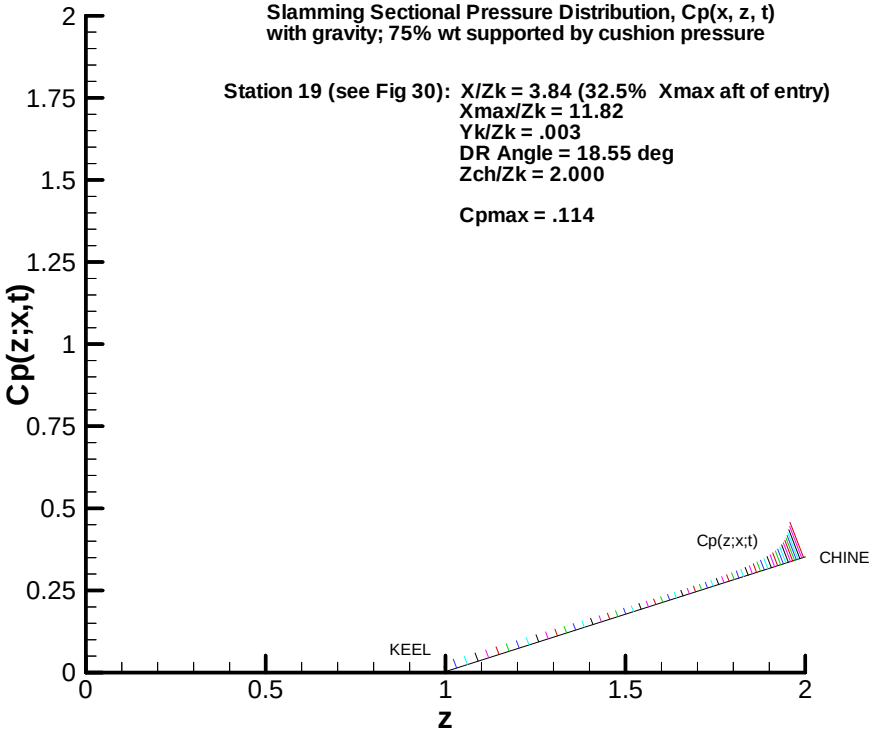

Figure 38: Half Demi-hull Section $C_p(x, z, t)$ at Station 32.5% of Wetted Length Aft of Entry (refer to Figure 30); 75% Wt by Cushion Pressure

Although hidden by the tic-mark at z = 1 on the latter four figures above, the keel pressure is equal to the cushion pressure; this is approximately C_{p0} = .01, referred to water.

V Comparison of Code Predictions with Model Tests

The EDITH 1-2g CatSeaAir code has been applied to the Bell-Halter 110 ft SES whose design was extensively model tested in the 1970's at the old Lockheed, San Diego facility (LOLTB), as reported in LMSC/D682700, December 1979. Figure 39 is the arrangement of the 1/15-scale (7 ft) model that was tested. Figures 40a and 40b are the body plan from which the geometry input for CatSeaAir was extracted.

A. *Analysis versus Experiments - Calm-Water*

The model experiments in calm water reported the following data needed for comparison with the analysis:

steady speed, U
weight, W
longitudinal center of gravity, xcg
air cushion pressure, p_{ac}
transom draft, Ht/Zk
trim
drag coefficient, Cd

The % air support, WA, was obtained from the cushion pressure by multiplying p_{ac} by the cushion ceiling area and dividing by the model weight, W. The transom draft was extrapolated from the measured mid-cushion draft using the measured trim angle.

The theoretical model has three degrees of freedom: heave, pitch, and surge. But the physical model was restrained in surge, so that drag representing the surge equation. This requires that of the seven variables listed above only three can be predicted by CatSeaAir and the others must be considered as input to the analysis. The normal choice for input would be U, W, xcg, and WA, with the trim, transom draft and drag considered as output to be compared with the experimental measurements. This is the context of the 10m analysis in Part A and the preceding sections of Part B, and was also the context of the experimental data presentation.

However, with trim, draft, and drag as the output, the calculations were very poorly behaved in some cases and failed to converge to reasonable values, if at all, in others. After a great deal of calculation it was decided that xcg and WA given for the tests were not consistent. WA had to be estimated from the cushion pressure measurement by assuming the cushion pressure uniform and constant over the wet deck. There was also some seeming confusion over the experimental xcg determination. Two xcg's were reported; one in air and a CG in "hover" on the air cushion at zero forward speed. They were different and it was not always clear which was being reported. These test were conducted 30 years ago, and while one or two of the TEXTRON people involved were still available and helpful, the xcg issue, particularly, remained confusing.

It was therefore finally decided to take the trim and draft as the two input variables, along with U and W, for the calm water analysis, and to calculate WA, xg and Cd for comparison to the tests data. This is reported below in Table 7 for the three model weights of Condition 1: W = 70, 81.5, and 93 lbs.

Figure 39: BH 110 Test Model

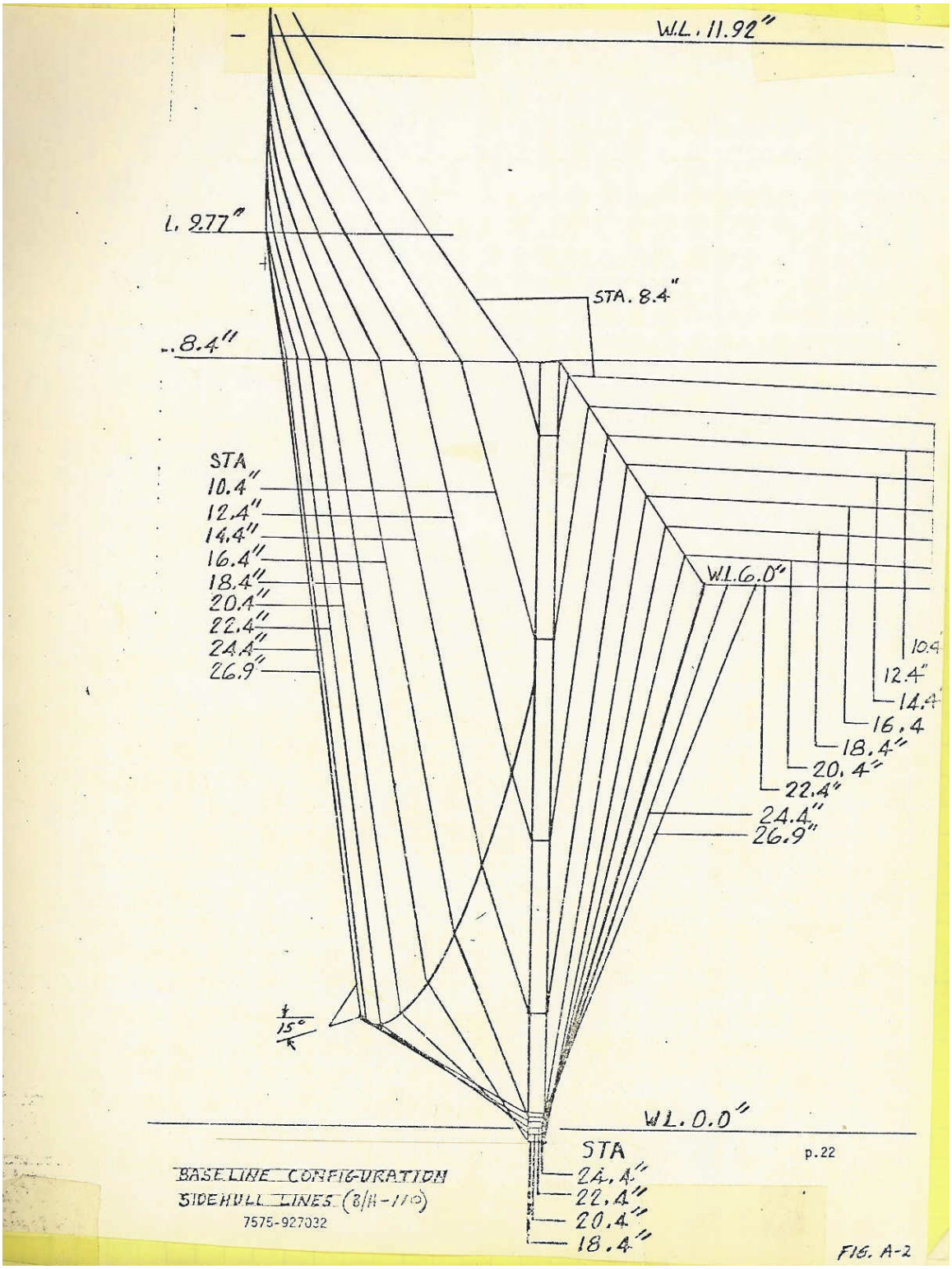

Figure 40a: BH110 (Model B-34C) Body Plan Forward

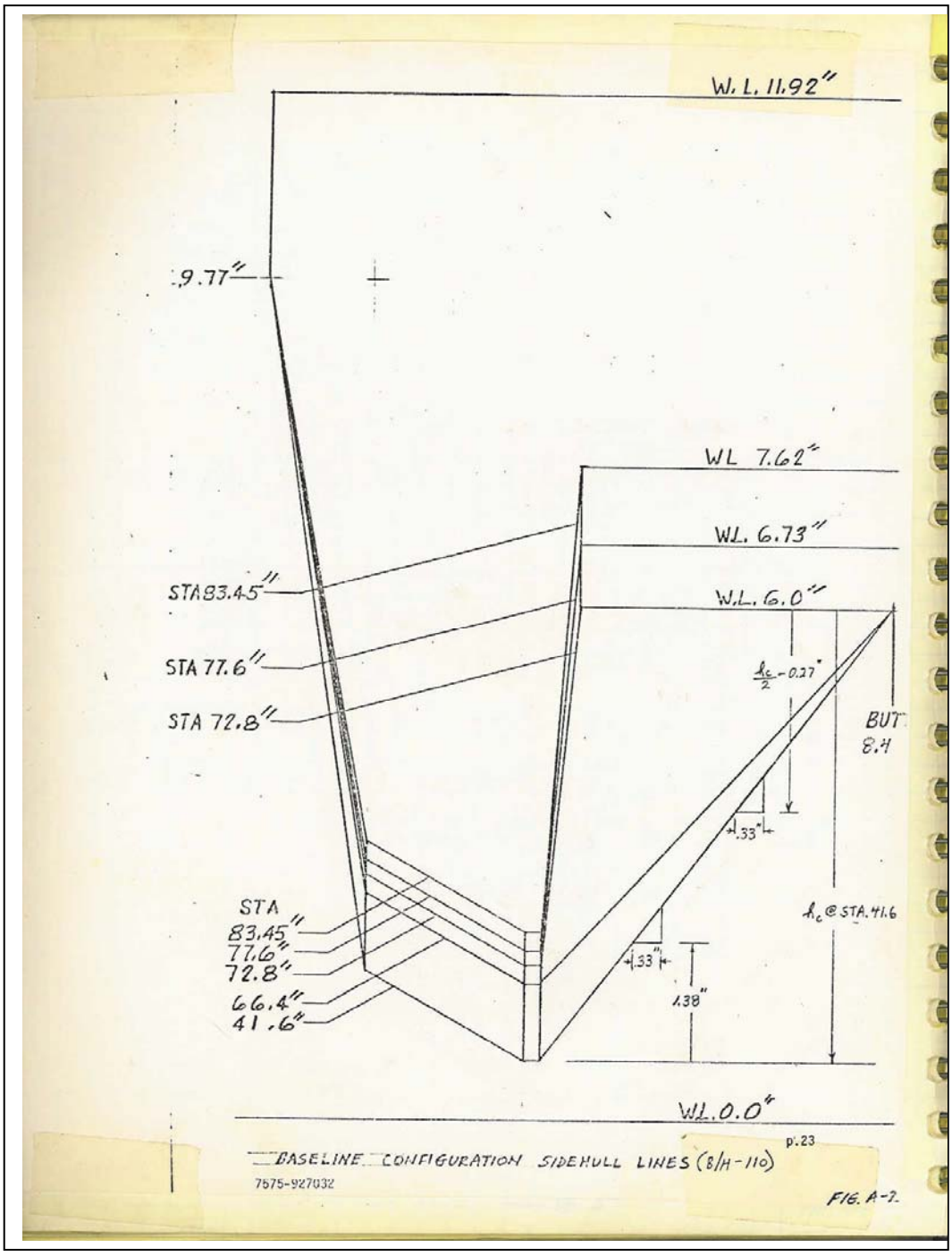

Figure 40b: BH110 (Model B-34C) Body Plan Aft

Note from these figures that the BH110 is a “rockered” hull with 2.6 degree of keel rocker aft.

Table 7

BH 110 Calm Water Runs, Model B34C, Configuration 1

LMSC/D682700, 12/79, Book 5

VAI Analysis of 9-06

No.	U(fps)	Vfs(k)	W(#)	%xge	Trim	Ht	Cl	%WAe	%WAc	xcge	xcgc	%xcgc	Cde	Cdc
362	12.91	29.60	70.0	0.0	1.28	.1229	.3935	87.5	81.0	2.623	2.485	-2.61	.0233	.0169
363	17.26	39.58	70.0	0.0	0.57	.0785	.2202	85.5	78.8	2.623	2.713	+1.70	.0126	.0194
364	13.10	30.04	70.0	-.70	1.59	.1273	.3822	78.7	81.9	2.586	2.465	-2.99	.0221	.0158
365	17.48	40.08	70.0	-.70	0.97	.0874	.2147	83.7	82.9	2.586	2.499	-2.52	.0103	.0118
366	24.28	55.68	70.0	-1.5	0.75	.0738	.1113	81.7	86.3	2.544	2.536	-1.65	.0069	.0095
367	13.12	30.08	70.0	-1.5	1.81	.1407	.3811	85.0	81.9	2.544	2.466	-2.97	.0215	.0161
368	17.48	40.08	70.0	-1.5	1.17	.1012	.2147	82.9	82.7	2.544	2.498	-2.37	.0108	.0118
370	24.08	55.22	70.0	-2.0	0.88	.0823	.1131	78.4	85.4	2.517	2.526	-1.84	.0068	.0094
371	30.90	70.86	70.0	-2.0	0.63	.0634	.0687	75.4	86.8	2.517	2.554	-1.31	.0049	.0083
372	9.20	21.10	70.0	-.50	2.27	.1233	.7751	82.6	87.0	2.597	2.433	-3.60	.0409	.0216
378	17.32	39.72	70.0	-1.0	1.00	.0941	.2187	82.0	84.4	2.571	2.502	-2.29	.0102	.0120
393	17.40	39.90	70.0	-1.0	1.14	.0980	.2168	86.7	83.0	2.571	2.495	-2.42	.0106	.0117
397	9.15	20.98	81.5	0.0	2.48	.2307	.9125	86.5	75.0	2.623	2.459	-3.10	.0549	.0393
398	13.08	30.00	81.5	0.0	1.45	.1315	.4465	89.1	79.1	2.623	2.478	-2.74	.0268	.0183
399	9.15	20.98	81.5	-.50	2.68	.2374	.9125	85.2	75.0	2.597	2.458	-3.12	.0562	.0397
400	13.08	30.00	81.5	-.50	1.74	.1344	.4465	87.7	82.3	2.597	2.460	-3.08	.0251	.0173
401	17.41	39.92	81.5	-.50	0.98	.0984	.2509	86.3	83.3	2.597	2.520	-1.95	.0132	.0134
402	24.00	55.03	81.5	-.50	0.61	.0777	.1326	85.1	79.5	2.597	2.743	+2.27	.0088	.0145
403	13.10	30.04	81.5	-1.0	1.96	.1499	.4451	87.4	81.9	2.571	2.462	-3.05	.0252	.0178
404	17.44	39.99	81.5	-1.0	1.22	.1103	.2509	84.7	81.5	2.571	2.504	-2.25	.0117	.0130
405	24.06	55.17	81.5	-1.0	0.85	.0834	.1320	84.0	85.4	2.571	2.537	-1.63	.0080	.0100
406	12.35	28.32	81.5	-1.5	2.37	.1775	.5008	85.4	81.3	2.544	2.458	-3.12	.0302	.0205
407	17.43	39.97	81.5	-1.5	1.38	.1113	.2514	83.6	83.4	2.544	2.488	-2.55	.0122	.0123
408	24.08	55.17	81.5	-1.5	0.94	.0830	.1317	81.1	84.4	2.544	2.523	-1.89	.0074	.0097
416	17.40	39.90	81.5	-1.0	1.24	.1104	.2524	84.3	81.8	2.571	2.501	-2.31	.0114	.0129
422	9.08	20.82	81.5	.50	2.30	.2215	.9265	85.9	74.6	2.649	2.469	-2.91	.0543	.0398
423	23.89	54.78	81.5	-2.0	1.05	.0953	.1339	81.4	83.0	2.517	2.531	-1.74	.0074	.0102
425	9.16	21.00	93.0	0.0	2.75	.2617	1.038	85.4	73.8	2.623	2.469	-2.91	.0657	.0485
426	13.09	30.02	93.0	0.0	1.75	.1500	.5082	86.7	79.8	2.623	2.469	-2.91	.0299	.0203
434	13.09	30.02	93.0	-.50	1.99	.1517	.5082	86.5	82.1	2.597	2.457	-3.14	.0293	.0195
435	17.29	39.65	93.0	-.50	1.17	.1125	.2913	83.6	83.0	2.597	2.506	-2.21	.0135	.0142
436	17.42	39.95	93.0	-1.0	1.40	.1160	.2870	84.4	82.9	2.571	2.489	-2.54	.0131	.0133
437	17.44	39.99	93.0	-1.5	1.54	.1271	.2863	83.4	82.4	2.544	2.493	-2.46	.0132	.0135

Key:
No. run number from test book 5
U: model speed in tank
Vfs: Froude scaled full scale speed in knots
W: weight of model, lbs
%xg: xcg shift as % of cushion length from cushion center from report
Trim: trim angle, deg, from report *(input)*
Ht: transom draft/Yk; Yk demi-hull keel offset from report *(input)*
Cl: hull lift coefficient, $W/1/2\rho U^2 Yk^2$ (*calc*)
%WA percent of W supported by air (*experimental and calc*)
xcg: location of center of gravity forward of transom/Yk (*experimental and calc*)
Cd: hull drag coefficient, $D/1/2\rho U^2 Yk^2$ (*experimental and calc*)
sub – e: experimental
sub – c: CatSeaAir calculation

Description of the data is provided at the bottom of the table. The comparisons were made for all of the data for model Condition 1. The differences in the several Conditions are generally superficial non-systematic variations in the model. Condition 1 was considered adequate coverage.

Choosing not to invert the equations of motion for trim and transom draft avoided the time stepping and actually made the CatSeaAir calculations much simpler. CarSeaAir was first run with WA set to zero with the trim and draft set to the Table 7 measured values. This produced W_h and xcg_h, with W_h being the weight supported by hydrodynamics/hydrostatics with zero air cushion pressure at the given trim and draft, with xcg_h being the center of application of W_h. Weight and moment component summation gives:

$$1 = \frac{WA}{W} + \frac{W_h}{W} \tag{9}$$

$$xcg = \frac{WA}{W} xcg_A + \frac{W_h}{W} xcg_h \tag{10}$$

with xcg_A being the known center of the air cushion from the transom.

Equation (9) is first solved for WA/W, which is substituted into (10) to calculate the required xcg. These are the values listed in Table 7 as %WAc and %xcgc[1].

Figures 41 is a plot of the trim and draft input values from Table 7 for each of the three model weights.

1: $\%xcg = 100(xcg - xcg_A)/xcg_A$

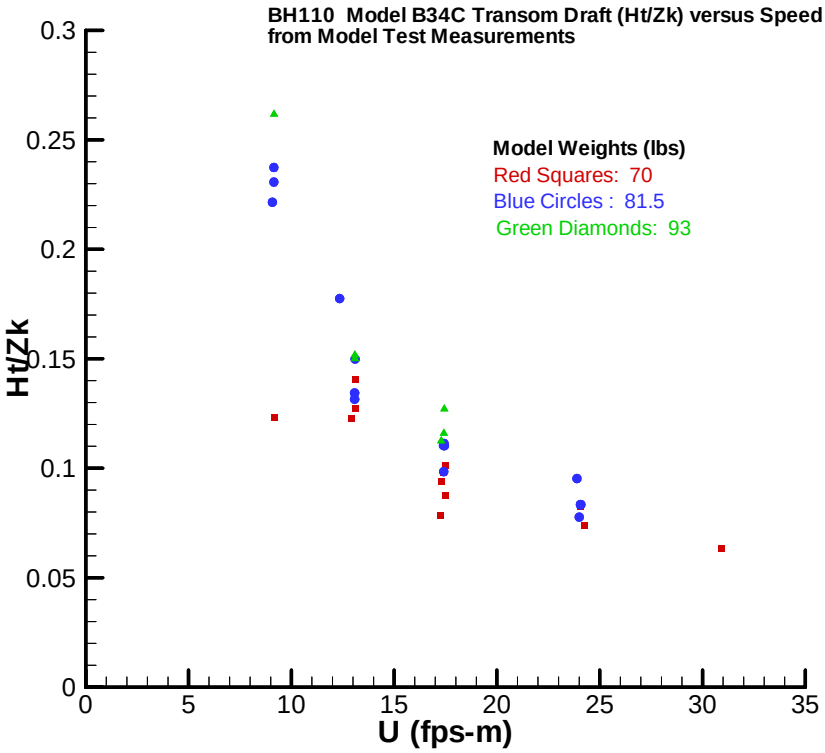

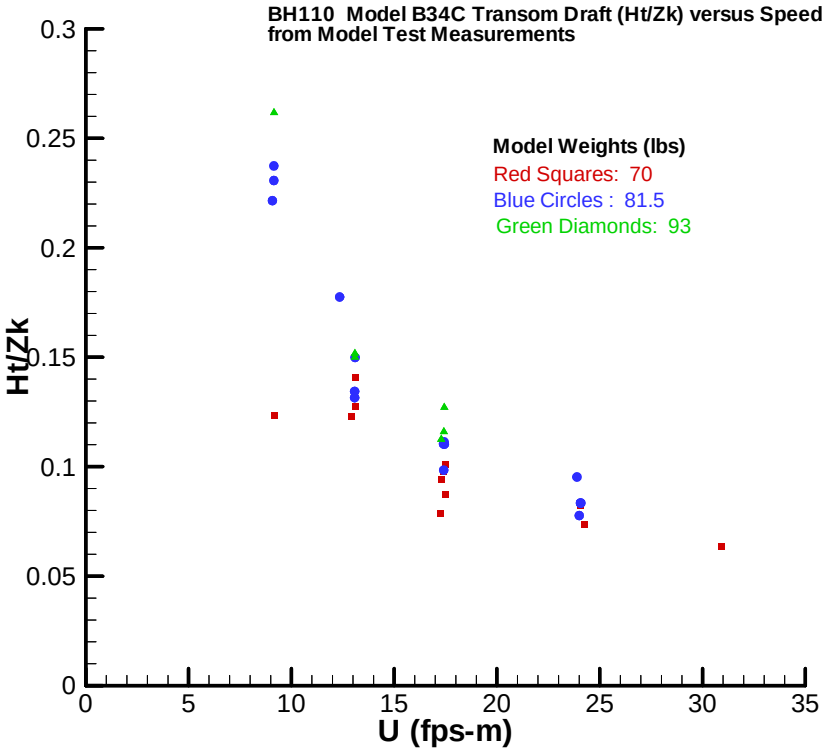

Figures 41: Measured Trim and transom Draft versus Speed for the Three Model Test Weights of 70, 81.5 and 93 lbs.

The data of Figure 41, and Table 7, is difficult to plot as conventional curves versus speed because so much is varying. Some of the variation is systematic input variation and some seems to be random experimental variability. It seems to be best displayed in terms of the unconnected data points as "scatter graphs," as on Figure 41.

Figures 42 to 47 are the calculated WA fraction and %xcg forward of mid-cushion from (9) and (10) via the Table 7 runs for each of the three weights.

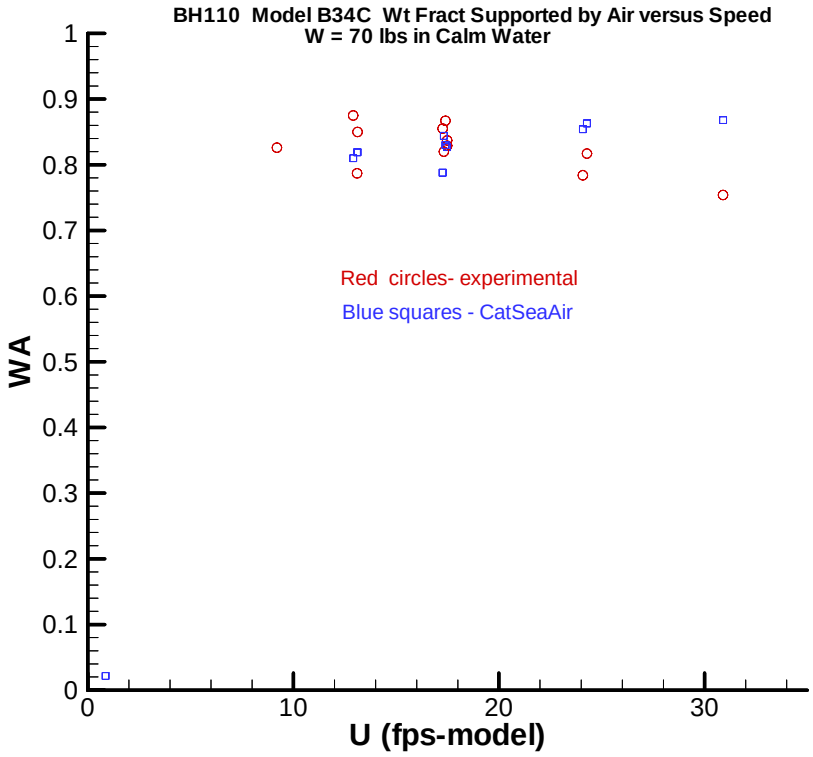

Figure 42: Calculated WA/W versus Model Speed for 70 lb Model Weight

The calculated WA/W displayed on Figures 42, 43, and 44 are considered to be quite close to the experimental in consideration of the variability of the input trim and transom draft measurements displayed on Figure 41.

As for the xcg data on Figures 47, 48, and 49, the test values were considered to be part of the test set-up. Except for a few irregular points the xcg required by CatSeaAir are lower (xcg further aft) and the variability, or sensitivity to speed differences, seems to be lower, in general. It should be kept in mind that a 1% CG shift is only about 3/8 inch relative to the length of the 7-foot model. It seems likely that movements of this magnitude would be hard to set by the simple balance and leveling methods used. And then there was uncertainty about "in air" or "in hover" cited in the preceding.

While the xcg comparisons may not so strongly contribute to establishing the validity of CatSeaAir, they are considered not to diminish it either.

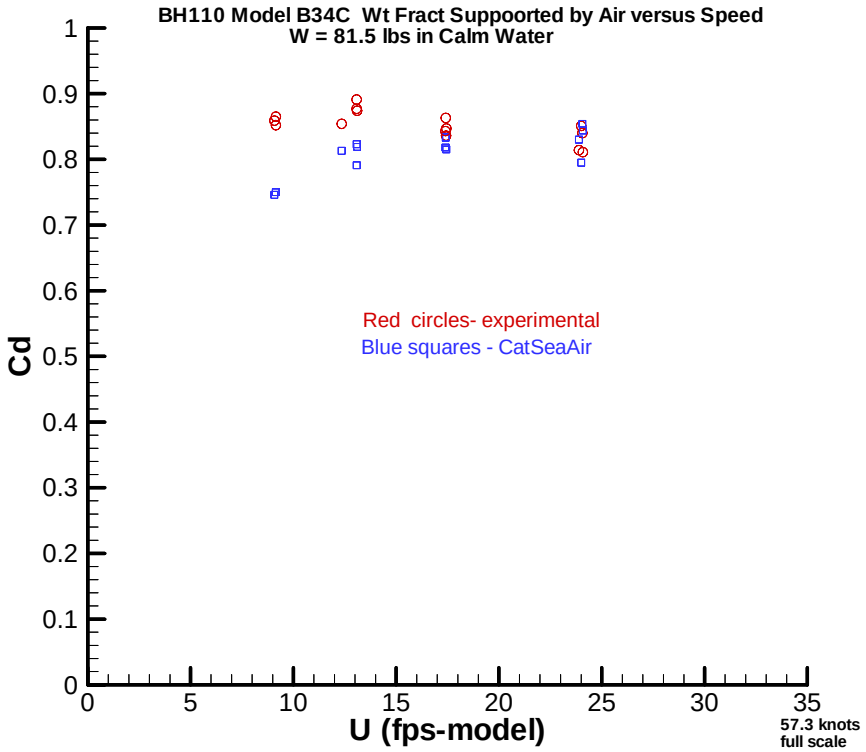

Figure 43: Calculated WA/W versus Model Speed for 81.5 lb Model Weight

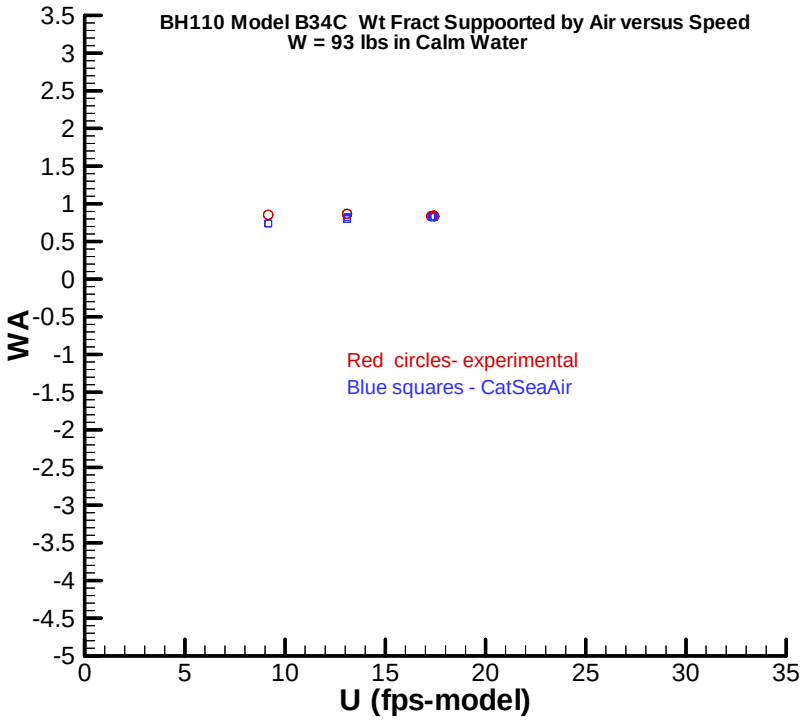

Figure 44: Calculated WA/W versus Model Speed for 93 lb Model Weight

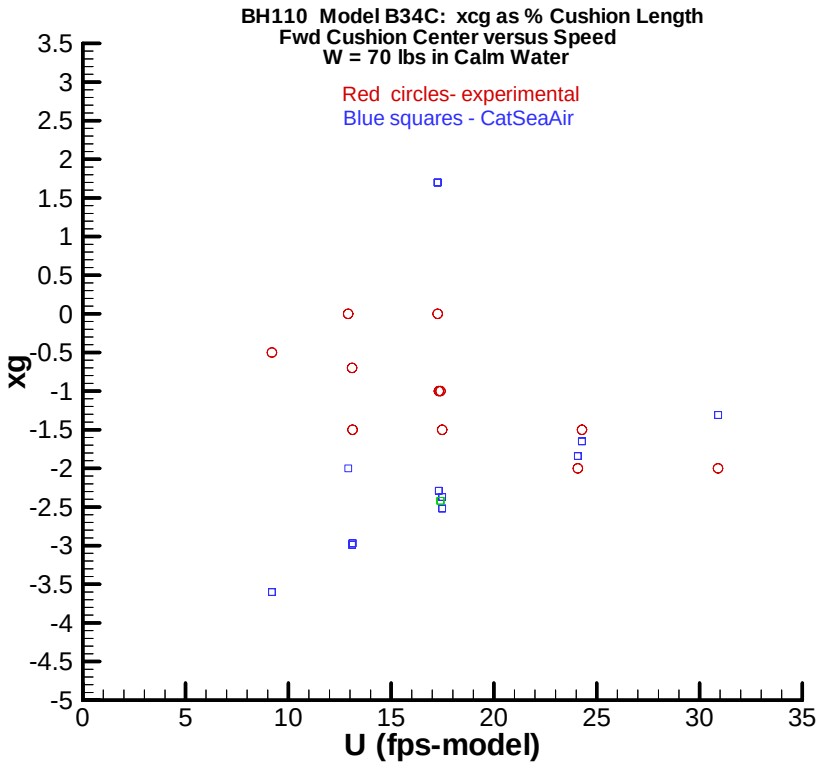

Figure 45: Calculated %xcg Versus Speed for 70lb Model Weight

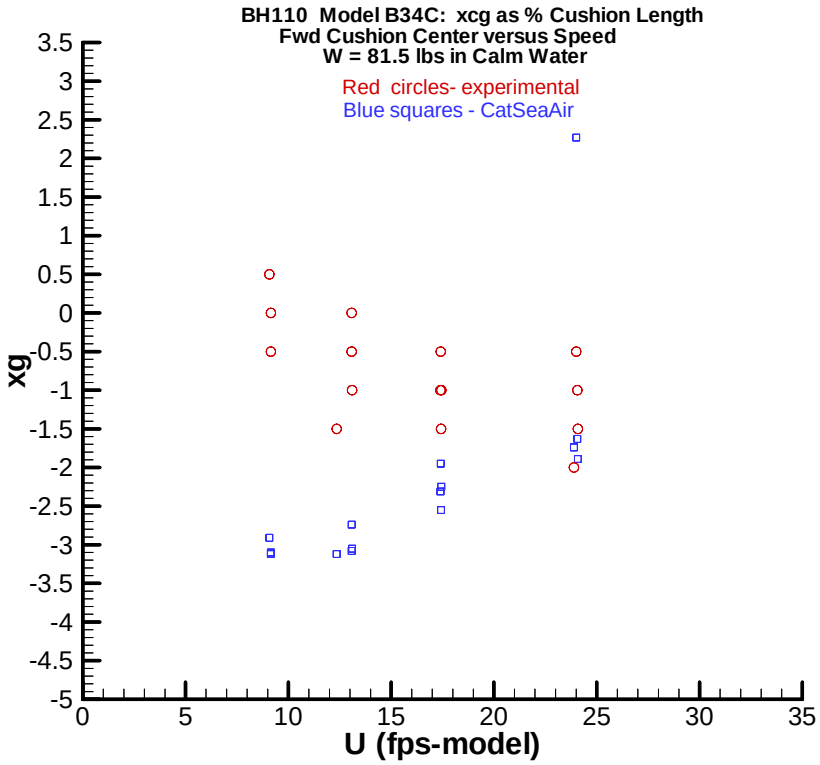

Figure 46: Calculated %xcg Versus Speed for 81.5lb Model Weight

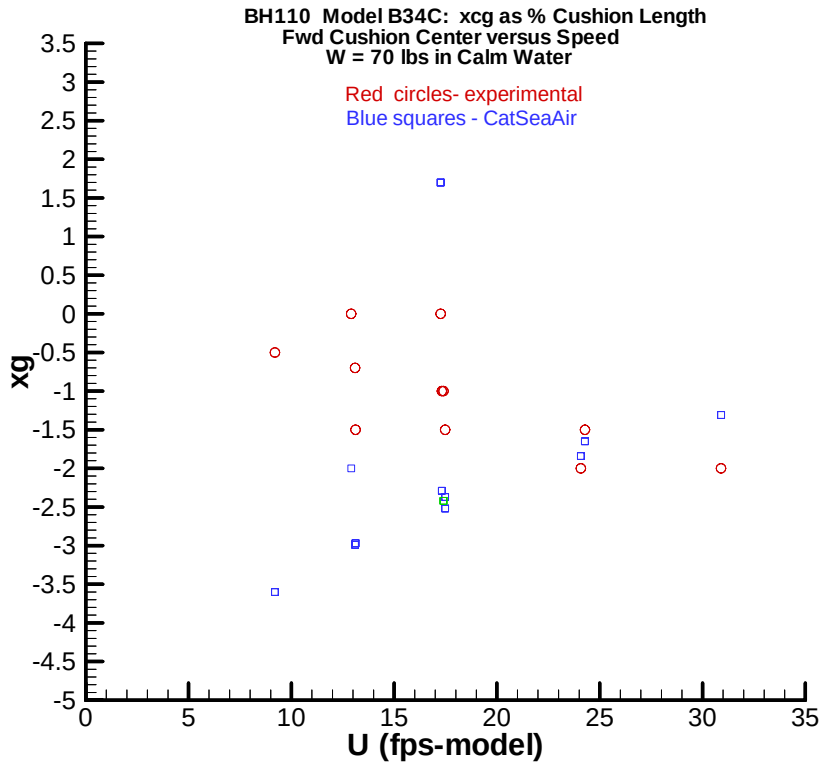

Figure 47: Calculated %xcg Versus Speed for 93lb Model Weight

A more supportive CatSeaAir calculation is considered to be that of the calm-water drag. This is Figures 48, 49, and 50, in the same format as the preceding comparisons.

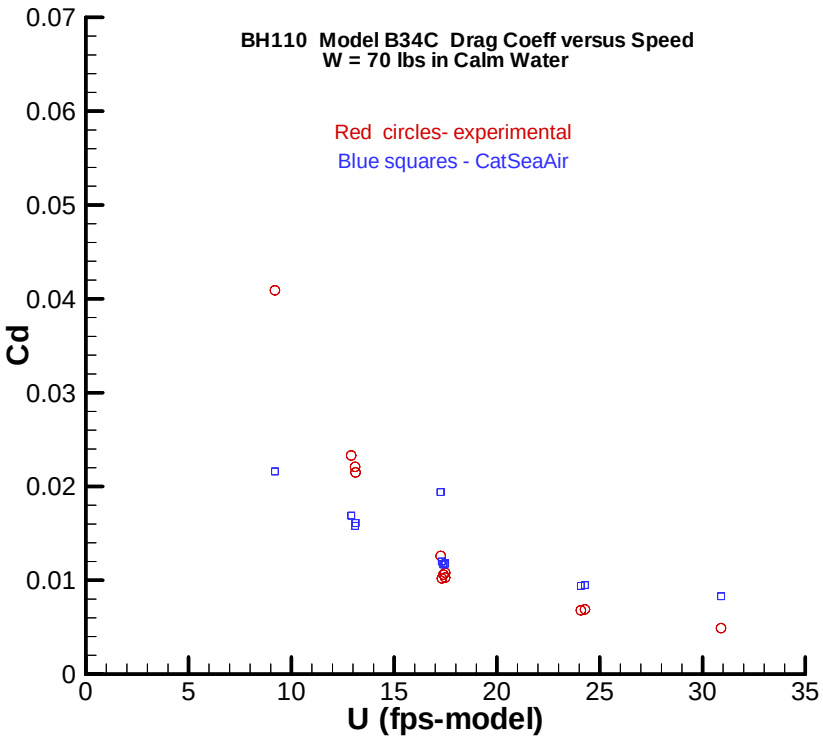

Figure 48: Calculated Cd Versus Speed for 70lb Model Weight

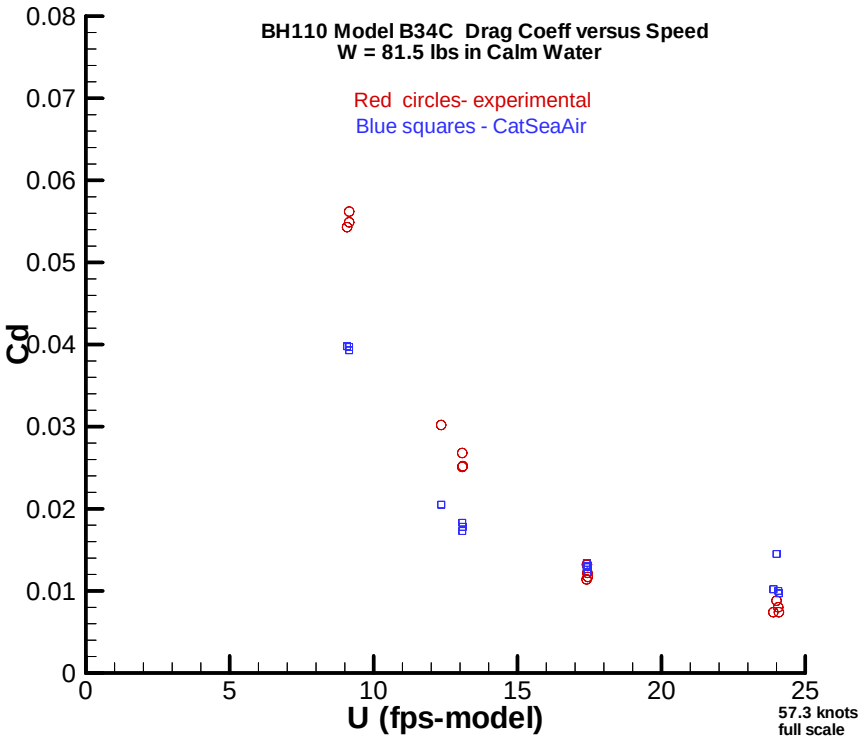

Figure 49: Calculated Cd Versus Speed for 81.5lb Model Weight

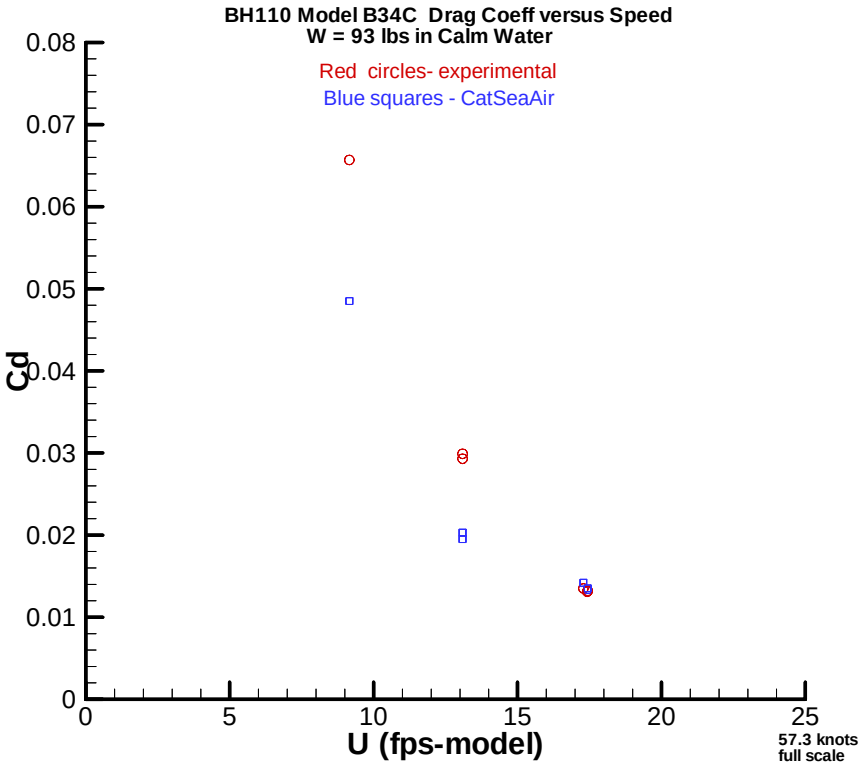

Figure 50: Calculated Cd Versus Speed for 93lb Model Weight

As a matter of record the drag coefficient is by the previous definition:

$$C_d = \frac{drag}{\frac{1}{2}\rho U^2 Z_k} \tag{11}$$

As these last three figures show, the calculated calm water drag is generally a little lower than the measured, but with the differences diminishing at the higher speeds. This is just as would be expected in consideration of the theory employed in CatSeaAir. The Maruo theory is a linearized theory and looses some effectiveness at lower Froude number of 9 ft/sec, which is the lowest speed evaluated. The length Froude number at U = 9 fps is .6, still high speed but associated with substantial wave-making and wave resistance. At the model speed of 30 fps, on the other hand, Fn = 2, for which the wave making should be small and within the linerized theory. This is the observation in Figures 48 to 50.

B. Analysis versus Experiments - Seaway Dynamics

The principal test data reported from the seaway measurements were statistical accelerations at the bow, center of gravity, and transom.

The model test procedure was somewhat different than that of the calculation by CatSeaAir; the model was accelerated to speed in the fully-developed wave system and then measurements were made for a distance of 110 ft down the tank. The data was then statistically processed.

In the CatSeaAir calculations the model is started with the calm water equilibrium at the test speed and the wave system ramped-up to the fully developed condition over a short time period. The statistical processing of the calculated data is delayed in the interest of achieving a statistically stationary response to the seaway.

The comparisons were limited to two of the seaway runs: #390 for Sea-State 2 and W = 70 lbs model weight and #438 for Sea-State 3 at W = 93 lbs model weight. The seaway runs were both fewer in number and time intensive to compute, as discussed. The speed for both runs is the design speed of nominally 17.45 fps (40 knots full scale). The starting calm-water runs are #393 at 70lbs and #437 at 93lbs. As shown on Table 7, the CG positions for these two cases are essentially identical; the calculated xcgc and WAc are used in all the seaway calculations. The results are summarized on Table 8.

There was a concern about achieving statistically stationary response from the numerical time-stepping solution in CatSeaAir, as well as in the model tests. The scaled Pierson-Moskowitz spectrum was inverted into the time domain for the time-stepping response solution by CatSeaAir. The wave input is thereby stationary random. The response output is meaningless as a statistical measure, e.g., RMS, unless it is likewise stationary. This was addressed in part A of the report; here the treatment is extended.

Figure 51 is a plot of displacement response components of the Run #438 computation at SS3.

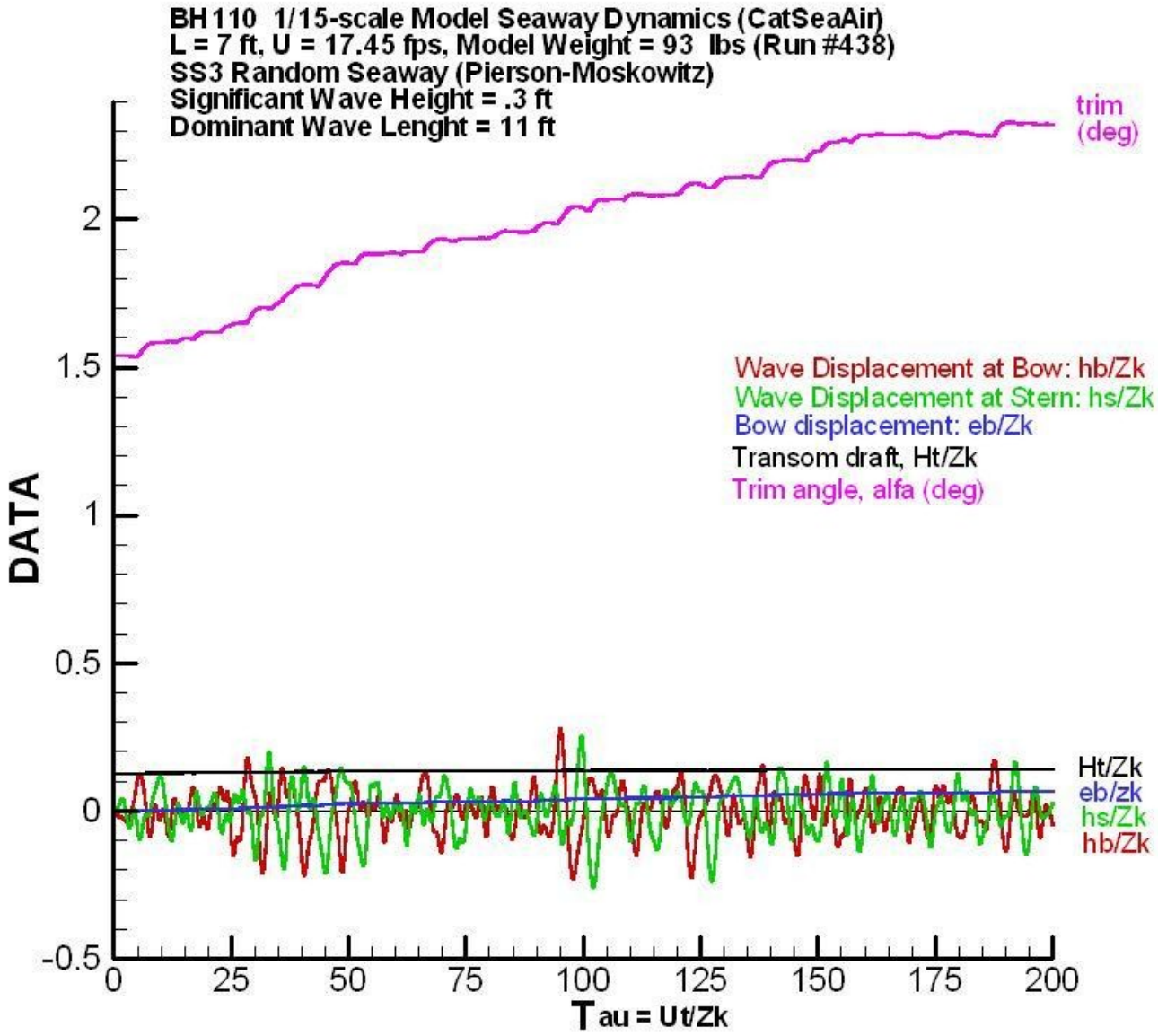

Figure 51: Displacement Distributions versus Time from Seaway Dynamic Analysis; Run 438, SS3, W = 93 lbs, U =17.43 fps, 10,000 time steps

The seawave dimensionless elevations at the bow as stern as converted from the Pierson-Moskowitz spectrum with the .3 ft significant wave height (4.5 ft full scale) plotted along the dimensionless time axis of Figure 51. The seaway is ramped-up as an inverse exponential from calm-water to its full stationary state at about $\tau = 10$, where the statistical data collection commences. Note that Ut is the distance the model has traveled down the tank, with the demi-hull keel offset Zk = 1.05 ft. So τ is approximately the distance the model has traveled down the tank, in feet.

Figure 51 clearly shows that the model is predicted to have risen in the time mean, more in the bow than in the stern. This is because the wave pounding is predominantly up, and predominantly in the bow, thus almost doubling the trim angle. The most relevant implication of Figure 51 is that the non-linear rise has essentially ceased at large time, which would imply that stationarity has been achieved. But it has taken 10,000 time steps at $\Delta\tau = .02$ to reach that state.

The companion SS2 analysis (Table 8) although not shown, exhibits the same character, but converges to the stationary random state slightly sooner.

Table 8
Seaway Dynamic Analysis – Calculations and Experiments

A. **Run #390 -** SS2, U = 17.43 fps, W = 70 lbs

				RMS g's (CatSeaAir)			Mean (CatSeaAir)		
No.	N	Tau	D(ft)	Bow	CG	Trans	Cl	Cd	L/D
390	2500	50.	52.5	.485	.103	.254	.229	.0150	15.3
	5000	110.	115.5	.400	.091	.221	.228	.0135	16.8
	6000	120	126.0	.420	.095	.246	.228	.0137	16.7
	8000	160	168.0	.374	.099	.245	.227	.0130	17.4
	10000	200	210.0	.351	.101	.240	.227	.0127	17.9
	From experiment						Calm Water Calculation		
390	4190	105	110.0	.250	.190	.140	.217	.0117	18.4

B. **Run# 438** – SS3, U = 17.43 fps, W = 93 lbs

				RMS g's (CatSeaAir)			Mean (CatSeaAir)		
No.	N	Tau	D(ft)	Bow	CG	Trans	Cl	Cd	L/D
438	3000	60	63.0	.418	.128	.158	.306	.0297	10.3
	5000	110.	115.5	.390	.129	.160	.305	.0273	11.2
	6000	120	126.0	.380	.125	.175	.304	.0258	11.8
	8000	160	168.0	.381	.123	.175	.304	.0248	13.1
	10000	200	210.0	.354	.115	.168	.303	.0231	21.2
	From experiment						Calm Water Calculation		
438	4190	105	110.0	.520	.330	.210	.286	.0135	21.2

Turning to Table 8, the 10,000 time step analysis was done using the dump-restart capability of CATSeaAir for both of the calculations; the files are written on the dump and saved (this is demonstrated in the Appendix). The total of 10,000 time steps is accomplished in 5 segments for each of the runs A and B; the distance down the tank corresponding to the advancing time is shown. It is being assumed that stationary response is achieved at 10,000 steps on the basis of Figure 51.

It is relevant to consider that the actual tank data collection was over 110 ft of tank length, with the measurements commencing from a transient start-up in the wave system.

The 4th column of Table 8 data would suggest that the stationary random state of the model response was hardly achieved in 110 ft.

The experimental statistics on RMS model acceleration is the last line in each of the Table 8 segments A and B. It is noteworthy that the Lockheed, San Diego tank tests were done under Bell-Halter (now TEXTRON) as an engineering design effort in the development of the BH110, and not as a research program. The model at 7 feet (1/15 scale) was really too small to expect high absolute accuracy. Relative, rather than absolute, accuracy is needed for continuous improvement in design development. In view of both the experimental and numerical modeling uncertainties, the Table 8 comparisons are considered to exhibit good approximate agreement.

One further Table 8 observation is worthy of attention. The right sides of the tables are calculated lift and drag coefficients. The upper-rights are the time means of the variations, with the last line being the calm-water calculated values of Table 7. There are no measurements available for the lift coefficients in the seaway. In this regard, the Cl might be expected to be the calm water value, even in waves. Cl is equivalent to the boat weight in calmwater. But continuing from Table 8B, for example, the predicted time mean Cl at $\tau = 200$ is 6% above the calm water Cl. It is this increased mean lift that produces the rise of the vessel above its calm water position, which is indicated and discussed on Figure 51.

The increase in mean drag over the calm water level indicated in Table 8 is believed to be consistent with expected levels of added resistance in waves. The drag increase is 71% over calm-water drag in the SS3 seaway at 40 knots full scale, by the predicted numbers of Table 8.

VI Summary and Conclusions – Report Part B

1. For the 10m catamaran at 50 knots, which was a subject of Part A, the length Froude number is 2.6. The analysis shows (Table 4) that gravity effects are weak at this high Fn. A speed reduction to 30 knots reduces the Froude number to 1.56, and results in stronger gravity effects in the hydrodynamics, as shown by Table 5. Large high speed ships have a Froude number typically around 1. at top speed. For these cases gravity would be needed in the hydrodynamics for good analysis.

2. For operation in the SES mode at the length Froude number of 2.6, the zero gravity analysis of Part A is also sufficient to approximate the physics well enough.

3. Pressure of the demi-hull bottom in a .5 m seaway are plotted across the bottom at a given time for maximum loading in the bow, and at several x-stations, with gravity and with and without air support (Figures 31 to 38). This is for the purpose of demonstrating the use of the extended CatSeaAir (EDITH 1-2g) code for dynamic load analysis in the seaway.

4. Calm water and seaway dynamic analysis was performed on the BH110 SES for which model test data was available, LMSC/D682700 (1979). The comparisons are reasonable. This is in consideration of the fact that the test program 30 years ago was on a 7 ft (1/15

scale) model for the purpose of engineering design development, and not as a research project. See section V.

5. CatSeaAir is a computation intensive theoretical tool which has demonstrated fairly good agreement with the limited test data available. Pending further validation it could provide reliable prediction of structural loads on high-speed SES/Catamaran hull forms in a seaway.

VII References – Report Part B

Von Karman, T. 1929 The impact of seaplane floats during landing. NACA TN 321 Washington, D.C., Oct.

Wagner, H. 1932 Uber stoss-und gleitvorgange an der oberflache von flussigkeiten. *Zeitschrift fur Angewandte Mathematik und Mechanik*, **12**, 193, Aug.

Maruo, H. 1967 High and low-aspect ratio approximation of planing surfaces. *Schiffstechnik*, **72**.

Tuck, E. 1975 Low-aspect ratio flat-ship theory. *Journal of Hydronautics*, **9**, 1, January.

Stability and Seakeeping Tests with a 1/15 Scale Model of the Bell Aerospace Company Model B-34C, LMSC/D682700, December 1979.

Vorus, W. 1996 A flat cylinder theory for vessel impact and steady planing resistance. *Journal of Ship Research*, **40**, 2, June.

SR1441 Report Appendix
CatSeaAir Input and Output

This Appendix includes samples of the I/O for CatSeaAir. Where numbers are given, they identify with segments of the BH110 analysis for SS2, which is covered in Table 8 of the text.

1. INPUT Data Files

CatSeaAir requires two user prepared input data files for cases not involving lifting strakes and trim tabs. These files are heavily commented with comment statements lifted directly from the source code. The description is believed to be adequate to give the correct impression of the usability of the code. The description is not intended as a user's manual for running the code.

The file descriptions each begin with the FORTRAN read statements from the source code, then list the data for the BH110 SS2 computation. This is followed by a description of each of the data read.

CatSeaAir Input File 1: CATSEA(W).IN (CONTROL DATA)

```
      OPEN(16,FILE='CATSEA(W).IN',STATUS='OLD')
      READ (16,*) RESTART,DUMP
      READ (16,2) (PROB(I),I=1,20)
      READ (16,*) KTABS,KDEF,KODE,KSTEP,KSTR,KEQ,KGRAV
      READ (16,*) MMZ,DSPZ,SBARZ,RATZ
      READ (16,*) CRIT(1),CRIT(2),FAC,KPRNT,KPLOT
      READ (16,*)DTOS,XMASS,GYRAD,XCG,ZCG,XLOA,XCOA,XCGA,CDA,CDMO,YCDA,
     ,DEPS,MALL
      READ (16,*) NPRNT
      IF (NPRNT .NE. 0) READ (16,*) (IPRNT(I),I=1,NPRNT)
      IF (KSTEP .EQ. 0) GO TO 5998
      READ (16,*) NSTEPS
      READ (16,*) (XLSTEP(I),I=1,NSTEPS)
 5998 READ (16,*) UK,ZKM,XTB,YTB,ANGTB,WTA
C
```

```
1 1
BH 110 SES (model data) U = 17.40 fps model scale, run# 390/393  DXCG =
-1.%  ss2
 0 0 3 0 0 0 1
60 .005 .03 2.
.005 .001 .8 0 0
.02 1.94 3.00 2.495 .701 5.794 5.285 2.623 .001 .0003327 .8 .2 10001
1
10000
10.3 .32 0. 0. 0. .83
4. 5.843 10. 1.7 3 200 1.



C
C  RESTART:  1, FOR RESTARTING FROM A DUMP FILE RENAMED RESTART; 0 FOR ORIGINAL.
C  DUMP:  1, WRITE DUMP FILE, 0 DO NOT WRITE DUMP FILE (FILE DUMP IS
C  RENAMED RESTART ON RESTARTING)
C  PROB: ALFANUMERIC IDENTIFICATION (1ST 80 COLS)
C
C  KTABS: 0 - NO TRIM TABS; 1 - TRIM TABS ACTIVE
C  KDEF: 0 -  NO FS DEFLS; 1 - OUTER BRANCH ONLY
C  KODE: 1 - REGULAR WAVES; 2 - IRREGULAR WAVES (JONSWAP SPECTRUM); 3 –
C  PIERSON-MOSKOWITZ SPECTRUM
C  KSTEP: 0 - NO STEPS
C  KSTR:  0 - NO LIFTING STRAKES
C  KEQ: 1 -  EQUIL RUN SEQUENCE WITH NO WAVES(thrust set to drag at
each time step);
C       0 - NONEQUIL RUN (thrust set to drag at IALL = 0)
C  KGRAV: 1 - WITH GRAVITY WAVE EFFECTS
C         0 - WITHOUT GRAVITY WAVE EFFECTS
C
C  MMZ: TOTAL NO SH ELE IN ZETA SPACE
C  DSPZ & SBARZ: SAME AS DZMIN & DELZ BUT IN 0 TO 1. ZETA SPACE; DSPZ
C  MIN AT 1.  (FOR DSPZ*MMZ .GT. 1., DSPZ SET TO 1./MMZ)
C  RATZ: EXPANSION FACTOR IN ZETA SPACE
C
C  CRIT1:  CONVERGENCE FACTOR FOR EXTERNAL (KW) JET VELOCITY (REC .0001)
C  CRIT2:  CONVERGENCE FACTOR FOR NEW VORTEX SHEET ELEMENT (REC .0001)
C  FAC: RELAXATION FACTOR IN BDOT SUB (REC .8)
C  KPRNT, KPLOT:  PRINT CONTROL PARAMETERS (0 NO PRINT)
C
C  DTOS: OSCILLATION TIME INCREMENT; dtime*U/ZK
C  XMASS: 2(W/gam*ZK**3)
C  GYRAD: rad of gyration about transom/ZK
C  XCG: dist cg from transom/ZK
C  ZCG: dist from transom base to CG/ZK
C  XLOA:  OVERALL BOAT LENGTH/ZK
C  XCOA: OVERALL CUSHION LENGHT/ZK FOR SES (XCOA=XLOA FOR NO CUSHION)
C  XCGA:  XCG OF AIR CUSHION
C  CDA:  Aerodynamic Drag Coefficient (referred to water)
```

```
C  YCDA: Vertical moment/ZK for aerodynamic drag effects
C  DEPS:  fractional artificial damping (C*DT/M; same for heave and c
C  pitch); use .01 - .02
C  MALL: NUMBER OF TIME STEPS (MALL = 1 FOR STEADY CASE ONLY)
C  NPRNT:  NO TIMES FOR DETAILED OUTPUT
C  IPRNT: TIME STEP NUMBERS FOR DETAILED OUTPUT (STEADY CASE: IALL = 0,
C  ALWAYS PRINTED)
C
C  NSTEPS = NUMBER OF STEPS (NUMBER OF TANDEM HULLS LESS 1)
C  XLSTEP(I)= DISTANCE BETWEEN STEPS/ZK
C  (FOR NSTEP = 1, XSTEP(1) IS STEP TO TRANSOM DISTANCE.)
C
C  UK:  VESSEL SPEED IN KNOTS
C  ZKM:  MAXIMUM HALF-KEEL OFFSET (M)
C  XTB,YTB: X/Zch AND Y/Zch POSITION OF THRUST BEARING RE BASELINE TRANSOM
C  ANGTB:  VERTICAL PLANE ANGLE OF THRUST LINE (+ UP LKNG FWD), DEG
C  WTA:  FRACTION OF CRAFT WEIGHT SUPPORTED BY INTERNAL AIR PRESSURE
C
C  DATA READ AND CONVERTED IN WAVE:
C
C  KODE = 1:  REGULAR WAVE;
C  READ (16,*) AHTA,WAVL,PHASE,WAVES
C
C  AHTA: MAX AMPLITUDE OF FREE-SURFACE OSCILLATION/ZK
C  WAVL: WAVE LENGTH/ZK
C  PHASE:  0 deg, NODE AT TRANSOM INITIALLY, TROUGH FWD; 180. NODE AT
C  TRANSOM INITIALLY, CREST FWD
C  OMEGA: FREQ OF TRANSOM DRAFT OSCILLATION; Omega*ZK/U = 2PI/Wavl
C  WAVES: HEAD = 1., FOLLOWING = -1.
C
C  KODE = 2: IRREGULAR WAVE (JONSWAP Spectrum)
C  READ (16,*) WMIN,W0,WMAX,GAM,NEW,WAVES
C
C  WMIN:  MIN SPECTRAL FREQ (RAD/SEC) (TYP: 1.)
C  W0:  FREQUENCY AT PEAK (TYP: 1.4)
C  WMAX:  MAX FREQUENCY (TYP 1.8)
C  GAM:  CONSTANT (USE 7.)
C  I1:  SEED FOR RANDOM PHASE IN IRREG SEA CALCS (3,5,7,9)
C  NEW:  NO FREQS IN SPECTRAL CALC (USE 200)
C  WAVES: HEAD = 1., FOLLOWING = -1.
C
C  KODE = 3; SAME READ AS KODE = 2 (GAM NOT USED)
C
C  DATA READ AND CONVERTED IN TABS:
C  READ (16,*) CTAB,WTAB,NTABS,ATAB0,ATAB,FTAB,RAMP,TUS
C
C  CTAB:  TAB CHORD/ZCH
C  WTAB:  TAB SPAN/ZCH
C  NTABS: NUMBER OF IDENTICAL TABS AT TRANSOM
C  ATAB0: MEAN TAB ANGLE (DEG); FROM 0 RE TRANSOM
```

```
C
C  ATAB: AMPLITUDE OF TAB OSCILLATION (deg)
C  FTAB: FREQUENCY OF TAB OSCILLATION (OMEGA*ZCH/U; OMEGA RADIANS/SEC)
C  RAMP: RAMP-UP RATE FOR TABS
C  TUS: NON-DIM TIME FOR COMMENCEMENT OF OSCILLATION
C
C  DATA READ AND CONVERTED IN STRAKES (FILE SDATA.IN)
C  NS - NO OF STRAKES
C  YS(I) - ELEVATION OF STRAKE I ABOVE BL/Zch
C  ZCHS(I) - WIDTH OF STRAKE FACE (IN)
C
C  TABULTAED DATA FOR INTERPOLATION:
C  NI,XL(I),NJ(I)
C  ALFA(I,J),CLL(I,J),XB(I,J)
C
```

CatSeaAir Input File 2: CATS(W).IN (HULL GEOMETRY)

```
OPEN(15,FILE='CATs(W).IN',STATUS='OLD')
READ (15,2) (PROB(I),I=1,20)
READ (15,*) HT,TRIM
READ (15,*) NGAM,NSEC
READ (15,*) ZC1,MM,DZMIN1,DELZ1,DZMIN2,DELZ2,KIT,NELE
READ (15,*) YK0,YK0P,YK0PP,YK1,YK1P,AKR,XMAX,XTRANS,XLA,XLC
READ (15,*) BETA0,BETA0P,BETA1,BETA1P,XLAB
READ (15,*) BET11,BET12,BET21,BET22
READ (15,*) ZK0,ZK0P,ZK1,ZK1P
READ (15,*) ZCI0,ZCI0P,ZCIM,ZCI1,ZCI1P,XLAC,XLCC
CLOSE(15)
C


BH 110 (model data #393)
.098 1.14
1 1
1.001 100 .005 .015 .01 .02 2 1
.4351 -1.088 0. -0. -0. 0. 5.798 0. 5.159 0.
74. -70. 30. 0. 4.84
74. 74. 30. 30.
1. 0. 1.  0.
1. .2 1.143 1.143 0. 4.84 0.
```

```
C
C  HT: TRANSOM DRAFT/ZK  (TRIAL OR CALM WATER)
C  TRIMD: BASELINE TRIM ANGLE, DEG  (TRIAL OR CALM WATER)
C
C  NWL: FORCE CALCS - NWL .NE. 0
C  NSEC:  SECTION PLOTS  -  NSEC .NE. 0
C
C  ZC1:  Z/ZK AT INITIAL CONDITION  (TYP 1.001)
C  MM: NUM ELEMENTS IN X0 - XMAX
C  DZMIN1:  MIN ELEMENT LENGTH IN ZCMIN TO ZC1 AT ZC1 (REC .0003 TO .001)
C  DELZ1:  INITIAL ELEMENT LENGTH AT STEM
C  DZMIN2:  FRACTION OF HULL LENGHT FOR DX2 (NONDIM ON XMAX)
C  DELZ2:  FINAL ELEMENT LENGTH AT TRANSOM
C  KIT:  EXTRAP ORDER FOR FIRST GUESS ON DB1 & VS2 (2 QUAD, 1 LINEAR, 0  CONST)
C  NELE:  NUM ELE IN CUW FREE SHEET DISCRETIZATION (for 1 ele of const
C  gamma set NELE=1) USE 1
C
C  YK0: KEEL UPSET AT ENTRY
C  YK0P: KEEL SLOPE AT ENTRY
C  YK0PP: KEEL CURVATURE AT ENTRY
C  YK1: KEEL UPSET AT TRANSOM
C  YK1P: KEEL SLOPE AT TRANSOM (NEGATIVE FOR CUP)
C  XMAX: TRIAL WL LENGTH
C  XTRANS: DISTANCE FROM HULL STEP TO TRANSOM (ZERO FOR NO STEPS).
C  XLA: FWD KEEL TANGENT POINT FWD FROM TRANSOM
C  XLC: AFT KEEL TANGENT POINT FWD FROM TRANSOM
C
C  BETA0:  DR ANGLE AT INITIAL CONDITION
C  BETA0P: SLOPE OF DEADRISE ANGLE AT X0
C  BETA1: DEADRISE ANGLE AT XMAX (DEG).
C  BETA1P: SLOPE OF DEADRISE ANGLE AT XMAX (DEG PER NON-DIM TIME)
C  XLAB: FWD DR TANGENT POINT FWD FROM TRANSOM  (zero for no const segment)
C  BET11:  DEADRISE ANGLE AT KEEL (TIP) @ T=TMIN
C  BET12:  DEADRISE ANGLE AT CHINE  @ T=TMIN
C  BET21:  DEADRISE ANGLE AT KEEL  @ T=XMAX
C  BET22:  DEADRISE ANGLE AT CHINE  @ T=XMAX
C  XCA: NO CAMBER INSIDE XCA; BET21 = BET22 = BETA1
C  (BETIJ: I=1,2 FWD AND AFT; J = 1,2 KEEL AND CHINE)
C
C  ZK0: KEEL OFFSET AT X0
C  ZK0P: KEEL OF CHINE OFFSET AT X0
C  ZK1:  KEEL OFFSET AT TRANSOM
C  ZK1P: SLOPE OF KEEL OFFSET AT XMAX
C
C  ZCI0: CHINE OFFSET AT ENTRY
C  ZCI0P: SLOPE OF CHINE OFFSET AT ENTRY
C  ZCIM: MAX CHINE OFFSET
C  ZCI1: CHINE OFFSET AT TRANSOM
C  ZCI1P: SLOPE OF CHINE OFFSET AT TRANSOM
C  XLAC: FWD TANGENT PT TO ZCIM FROM TRANSOM
C  XLCC: AFT TANGENT PT TO ZCIM FROM TRANSOM
C
```

2. OUTPUT Data Files

The output is either the spatially lumped quantities versus time, or the spatial distribution versus x over the instantaneous vessel length; see Report Part A for a description of the logic of the computation.

CATSEA(W).OUT

The principal output file: CATSEA(W).OUT is of the first type. The file shown is from the 8,000 to 10,000 restart segment of Table 8 in the text. At 2,000 time steps this file is still quited lengthy and has been truncated in the middle, as shown below. The lines have also been wrapped as needed due to page width limitations. Identification of the listed output variables follows the file copy.

```
Catamaran Planning Boat Dynamics, Vorus and Associates, Inc  2001 – 2006
CatSeaAir EDITH1-2g

 ANALYSIS OF CATAMARANS and SES

 NO OF STEPS (no tandem hulls-1); FWD TO AFT:           0
 DISTANCE BETWEEN STEPS/ZK:


BH 110 SES (model data) U = 17.40 fps model scale, run# 390/393  DXCG = -1.%  ss2
 IRREGULAR WAVE ANALYSIS; PIERSON-MOSKOWITZ SPECTRUM
 HEAD SEAS

 WMIN,W0,WMAX,GAM,I1,NEW:
   4.00000000000000        5.84300000000000        10.0000000000000
   1.70000000000000                3         200
 WAVE LENGHT/ZK & W0*ZK/U @ W0 =    5.64897121624901
  0.352527359120678

 SIG WAVE HEIGHT =   4.298041097415504E-002 M     0.140975746765549      FT
 WAVE LENGHT =    1.80767078919968      M      5.92916013685708      FT

 DTOS,XMASS,GYRAD,XCG,ZCG,G,XLOA,XCOA,DEPS:   2.000000000000000E-002
   1.94000000000000        3.00000000000000        2.49500000000000
  0.701000000000000       0.111731373139073        5.79400000000000
   5.28500000000000       0.200000000000000

 AERODYNAMIC CDM,CDA,YCDA:   3.327000000000000E-004  1.000000000000000E-003
  0.800000000000000
 THRUST CENTER AND ORIENTATION: XTB,YTB,ANGTB (deg)
  0.000000000000000E+000  0.000000000000000E+000  0.000000000000000E+000

 FRACTION OF WT SUPPORTED BY AIR, WTA:   0.830000000000000
 AIR PRESSURE COEF, CPA:    14.1086331853823

 VESSEL UK(KNOTS), ZK(M), PA(PSI):    10.3000000000000
  0.320000000000000       3.464341817286686E-002
 Trim Tabs Inactive
 STEADY PLANING CLT0,CMT0:   0.216758863889801       0.540813365405054
```

```
 IALL     TOS        XMAX         XCW         HFSe        HFSs         HT          TRIMD       Evbpp      Evtpp
Espp       DC3T         DC5T

 8001  0.1600D+03  0.4484D+01  0.3811D+01  0.3273D-01  0.3662D-01  0.11826D+00  0.19292D+01  0.4392D+00 -
0.3694D+00  0.9423D-01 -0.4595D-02  0.5816D-01
 8002  0.1600D+03  0.4465D+01  0.3833D+01  0.3209D-01  0.3699D-01  0.11826D+00  0.19293D+01  0.4466D+00 -
0.3690D+00  0.9505D-01 -0.3855D-02  0.6061D-01
 8003  0.1601D+03  0.4446D+01  0.3853D+01  0.3147D-01  0.3732D-01  0.11827D+00  0.19295D+01  0.4461D+00 -
0.3677D+00  0.9491D-01 -0.3741D-02  0.6074D-01
 8004  0.1601D+03  0.4427D+01  0.3837D+01  0.3083D-01  0.3759D-01  0.11828D+00  0.19298D+01  0.4539D+00 -
0.3683D+00  0.9592D-01 -0.3083D-02  0.6309D-01
 8005  0.1601D+03  0.4408D+01  0.3856D+01  0.3019D-01  0.3781D-01  0.11829D+00  0.19301D+01  0.4537D+00 -
0.3645D+00  0.9546D-01 -0.2630D-02  0.6387D-01
 8006  0.1601D+03  0.4389D+01  0.3839D+01  0.2957D-01  0.3799D-01  0.11831D+00  0.19304D+01  0.4593D+00 -
0.3625D+00  0.9589D-01 -0.1870D-02  0.6609D-01

                  .

                  .

                  .

9990  0.1998D+03  0.3721D+01  0.1887D+01  0.1326D-01  0.5067D-02  0.11806D+00  0.20218D+01 -0.4620D-01
0.1502D+00 -0.1999D-01  0.1423D-01  0.1814D-01
9991  0.1998D+03  0.3705D+01  0.1855D+01  0.1268D-01  0.6852D-02  0.11806D+00  0.20217D+01 -0.4611D-01
0.1765D+00 -0.2375D-01  0.1749D-01  0.2412D-01
 9992  0.1998D+03  0.3688D+01  0.1837D+01  0.1210D-01  0.8715D-02  0.11805D+00  0.20217D+01 -0.4721D-01
0.1670D+00 -0.2258D-01  0.1621D-01  0.2163D-01
 9993  0.1999D+03  0.3672D+01  0.1819D+01  0.1152D-01  0.1065D-01  0.11804D+00  0.20216D+01 -0.4727D-01
0.1565D+00 -0.2117D-01  0.1491D-01  0.1925D-01
 9994  0.1999D+03  0.3655D+01  0.1811D+01  0.1093D-01  0.1266D-01  0.11804D+00  0.20215D+01 -0.4617D-01
0.1417D+00 -0.1902D-01  0.1318D-01  0.1627D-01
 9995  0.1999D+03  0.3638D+01  0.1783D+01  0.1034D-01  0.1474D-01  0.11803D+00  0.20214D+01 -0.4666D-01
0.1651D+00 -0.2243D-01  0.1602D-01  0.2139D-01
 9996  0.1999D+03  0.3622D+01  0.1765D+01  0.9746D-02  0.1687D-01  0.11803D+00  0.20214D+01 -0.4581D-01
0.1553D+00 -0.2102D-01  0.1489D-01  0.1947D-01
 9997  0.1999D+03  0.3605D+01  0.1744D+01  0.9156D-02  0.1906D-01  0.11802D+00  0.20213D+01 -0.4486D-01
0.1470D+00 -0.1981D-01  0.1396D-01  0.1792D-01
 9998  0.2000D+03  0.3588D+01  0.1736D+01  0.8558D-02  0.2129D-01  0.11802D+00  0.20212D+01 -0.4229D-01
0.1326D+00 -0.1756D-01  0.1241D-01  0.1549D-01
 9999  0.2000D+03  0.3571D+01  0.1728D+01  0.7958D-02  0.2357D-01  0.11801D+00  0.20211D+01 -0.3945D-01
0.1192D+00 -0.1545D-01  0.1103D-01  0.1340D-01
10000  0.2000D+03  0.3554D+01  0.1693D+01  0.7360D-02  0.2588D-01  0.11800D+00  0.20211D+01 -0.4060D-01
0.1431D+00 -0.1899D-01  0.1387D-01  0.1842D-01

     2xRMS VERT ACCELERATIONS AT BOW, TRANSOM, AND CG
      0.70216E+00  0.47952E+00  0.20157E+00
     2xRMS AXIAL ACCELERATION:   0.103779104162324

     TIME MEAN CL, CD, AND CL/CD
      0.22745E+00  0.12667E-01  0.17956E+02
     TIME MEAN TRIM AND HT/Zch:
      0.17166E+01  0.11383E+00
```

All of the initial data in the file (on p. 5A) is input. The variables in the output list above are identified as follows:

IALL – time step number, $\tau = 0$ being IALL = 1.

TOS – dimensionless time τ

XMAX - wetted length/Zk

XCW – chine-wetting distance forward of the transom/Zk (0 is fully chine-unwetted).

HFSe – wave elevation at entry/Zk (XMAX forward of the transom)

HFSs – wave elevation at the stern, or transom

HT – transom draft/Zk

TRIMD – trim angle, degrees

Evbpp – vertical acceleration at bow, g's

Evtpp – vertical acceleration at transom, g's

Espp – surge acceleration, g's

DC3T – coefficients of instantaneous hydrodynamic lift less calm water lift

DC5T - coefficients of instantaneous hydrodynamic moment less calm water moment

The remaining output files are for specified times and list data versus x; the data is always listed at the last computation time (τ = 200 in this example).

CATS (W)a.OUT

```
Version CATSea2-0(s)
PLANING CATAMARAN SEAKEPING
BH 110 (model data #393)

IALL =        10000

 CRIT(1),CRIT(2),FAC,KIT
    5.000000000000000E-003  1.000000000000000E-003  0.800000000000000  2

 Rocker Angle AKR (deg) =   2.600000000000000E+000

  Discretization Parameters ZC1,DZMIN1,DELZ1,DZMIN2,DELZ2:
   1.00100000000000       5.000000000000000E-003  1.500000000000000E-002
   1.000000000000000E-002  2.000000000000000E-002
   NUMBER X STEPS =          100
```

```
      TRANSOM DRAFT/ZK =   0.118004432383109
      TRANSOM OPENING/ZK, H0 =   0.000000000000000E+000
      TRIM ANGLE, DEG:    2.02107339463515

      TIME STEP*U/ZK =   2.000000000000000E-002
      MEMORY EFFECTS IN CUW FLOW, NELE =            1

      ZERO CAMBER

      INITIAL AND FINAL DR ANGLES (DEG) & XLAB:    30.0000000000000
        30.0000000000000        4.84000000000000
      ENTRY ANGLE ALLOWING FOR CAMBER =    30.0000000000000


 I   Zc(I)   Zk(I)  Zci(I)  Zw  YwL   BETA(I)     VV        X(I)        Vs(I,1)      Zb(I,1)      Vs(I,2)
              Zb(I,2)    ITB1 ITB2 ISLAST IS1 IS2 ISL
 1  1.001  1.000  1.143  1.000  0.002 30.00  0.69297E-01  0.17768E-01 -0.13141E+00  0.99883E+00  0.35065E+00
             0.10040E+01   4   4   0   0   0   0
 2  1.008  1.000  1.143  1.001  0.004 30.00  0.68414E-01  0.35447E-01 -0.65935E-02  0.99654E+00
             0.41130E+00  0.10091E+01   7   0   0   0   0   0
 3  1.013  1.000  1.143  1.002  0.006 30.00  0.67511E-01  0.53127E-01 -0.23720E-02  0.99425E+00
             0.45157E+00  0.10141E+01   5   0   0   0   0   0
 4  1.019  1.000  1.143  1.005  0.007 30.00  0.66591E-01  0.70806E-01 -0.22156E-02  0.99195E+00
             0.49546E+00  0.10195E+01   4   0   0   0   0   0
 5  1.023  1.000  1.143  1.008  0.009 30.00  0.65633E-01  0.88873E-01 -0.18705E-02  0.98961E+00
             0.50818E+00  0.10243E+01   4   0   0   0   0   0
                                  .
                                  .
                                  .
 96  1.143  1.000  1.143  1.143  0.155 30.00  0.53525E-01  0.33751E+01 -0.10000E-02  0.64145E+00
             0.18544E+00  0.12395E+01   4   4   0   0   0   0
 97  1.143  1.000  1.143  1.143  0.153 30.00  0.54280E-01  0.34114E+01 -0.10000E-02  0.63824E+00
             0.18581E+00  0.12413E+01   4   4   0   0   0   0
 98  1.143  1.000  1.143  1.143  0.150 30.00  0.54890E-01  0.34474E+01 -0.10000E-02  0.63508E+00
             0.18584E+00  0.12430E+01   4   4   0   0   0   0
 99  1.143  1.000  1.143  1.143  0.148 30.00  0.55349E-01  0.34829E+01 -0.10000E-02  0.63197E+00
             0.18560E+00  0.12448E+01   4   4   0   0   0   0
100  1.143  1.000  1.143  1.143  0.146 30.00  0.55656E-01  0.35183E+01 -0.10000E-02  0.62889E+00
             0.18509E+00  0.12466E+01   4   4   0   0   0   0
101  1.143  1.000  1.143  1.143  0.144 30.00  0.55810E-01  0.35536E+01 -0.10000E-02  0.62581E+00
             0.18435E+00  0.12484E+01   4   4   0   0   0   0

      INDICES FOR CP CALCS;  NGAMS =           69
   1    3    5    7   10   13   14   15   16   17   18   19   20   21   22
  23   24   25   26   27   28   29   30   31   32   33   34   35   36   37
  38   39   40   41   42   43   44   45   46   47   48   49   50   51   52
  53   54   55   56   57   58   59   61   62   63   65   67   70   73   76
  79   82   85   88   91   94   97  100  101
```

XLL,FNL:
  0.35536D+01 0.15874D+01

DX(I), I = 1, NXX

0.17768D-01	0.17679D-01	0.17679D-01	0.17679D-01	0.18067D-01
0.18834D-01	0.19589D-01	0.20331D-01	0.21061D-01	0.21778D-01
0.22483D-01	0.23175D-01	0.23854D-01	0.24522D-01	0.25176D-01
0.25819D-01	0.26448D-01	0.27065D-01	0.27670D-01	0.28262D-01
0.28842D-01	0.29409D-01	0.29964D-01	0.30506D-01	0.31036D-01
0.31553D-01	0.32058D-01	0.32550D-01	0.33030D-01	0.33497D-01
0.33952D-01	0.34394D-01	0.34824D-01	0.35241D-01	0.35646D-01
0.36038D-01	0.36418D-01	0.36785D-01	0.37140D-01	0.37482D-01
0.37812D-01	0.38130D-01	0.38434D-01	0.38727D-01	0.39007D-01
0.39274D-01	0.39529D-01	0.39771D-01	0.40001D-01	0.40218D-01
0.40423D-01	0.40615D-01	0.40795D-01	0.40963D-01	0.41117D-01
0.41260D-01	0.41390D-01	0.41507D-01	0.41612D-01	0.41704D-01
0.41784D-01	0.41852D-01	0.41906D-01	0.41949D-01	0.41979D-01
0.41996D-01	0.42001D-01	0.41993D-01	0.41973D-01	0.41941D-01
0.41896D-01	0.41838D-01	0.41768D-01	0.41686D-01	0.41590D-01
0.41483D-01	0.41363D-01	0.41230D-01	0.41085D-01	0.40928D-01
0.40758D-01	0.40575D-01	0.40380D-01	0.40173D-01	0.39953D-01
0.39720D-01	0.39475D-01	0.39218D-01	0.38948D-01	0.38665D-01
0.38370D-01	0.38063D-01	0.37743D-01	0.37410D-01	0.37065D-01
0.36708D-01	0.36338D-01	0.35955D-01	0.35560D-01	0.35359D-01
0.35359D-01				

XMAX : 3.55363037295488

NI	XI(NIP)	SS(NIP)	BB(NI)	BBP(NI)	VV	G(0)	GI(0)
1	0.018	0.001	30.000	0.00	0.0353	0.61809D-05	0.61809D-05
2	0.035	0.008	30.000	0.00	0.0353	0.38467D-03	0.38467D-03
3	0.053	0.013	30.000	0.00	0.0353	0.90826D-03	0.90817D-03
4	0.071	0.019	30.000	0.00	0.0353	0.16183D-02	0.16176D-02
5	0.089	0.023	30.000	0.00	0.0353	0.21689D-02	0.21657D-02
6	0.108	0.028	30.000	0.00	0.0353	0.26022D-02	0.25924D-02
			.				
			.				
			.				
95	3.338	0.143	30.000	0.00	0.0353	0.66641D-02	-0.10126D-07
96	3.375	0.143	30.000	0.00	0.0353	0.71983D-02	-0.87753D-08
97	3.411	0.143	30.000	0.00	0.0353	0.73576D-02	-0.76087D-08
98	3.447	0.143	30.000	0.00	0.0353	0.71076D-02	-0.66006D-08
99	3.483	0.143	30.000	0.00	0.0353	0.65595D-02	-0.57292D-08
100	3.518	0.143	30.000	0.00	0.0353	0.58917D-02	-0.49419D-08
101	3.554	0.143	30.000	0.00	0.0353	0.53551D-02	-0.42346D-08

i) The first data set in CATS(W)a.OUT is again input data for checking. In the second set:

I – x-station number, with 1 at Xmax forward of the stern.
Zc – zero pressure point offset
Zci – chine offset
Zw – waterline offset
Ywl – waterline elevation above the transom baseline
Beta – deadrise angle
VV – vertical onset velocity at baseline
X – dimensionless distance of I section downstream of entry
Vs(1) – outer jet-head velocity
Zb(1) – outer jet-head offset
Vs(2) – inner jet-head velocity
Zb(2) – inner jet-head offset
ITB ...ISL - convergence control parameters

ii) The second data set labeled “INDICES …” are the station numbers where pressures are calculated for force integration; the pressure distribution at not all 101 stations is evaluated, to conserve run time.

iii) XLL and FNL are the wetted length and length Froude number

iv) DX is the dimensionless station spacing at IALL

v) The last set in this file is the computation of the gravity wave effect:

NI – station number, same as I above
XI – same as x above
SSP – jet head offset, same as Zc above
BB – deadrise angle, same as Beta above
VV – same as VV above
G(0)- non-infinite Fn transverse vortex strength on x-axis; see eq. (2) and related discussion
GI(0) - infinite Fn transverse vortex strength on x-axis; see eq. (2) and related discussion.

CATS (W)b.OUT

```
          (PRESSURE AND FORCE CALCULATION RESULTS)

          BH 110 (model data #393)

           IALL =        10000


           INITIAL DEADRISE ANGLE =    74.0000000000000      DEGREES
```

```
TOTAL PRESSURE EFFECTS

Z-VALUES AT I =           1
 0.10000E+01  0.10000E+01  0.10001E+01  0.10001E+01  0.10001E+01
 0.10001E+01  0.10002E+01  0.10002E+01  0.10002E+01  0.10003E+01
 0.10003E+01  0.10003E+01  0.10003E+01  0.10004E+01  0.10004E+01
 0.10004E+01  0.10004E+01  0.10005E+01  0.10005E+01  0.10005E+01
 0.10005E+01  0.10005E+01  0.10006E+01  0.10006E+01  0.10006E+01
 0.10006E+01  0.10006E+01  0.10007E+01  0.10007E+01  0.10007E+01
 0.10007E+01  0.10007E+01  0.10007E+01  0.10008E+01  0.10008E+01
 0.10008E+01  0.10008E+01  0.10008E+01  0.10008E+01  0.10008E+01
 0.10009E+01  0.10009E+01  0.10009E+01  0.10009E+01  0.10009E+01
 0.10009E+01  0.10009E+01  0.10009E+01  0.10009E+01  0.10009E+01
 0.10009E+01  0.10010E+01  0.10010E+01  0.10010E+01  0.10010E+01
 0.10010E+01  0.10010E+01  0.10010E+01  0.10010E+01  0.10010E+01
 0.10010E+01


CP @ S
 0.00000E+00  0.00000E+00  0.00000E+00  0.00000E+00  0.00000E+00
 0.00000E+00  0.00000E+00  0.00000E+00  0.00000E+00  0.00000E+00
 0.00000E+00  0.00000E+00  0.00000E+00  0.00000E+00  0.00000E+00
 0.00000E+00  0.00000E+00  0.00000E+00  0.00000E+00  0.00000E+00
 0.00000E+00  0.00000E+00  0.00000E+00  0.00000E+00  0.00000E+00
 0.00000E+00  0.00000E+00  0.00000E+00  0.00000E+00  0.00000E+00
 0.00000E+00  0.00000E+00  0.00000E+00  0.00000E+00  0.00000E+00
 0.00000E+00  0.00000E+00  0.00000E+00  0.00000E+00  0.00000E+00
 0.00000E+00  0.00000E+00  0.00000E+00  0.00000E+00  0.00000E+00
 0.00000E+00  0.00000E+00  0.00000E+00  0.00000E+00  0.00000E+00
 0.00000E+00  0.00000E+00  0.00000E+00  0.00000E+00  0.00000E+00
 0.00000E+00  0.00000E+00  0.00000E+00  0.00000E+00  0.00000E+00
 0.00000E+00

  Cl = F/.5*RHO*U**2*ZK =   0.000000000000000E+000
  Cd = D/.5*RHO*U**2*ZK =   0.000000000000000E+000

Lift-to-Drag-Ratio =   0.000000000000000E+000


TOTAL PRESSURE EFFECTS

Z-VALUES AT I =           3
 0.10000E+01  0.10004E+01  0.10008E+01  0.10012E+01  0.10016E+01
 0.10019E+01  0.10023E+01  0.10027E+01  0.10030E+01  0.10034E+01
 0.10037E+01  0.10041E+01  0.10044E+01  0.10047E+01  0.10050E+01
 0.10054E+01  0.10057E+01  0.10060E+01  0.10063E+01  0.10066E+01
 0.10068E+01  0.10071E+01  0.10074E+01  0.10076E+01  0.10079E+01
 0.10082E+01  0.10084E+01  0.10086E+01  0.10089E+01  0.10091E+01
 0.10093E+01  0.10095E+01  0.10097E+01  0.10099E+01  0.10101E+01
 0.10103E+01  0.10105E+01  0.10107E+01  0.10108E+01  0.10110E+01
```

```
 0.10112E+01  0.10113E+01  0.10115E+01  0.10116E+01  0.10117E+01
 0.10118E+01  0.10120E+01  0.10121E+01  0.10122E+01  0.10123E+01
 0.10124E+01  0.10125E+01  0.10125E+01  0.10126E+01  0.10127E+01
 0.10128E+01  0.10128E+01  0.10129E+01  0.10129E+01  0.10130E+01
 0.10131E+01


CP @ S
 0.18279E-01  0.19760E+00  0.20220E+00  0.20353E+00  0.20424E+00
 0.20472E+00  0.20507E+00  0.20535E+00  0.20559E+00  0.20580E+00
 0.20600E+00  0.20618E+00  0.20636E+00  0.20654E+00  0.20672E+00
 0.20689E+00  0.20707E+00  0.20725E+00  0.20744E+00  0.20764E+00
 0.20783E+00  0.20804E+00  0.20826E+00  0.20848E+00  0.20871E+00
 0.20894E+00  0.20919E+00  0.20945E+00  0.20971E+00  0.20998E+00
 0.21025E+00  0.21053E+00  0.21082E+00  0.21113E+00  0.21145E+00
 0.21176E+00  0.21207E+00  0.21237E+00  0.21266E+00  0.21293E+00
 0.21316E+00  0.21336E+00  0.21351E+00  0.21360E+00  0.21360E+00
 0.21349E+00  0.21324E+00  0.21280E+00  0.21213E+00  0.21115E+00
 0.20976E+00  0.20784E+00  0.20520E+00  0.20160E+00  0.19662E+00
 0.18941E+00  0.17797E+00  0.15739E+00  0.11083E+00  0.00000E+00
 0.00000E+00

  Cl = F/.5*RHO*U**2*ZK =   5.289732860016444E-003
  Cd = D/.5*RHO*U**2*ZK =   1.865920743021828E-004

Lift-to-Drag-Ratio =    28.3491829961106


TOTAL PRESSURE EFFECTS

Z-VALUES AT I =            5
 0.10000E+01  0.10007E+01  0.10014E+01  0.10021E+01  0.10028E+01
 0.10035E+01  0.10041E+01  0.10048E+01  0.10054E+01  0.10060E+01
 0.10066E+01  0.10072E+01  0.10078E+01  0.10084E+01  0.10090E+01
 0.10096E+01  0.10101E+01  0.10106E+01  0.10112E+01  0.10117E+01
 0.10122E+01  0.10127E+01  0.10131E+01  0.10136E+01  0.10141E+01
 0.10145E+01  0.10150E+01  0.10154E+01  0.10158E+01  0.10162E+01
 0.10166E+01  0.10170E+01  0.10173E+01  0.10177E+01  0.10180E+01
 0.10184E+01  0.10187E+01  0.10190E+01  0.10193E+01  0.10196E+01
 0.10199E+01  0.10201E+01  0.10204E+01  0.10206E+01  0.10209E+01
 0.10211E+01  0.10213E+01  0.10215E+01  0.10217E+01  0.10219E+01
 0.10220E+01  0.10222E+01  0.10223E+01  0.10225E+01  0.10226E+01
 0.10227E+01  0.10228E+01  0.10230E+01  0.10231E+01  0.10232E+01
 0.10233E+01


CP @ S
 0.19078E-01  0.25053E+00  0.25620E+00  0.25781E+00  0.25866E+00
 0.25920E+00  0.25959E+00  0.25989E+00  0.26014E+00  0.26035E+00
 0.26053E+00  0.26069E+00  0.26085E+00  0.26100E+00  0.26114E+00
 0.26128E+00  0.26142E+00  0.26156E+00  0.26171E+00  0.26186E+00
 0.26201E+00  0.26218E+00  0.26235E+00  0.26253E+00  0.26272E+00
 0.26292E+00  0.26313E+00  0.26335E+00  0.26358E+00  0.26386E+00
```

```
 0.26417E+00  0.26449E+00  0.26483E+00  0.26518E+00  0.26554E+00
 0.26591E+00  0.26629E+00  0.26669E+00  0.26709E+00  0.26751E+00
 0.26792E+00  0.26835E+00  0.26876E+00  0.26917E+00  0.26956E+00
 0.26992E+00  0.27024E+00  0.27049E+00  0.27065E+00  0.27069E+00
 0.27055E+00  0.27018E+00  0.26948E+00  0.26832E+00  0.26653E+00
 0.26373E+00  0.25908E+00  0.25040E+00  0.23000E+00  0.13529E+00
 0.00000E+00

  Cl = F/.5*RHO*U**2*ZK =   1.198288615641586E-002
  Cd = D/.5*RHO*U**2*ZK =   4.226889416199356E-004

Lift-to-Drag-Ratio =    28.3491829961106


TOTAL PRESSURE EFFECTS

Z-VALUES AT I =            7
 0.10000E+01  0.10010E+01  0.10020E+01  0.10030E+01  0.10040E+01
 0.10049E+01  0.10059E+01  0.10068E+01  0.10077E+01  0.10086E+01
 0.10094E+01  0.10103E+01  0.10111E+01  0.10120E+01  0.10128E+01
 0.10136E+01  0.10143E+01  0.10151E+01  0.10158E+01  0.10166E+01
 0.10173E+01  0.10180E+01  0.10187E+01  0.10193E+01  0.10200E+01
 0.10206E+01  0.10212E+01  0.10218E+01  0.10224E+01  0.10230E+01
 0.10236E+01  0.10241E+01  0.10246E+01  0.10251E+01  0.10256E+01
 0.10261E+01  0.10265E+01  0.10270E+01  0.10274E+01  0.10278E+01
 0.10282E+01  0.10286E+01  0.10290E+01  0.10293E+01  0.10297E+01
 0.10300E+01  0.10303E+01  0.10306E+01  0.10308E+01  0.10311E+01
 0.10313E+01  0.10315E+01  0.10317E+01  0.10319E+01  0.10321E+01
 0.10323E+01  0.10324E+01  0.10326E+01  0.10328E+01  0.10329E+01
 0.10331E+01


CP @ S
 0.19889E-01  0.25746E+00  0.26346E+00  0.26511E+00  0.26594E+00
 0.26646E+00  0.26681E+00  0.26707E+00  0.26727E+00  0.26743E+00
 0.26756E+00  0.26767E+00  0.26777E+00  0.26787E+00  0.26795E+00
 0.26804E+00  0.26812E+00  0.26821E+00  0.26830E+00  0.26839E+00
 0.26849E+00  0.26860E+00  0.26872E+00  0.26884E+00  0.26898E+00
 0.26912E+00  0.26928E+00  0.26945E+00  0.26966E+00  0.26993E+00
 0.27022E+00  0.27052E+00  0.27083E+00  0.27117E+00  0.27152E+00
 0.27188E+00  0.27227E+00  0.27268E+00  0.27310E+00  0.27355E+00
 0.27401E+00  0.27450E+00  0.27500E+00  0.27552E+00  0.27606E+00
 0.27660E+00  0.27715E+00  0.27769E+00  0.27822E+00  0.27872E+00
 0.27916E+00  0.27951E+00  0.27974E+00  0.27977E+00  0.27952E+00
 0.27886E+00  0.27743E+00  0.27429E+00  0.26606E+00  0.22337E+00
 0.00000E+00

  Cl = F/.5*RHO*U**2*ZK =   1.750834672242974E-002
  Cd = D/.5*RHO*U**2*ZK =   6.175961658165536E-004

Lift-to-Drag-Ratio =    28.3491829961106
```

```
TOTAL PRESSURE EFFECTS

Z-VALUES AT I =           10
 0.10000E+01  0.10015E+01  0.10029E+01  0.10043E+01  0.10057E+01
 0.10071E+01  0.10085E+01  0.10098E+01  0.10111E+01  0.10124E+01
 0.10137E+01  0.10149E+01  0.10161E+01  0.10173E+01  0.10185E+01
 0.10197E+01  0.10208E+01  0.10219E+01  0.10230E+01  0.10240E+01
 0.10251E+01  0.10261E+01  0.10271E+01  0.10280E+01  0.10290E+01
 0.10299E+01  0.10308E+01  0.10317E+01  0.10325E+01  0.10333E+01
 0.10341E+01  0.10349E+01  0.10357E+01  0.10364E+01  0.10371E+01
 0.10378E+01  0.10385E+01  0.10391E+01  0.10397E+01  0.10403E+01
 0.10409E+01  0.10415E+01  0.10420E+01  0.10425E+01  0.10430E+01
 0.10434E+01  0.10439E+01  0.10443E+01  0.10447E+01  0.10450E+01
 0.10454E+01  0.10457E+01  0.10460E+01  0.10463E+01  0.10465E+01
 0.10468E+01  0.10470E+01  0.10472E+01  0.10475E+01  0.10477E+01
 0.10480E+01


CP @ S
 0.21107E-01  0.24179E+00  0.24736E+00  0.24883E+00  0.24952E+00
 0.24992E+00  0.25017E+00  0.25033E+00  0.25044E+00  0.25052E+00
 0.25056E+00  0.25060E+00  0.25062E+00  0.25063E+00  0.25064E+00
 0.25066E+00  0.25067E+00  0.25068E+00  0.25070E+00  0.25073E+00
 0.25076E+00  0.25080E+00  0.25086E+00  0.25092E+00  0.25099E+00
 0.25108E+00  0.25117E+00  0.25129E+00  0.25152E+00  0.25178E+00
 0.25204E+00  0.25233E+00  0.25263E+00  0.25295E+00  0.25328E+00
 0.25364E+00  0.25403E+00  0.25443E+00  0.25486E+00  0.25532E+00
 0.25580E+00  0.25631E+00  0.25686E+00  0.25743E+00  0.25803E+00
 0.25867E+00  0.25933E+00  0.26002E+00  0.26074E+00  0.26147E+00
 0.26220E+00  0.26293E+00  0.26363E+00  0.26427E+00  0.26482E+00
 0.26524E+00  0.26543E+00  0.26508E+00  0.26309E+00  0.24986E+00
 0.00000E+00

  Cl = F/.5*RHO*U**2*ZK =   2.377254977778815E-002
  Cd = D/.5*RHO*U**2*ZK =   8.385620771169899E-004

Lift-to-Drag-Ratio =    28.3491829961106
           .

           .

           .


TOTAL PRESSURE EFFECTS

Z-VALUES AT I =           97
 0.10000E+01  0.10044E+01  0.10087E+01  0.10130E+01  0.10171E+01
 0.10213E+01  0.10253E+01  0.10293E+01  0.10332E+01  0.10370E+01
 0.10408E+01  0.10445E+01  0.10481E+01  0.10517E+01  0.10552E+01
 0.10586E+01  0.10620E+01  0.10653E+01  0.10685E+01  0.10716E+01
 0.10747E+01  0.10777E+01  0.10807E+01  0.10836E+01  0.10864E+01
 0.10891E+01  0.10918E+01  0.10944E+01  0.10969E+01  0.10994E+01
```

```
 0.11018E+01  0.11041E+01  0.11064E+01  0.11086E+01  0.11107E+01
 0.11127E+01  0.11147E+01  0.11166E+01  0.11185E+01  0.11203E+01
 0.11220E+01  0.11236E+01  0.11252E+01  0.11267E+01  0.11281E+01
 0.11295E+01  0.11308E+01  0.11320E+01  0.11332E+01  0.11343E+01
 0.11353E+01  0.11363E+01  0.11371E+01  0.11380E+01  0.11387E+01
 0.11394E+01  0.11401E+01  0.11409E+01  0.11416E+01  0.11423E+01
 0.11430E+01


CP @ S
 0.35460E-01  0.63567E-01  0.65487E-01  0.65808E-01  0.65846E-01
 0.65863E-01  0.65785E-01  0.65591E-01  0.65128E-01  0.64481E-01
 0.63788E-01  0.63122E-01  0.62499E-01  0.61911E-01  0.61343E-01
 0.60783E-01  0.60222E-01  0.59655E-01  0.59078E-01  0.58491E-01
 0.57894E-01  0.57292E-01  0.56689E-01  0.56089E-01  0.55498E-01
 0.54917E-01  0.54348E-01  0.53791E-01  0.53250E-01  0.52728E-01
 0.52225E-01  0.51737E-01  0.51255E-01  0.50763E-01  0.50245E-01
 0.49697E-01  0.49121E-01  0.48530E-01  0.47934E-01  0.47343E-01
 0.46766E-01  0.46199E-01  0.45626E-01  0.45041E-01  0.44448E-01
 0.43827E-01  0.43149E-01  0.42390E-01  0.41504E-01  0.40413E-01
 0.39013E-01  0.37174E-01  0.34737E-01  0.31455E-01  0.26851E-01
 0.19880E-01  0.81330E-02  0.00000E+00  0.00000E+00  0.00000E+00
 0.00000E+00

  Cl = F/.5*RHO*U**2*ZK =   1.577478425336537E-002
  Cd = D/.5*RHO*U**2*ZK =   5.564458155823966E-004

Lift-to-Drag-Ratio =    28.3491829961106

TOTAL PRESSURE EFFECTS

Z-VALUES AT I =          100
 0.10000E+01  0.10044E+01  0.10087E+01  0.10130E+01  0.10171E+01
 0.10213E+01  0.10253E+01  0.10293E+01  0.10332E+01  0.10370E+01
 0.10408E+01  0.10445E+01  0.10481E+01  0.10517E+01  0.10552E+01
 0.10586E+01  0.10620E+01  0.10653E+01  0.10685E+01  0.10716E+01
 0.10747E+01  0.10777E+01  0.10807E+01  0.10836E+01  0.10864E+01
 0.10891E+01  0.10918E+01  0.10944E+01  0.10969E+01  0.10994E+01
 0.11018E+01  0.11041E+01  0.11064E+01  0.11086E+01  0.11107E+01
 0.11127E+01  0.11147E+01  0.11166E+01  0.11185E+01  0.11203E+01
 0.11220E+01  0.11236E+01  0.11252E+01  0.11267E+01  0.11281E+01
 0.11295E+01  0.11308E+01  0.11320E+01  0.11332E+01  0.11343E+01
 0.11353E+01  0.11363E+01  0.11371E+01  0.11380E+01  0.11387E+01
 0.11394E+01  0.11401E+01  0.11409E+01  0.11416E+01  0.11423E+01
 0.11430E+01


CP @ S
 0.35460E-01  0.60132E-01  0.62778E-01  0.63250E-01  0.63388E-01
 0.63411E-01  0.63420E-01  0.63372E-01  0.63101E-01  0.62593E-01
 0.61968E-01  0.61326E-01  0.60711E-01  0.60131E-01  0.59579E-01
 0.59042E-01  0.58510E-01  0.57979E-01  0.57445E-01  0.56908E-01
```

```
 0.56372E-01  0.55838E-01  0.55309E-01  0.54785E-01  0.54268E-01
 0.53759E-01  0.53265E-01  0.52789E-01  0.52333E-01  0.51896E-01
 0.51470E-01  0.51044E-01  0.50606E-01  0.50147E-01  0.49667E-01
 0.49168E-01  0.48656E-01  0.48139E-01  0.47632E-01  0.47149E-01
 0.46688E-01  0.46230E-01  0.45764E-01  0.45291E-01  0.44810E-01
 0.44304E-01  0.43742E-01  0.43077E-01  0.42239E-01  0.41145E-01
 0.39710E-01  0.37818E-01  0.35272E-01  0.31770E-01  0.26807E-01
 0.19252E-01  0.64738E-02  0.00000E+00  0.00000E+00  0.00000E+00
 0.00000E+00

  Cl = F/.5*RHO*U**2*ZK =   1.539675194694321E-002
  Cd = D/.5*RHO*U**2*ZK =   5.431109584024200E-004

Lift-to-Drag-Ratio =    28.3491829961106


TOTAL PRESSURE EFFECTS

Z-VALUES AT I =          101
 0.10000E+01  0.10044E+01  0.10087E+01  0.10130E+01  0.10171E+01
 0.10213E+01  0.10253E+01  0.10293E+01  0.10332E+01  0.10370E+01
 0.10408E+01  0.10445E+01  0.10481E+01  0.10517E+01  0.10552E+01
 0.10586E+01  0.10620E+01  0.10653E+01  0.10685E+01  0.10716E+01
 0.10747E+01  0.10777E+01  0.10807E+01  0.10836E+01  0.10864E+01
 0.10891E+01  0.10918E+01  0.10944E+01  0.10969E+01  0.10994E+01
 0.11018E+01  0.11041E+01  0.11064E+01  0.11086E+01  0.11107E+01
 0.11127E+01  0.11147E+01  0.11166E+01  0.11185E+01  0.11203E+01
 0.11220E+01  0.11236E+01  0.11252E+01  0.11267E+01  0.11281E+01
 0.11295E+01  0.11308E+01  0.11320E+01  0.11332E+01  0.11343E+01
 0.11353E+01  0.11363E+01  0.11371E+01  0.11380E+01  0.11387E+01
 0.11394E+01  0.11401E+01  0.11409E+01  0.11416E+01  0.11423E+01
 0.11430E+01


CP @ S
 0.35460E-01  0.58656E-01  0.61649E-01  0.62165E-01  0.62328E-01
 0.62357E-01  0.62376E-01  0.62350E-01  0.62136E-01  0.61681E-01
 0.61089E-01  0.60463E-01  0.59855E-01  0.59278E-01  0.58729E-01
 0.58196E-01  0.57672E-01  0.57152E-01  0.56633E-01  0.56116E-01
 0.55601E-01  0.55090E-01  0.54582E-01  0.54079E-01  0.53584E-01
 0.53100E-01  0.52633E-01  0.52185E-01  0.51759E-01  0.51348E-01
 0.50944E-01  0.50535E-01  0.50111E-01  0.49668E-01  0.49208E-01
 0.48732E-01  0.48244E-01  0.47756E-01  0.47286E-01  0.46845E-01
 0.46422E-01  0.45997E-01  0.45565E-01  0.45133E-01  0.44697E-01
 0.44233E-01  0.43702E-01  0.43051E-01  0.42213E-01  0.41116E-01
 0.39674E-01  0.37757E-01  0.35155E-01  0.31561E-01  0.26466E-01
 0.18697E-01  0.55428E-02  0.00000E+00  0.00000E+00  0.00000E+00
 0.00000E+00

  Cl = F/.5*RHO*U**2*ZK =   1.519733154922007E-002
  Cd = D/.5*RHO*U**2*ZK =   5.360765264842055E-004

Lift-to-Drag-Ratio =    28.3491829961106
```

SECTION GEOMETRIC CHARACTERISTICS

I	X(I)	YWL(I)	ZWL0(I)	ZWLI(I)	YB(I)	AC(I)	SL(I)
1	0.17768D-01	0.19234D-02	0.10000D+01	0.10033D+01	-0.64115D-03	0.32040D-05	0.38469D-02
2	0.35447D-01	0.37984D-02	0.10000D+01	0.10064D+01	-0.10967D-02	0.96849D-05	0.99073D-02
3	0.53127D-01	0.56327D-02	0.10000D+01	0.10093D+01	-0.17147D-02	0.23430D-04	0.15687D-01
4	0.70806D-01	0.74244D-02	0.10000D+01	0.10122D+01	-0.23178D-02	0.42428D-04	0.21466D-01
5	0.88873D-01	0.92095D-02	0.10000D+01	0.10157D+01	-0.29201D-02	0.66796D-04	0.27245D-01
			.				
			.				
			.				
95	0.33384D+01	0.15698D+00	0.10000D+01	0.11430D+01	-0.60304D-01	0.16545D-01	0.16512D+00
96	0.33751D+01	0.15480D+00	0.10000D+01	0.11430D+01	-0.59261D-01	0.16233D-01	0.16512D+00
97	0.34114D+01	0.15258D+00	0.10000D+01	0.11430D+01	-0.58202D-01	0.15916D-01	0.16512D+00
98	0.34474D+01	0.15036D+00	0.10000D+01	0.11430D+01	-0.57142D-01	0.15598D-01	0.16512D+00
99	0.34829D+01	0.14816D+00	0.10000D+01	0.11430D+01	-0.56095D-01	0.15283D-01	0.16512D+00
100	0.35183D+01	0.14599D+00	0.10000D+01	0.11430D+01	-0.55068D-01	0.14974D-01	0.16512D+00
101	0.35536D+01	0.14388D+00	0.10000D+01	0.11430D+01	-0.54067D-01	0.14671D-01	0.16512D+00

TOTAL LIFT AND DRAG (all segments)
CL = L/.5*RHO*U**2*ZK**2 = 0.230629087887093
CL required, CLT0 = 0.216758863889801
Center of LIFT/ZK, from transom = 2.41534671432768
Xcg/ZK required = 2.49500000000000
TOTAL DRAG COEF, CDT = D/.5*RHO*U**2*ZK**2 = 1.104890971092080E-002
Equil thrust coef = 1.174913208509830E-002
HULL WETTED AREA/ZK**2 = 0.886244640975916
VISCOUS DRAG COEF = 3.585053605857132E-003
TRANSOM DRAG COEF = 5.155638495162291E-004
TOTAL CUSHION DRAG COEF = 9.012412293392775E-004
MOMENTUM DRAG COEF = 3.327000000000000E-004
SEAL VISCOUS DRAG COEF = 2.925261341841714E-003
Center of drag/ZK above transom base = 0.197907421973998
Center of THRUST above transom base = 0.000000000000000E+000
Lift-to-Drag-Ratio = 20.8734702265815

i) The primary data in CATS(W)b.OUT is the pressure coefficient distribution in x at time τ for the force calculation. This is the data plotted on Figures 33 to 40 of the Part B report.

ii) The second data set labeled section geometric characteristics is the geometric data for the hydrodynamic and hydrostatic load calculations. It is as follows:

X – station position downstream from entry (same as from CATS(W)a.OUT).
YWL – waterline elevation (same as from CATS(W)a.OUT).
ZWL0 – demihull (dimensionless) keel offset

ZWLI - demihull offset at YWL
YB – elevation of center of buoyancy
AC – cross-sectional area
SL – streamline length keel to waterline

iii) The final data set is the load summary at τ. It is:

CL - instantaneous vessel lift coefficient.
CLT0 – required CL at calm water equilibrium
Lift/Zk – instantaneous total lift center forward of transom
Xcg/Zk - required lift center forward of transom at calm water Equilibrium
CDT – total drag coefficient
Thrust coefficient – taken as equal to equil drag coef
AS – dimensionless wetted surface area
(various drag components and centers)
L/D – instantaneous lift/drag ratio

2. Plot Files

Plotting, with TECHPLOT, is used extensively to display both input and output data. The Techplot.plt files, which are left in the run folder after execution, are identified as follows:

BETA – wetted deadrise angle versus x at τ, deg
YKEEL – wetted keel upset versus x at τ(dimensionless on Zk)
CHINE – wetted chine offset versus x at τ(dimensionless on Zk)
BPLAN – wetted half-body plan versus x at τ(dimensionless on Zk)
PLAN – wetted plan showing separated streamlines versus x at τ (dimensionless on Zk)
W0 – jet velocities at τ
FORC – normal force coefficient distribution in x at τ
DUMP – active data at end of run; change name to RESTART for restarting at end time
SEAOUT1 – impact vertical accelerations in τ
SEAOUT2 – wetted length and wetted chine length in τ
SEAOUT3 – wave and craft displacements in τ
SEAOUT4 – surge acceleration in τ
SEAOUT5 – lift and drag coefficients in τ

PROJECT TECHNICAL COMMITTEE MEMBERS

The following persons were members of the committee that represented the Ship Structure Committee to the Contractor as resident subject matter experts. As such they performed technical review of the initial proposals to select the contractor, advised the contractor in cognizant matters pertaining to the contract of which the agencies were aware, performed technical review of the work in progress and edited the final report.

Chairman

Members
Contracting Officer's Technical Representative:

Marine Board Liaison:

Executive Director Ship Structure Committee:

SHIP STRUCTURE COMMITTEE LIAISON MEMBERS

LIAISON MEMBERS

American Society of Naval Engineers	Captain Dennis K. Kruse (USN Ret.)
Bath Iron Works	Mr. Steve Tarpy
Colorado School of Mines	Dr. Stephen Liu
Edison Welding Institute	Mr. Rich Green
International Maritime Organization	Mr. Igor Ponomarev
Int'l Ship and Offshore Structure Congress	Dr. Alaa Mansour
INTERTANKO	Mr. Dragos Rauta
Massachusetts Institute of Technology	
Memorial University of Newfoundland	Dr. M. R. Haddara
National Cargo Bureau	Captain Jim McNamara
National Transportation Safety Board - OMS	Dr. Jack Spencer
Office of Naval Research	Dr. Yapa Rajapaksie
Oil Companies International Maritime Forum	Mr. Phillip Murphy
Samsung Heavy Industries, Inc.	Dr. Satish Kumar
United States Coast Guard Academy	Commander Kurt Colella
United States Merchant Marine Academy	William Caliendo / Peter Web
United States Naval Academy	Dr. Ramswar Bhattacharyya
University of British Columbia	Dr. S. Calisal
University of California Berkeley	Dr. Robert Bea
Univ. of Houston - Composites Eng & Appl.	
University of Maryland	Dr. Bilal Ayyub
University of Michigan	Dr. Michael Bernitsas
Virginia Polytechnic and State Institute	Dr. Alan Brown
Webb Institute	Prof. Roger Compton

RECENT SHIP STRUCTURE COMMITTEE PUBLICATIONS

Ship Structure Committee Publications on the Web - All reports from SSC 1 to current are available to be downloaded from the Ship Structure Committee Web Site at URL: http://www.shipstructure.org

SSC 445 – SSC 393 are available on the SSC CD-ROM Library. Visit the National Technical Information Service (NTIS) Web Site for ordering hard copies of all SSC research reports at URL: http://www.ntis.gov

SSC Report Number	Report Bibliography
SSC 448	Fracture Mechanics Characterization of Aluminum Alloys for Marine Structural Applications, Donald J.K., Blair A. 2007
SSC 447	Fatigue and Fracture Behavior of Fusion and Friction Stir Welded Aluminum Components, Kramer R. 2007
SSC 446	Comparative Study of Naval and Commercial Ship Structure Design Standards, Kendrick, A., Daley C. 2007
SSC 445	Structural Survivability of Modern Liners, Iversen R. 2005
SSC 444	In-Service Non-Destructive Estimation of the Remaining Fatigue Life of Welded Joints, Dexter R.J., Swanson K.M., Shield C.K. 2005
SSC 443	Design Guidelines for Doubler Plate Repairs on Ship Structures Sensharma P.K., Dinovitzer A., Traynham Y. 2005
SSC 442	Labor-Saving Passive Fire Protection Systems For Aluminum And Composite Construction E. Greene, 2005
SSC 441	Fire Degradation, Failure Prediction And Qualification Methods For Fiber Composites R. Asaro, M. Dao, 2005
SSC 440	Deterioration of Structural Integrity Due to Chemical Treatment of Ballast Water S. Tiku, 2005
SSC 439	Comparative Structural Requirements For High Speed Crafts K. Stone, 2005
SSC 438	Structural Optimization for Conversion of Aluminum Car Ferry to Support Military Vehicle Payload, R.Kramer, 2005